Profile derived fluxes above inhomogeneous terrain:
a numerical approach

L. J. M. Kroon

Profile derived fluxes above inhomogeneous terrain: a numerical approach

Proefschrift

ter verkrijging van de graad van
doctor in de landbouwwetenschappen,
op gezag van de rector magnificus,
dr. C. C. Oosterlee,
in het openbaar te verdedigen
op woensdag 6 maart 1985
des namiddags te vier uur in de aula
van de Landbouwhogeschool te Wageningen

"If we knew all the laws of Nature, we should need only one fact, or the description of one actual phenomenon, to infer all the particular results at that point. Now we know only a few laws, and our result is vitiated, not, of course, by any confusion or irregularity in Nature, but by our ignorance of essential elements in the calculation. Our notions of law and harmony are commonly confined to those instances which we detect; but the harmony which results from a far greater number of seemingly conflicting, but really concurring, laws, which we have not detected, is still more wonderful. The particular laws are as our points of view, as, to the traveller, a mountain outline varies with every step, and it has an infinite number of profiles, though absolutely but one form. Even when cleft or bored through it is not comprehended in its entireness."

from: Walden
Henry David Thoreau
(1817-1862)

Aan mijn ouders
en aan Marja en Emily

Voorwoord

Het verrichte onderzoek, waarvan deze dissertatie een van de eindprodukten is, had een aanpak die omschreven wordt door de term modellering. Een dergelijke aanpak brengt met zich mee dat slechts een relatief gering aantal mensen naast de onderzoeker zelf een inbreng in het geheel heeft. Maar die inbreng zelf hoeft op zich niet gering te zijn.

Mijn promotoren Bert Wartena en Hans Vugts dank ik voor hun begeleiding tijdens de afgelopen jaren. Bert, hoewel onze discussies over het onderzoek niet frequent waren, slaagde jij er toch in mij in de beginfase op het juiste spoor te zetten. Bij de voortgang van het werk was jij degene die de grote lijnen niet uit het oog verloor, juist daar, waar ik mijzelf in details dreigde te verliezen.

Hans Vugts, ik ben je erkentelijk voor het in het juiste perspectief zetten van de resultaten van dit onderzoek. Juist jouw enorme ervaring uit de praktijk kwam hierbij goed van pas.

In de lange aanloopfase kwam in de gesprekken met K. Krishna Prasad ook een geheel andere mogelijke aanpak van het probleem ter sprake. Hoewel ik uiteindelijk toch niet voor die mogelijkheid heb gekozen, bedank ik hem voor zijn hulp en inbreng.

Een nieuw onderzoek moet door anderen bedacht, aangevraagd en verdedigd worden voordat de onderzoeker zelf nog maar iets heeft gedaan. Voor dit voorbereidende en essentiële werk ben ik vooral Frits Bottemanne zeer dankbaar.

Om je gedachten, de theorie en de resultaten goed geformuleerd op papier te krijgen is meestal een iteratieproces nodig. Jacques Schols, Adrie Jacobs en Henk de Bruin wil ik hierbij bedanken voor het toevoegen van enige onmisbare cycli aan dit proces.

Voor de uiteindelijke vormgeving hebben vooral zorg gedragen: Paul van Espelo, die met voortvarende hand het tekenwerk verzorgde, en Len Weldring die in een hoog tempo het typewerk heeft geleverd. Mijn dank voor hun doorzettingsvermogen is zeer groot.

Tenslotte, lieve Marja en Emily, wil ik jullie bedanken voor het feit dat jullie, vooral in de laatste maanden, mijn afwezigheid (ook geestelijk) zonder al te veel protest hebben doorstaan.

Bennekom, 15 oktober 1984.

Contents

List of symbols

Symbol	Description	S.I. unit	Introduced in:
a	factor in Elliott's expression for the height of the internal boundary layer	-	3.2.2
a	constant in Mulhearn's model	-	3.3.1
a_1	constant in Bradshaw's model	-	3.5.1
a_1, a_2	constants used in the modeling of the pressure terms	-	A3.1
a_t	constant used in the modeling of the turbulent transport terms	-	4.1.2
b	constant used in the modeling of the destruction terms	-	4.1.2
c	constant used in the modeling of the dissipation terms	-	4.1.2
c_{13}	constant used in the modeling of the pressure covariance	-	A2.1
C, C_1, C_2	constants used in the modeling of the pressure covariance	-	A3.1
c_{pd}	specific heat of dry air at constant pressure	$J\ kg^{-1}K^{-1}$	2.3
$d(x)$	height of the internal boundary layer	m	2.1
d_1, d_3	constants used in the modeling of the destruction terms	-	A3.1
e	used in the turbulent kinetic energy defined by: TKE = $\overline{e^2}$	m^2s^{-2}	3.5.1
E	water vapour flux density	$kg\ m^{-2}s^{-1}$	4.3.2
Ei, E_1	exponential integral functions	-	3.3.1
f, F	universal functions in the models of Townsend and Mulhearn	-	3.3.1
f	Coriolis parameter	s^{-1}	3.4.1
g_i	acceleration of gravity, g_i = (0,0,g)	ms^{-2}	2.3

Symbol	Description	S.I. unit	Introduced in:
g, G	universal functions in Mulhearn's model	–	3.3.1
G	Geostrophic wind speed	ms^{-1}	3.4.1
G	function in Bradshaw's model	–	3.5.1
G	soil heat flux density	Wm^{-2}	5.2
h_o	average height of roughness elements	m	6.3
h_{BR}	height at which the fluxes determined with the Bowen ratio method deviate 10% from the surface fluxes	m	6.2
H_α	scale height of the atmosphere	m	2.3
H	sensible heat flux	Wm^{-2}	4.3.2
I	vertical flux of horizontal momentum	$kg\ m^{-1}s^{-2}$	5.2
k	von Karman constant (k = 0.41)	–	3.2.1
k	thermal conductivity	$Jm^{-1}s^{-1}K^{-1}$	2.3
$K_{m,h,w}$	scalar eddy transfer coefficients for momentum, heat and water vapour	m^2s^{-1}	3.2.1/5.2
k	turbulent kinetic energy $k = \overline{e^2}$	m^2s^{-2}	3.5.1
ℓ_w	length scale of the vertical velocity	m	2.3
ℓ_α	length scale for the vertical variation of specific volume (α)	m	2.3
ℓ_H	length scale for the horizontal motion	m	2.3
ℓ	mixing length	m	3.2.1
ℓ_o	length scale in the models of Townsend and Mulhearn	m	3.3.1
L	length scale in Bradshaw's model	m	3.5.1
L	Obukhov length	m	5.2
ℓ_1, ℓ_ϵ	length scales in the model of Huang and Nickerson	m	3.5.1

Symbol	Description	S.I. unit	Introduced in:
m	ratio of upstream and downstream roughness length $m = z_{01}/z_{02}$	–	3.2.2
M	$M = \ln(z_{01}/z_{02})$	–	3.2.2
$\underset{\sim}{P}$	(instantaneous) pressure $\underset{\sim}{P} = P_r + \tilde{P}$	Pa	2.3
$\tilde{P}$	perturbation pressure $\tilde{P} = P + p$	Pa	
P	production rate of turbulent kinetic energy	$m^2 s^{-3}$	3.5.1
$P_{1,2,3}$	terms in the transformation of the $\overline{uw}$ equation	–	A5
$\tilde{q}$	specific humidity $\tilde{q} = Q + q$	–	2.3
q_*	specific humidity scale, $q_* = -\overline{wq}/u_*$	–	4.2.1
Q_s	saturation specific humidity	–	A3.1
R_o	surface relative humidity (defined at $z = z_o$)	–	A3.2
R_d	gas constant for dry air	$J\ kg^{-1}K^{-1}$	2.3
R_i	Richardson number	–	A3.1
R_n	net radiation	Wm^{-2}	5.2
$r_{\theta q}$	correlation coefficient	–	5.4.2
r_a	aerodynamic resistance	sm^{-1}	A4
r_s	surface resistance	sm^{-1}	A4
s	slope of the saturation specific humidity curve	K^{-1}	A4
S	specific entropy	$J\ kg^{-1}K^{-1}$	2.3
t	time	s	2.3
$\underset{\sim}{T}$	(instantaneous) temperature $\underset{\sim}{T} = T_r + \tilde{T}$	K	2.3
$\tilde{T}$	perturbation temperature	K	2.3
T_*	temperature scale, $T_* = \overline{w\theta}/u_*$	K	4.1.2
$\underset{\sim}{u}_i$	(instantaneous) Eulerian velocity with components $(\underset{\sim}{u}, \underset{\sim}{v}, \underset{\sim}{w})$ and $\underset{\sim}{u}_i = u_{i,r} + \tilde{u}_i$	ms^{-1}	2.3
$\tilde{u}_i$	perturbation velocity $\tilde{u}_i = U_i + u_i$	ms^{-1}	2.3
u_*	friction velocity, $u_* = (\tau_o/\rho_o)^{\frac{1}{2}}$	ms^{-1}	A2

Symbol	Description	S.I. unit	Introduced in:
u_o	velocity scale in Townsend's model	ms^{-1}	3.3.1
x_i	position vector with components (x,y,z)	m	2.1
x_{max}	downstream distance where $d(x) = z_{max}$	m	2.1
z_o	surface roughness length	m	2.1
z_I	PBL height	m	A3.2
z_{max}	upper grid level	m	A3.2
z_1, z_2	lowest two grid levels	m	A3.2

Greek symbols

Symbol	Description	S.I. unit	Introduced in:
α	specific volume	$m^3 kg^{-1}$	2.3
β	Bowen ratio (gradient)	–	5.2
β^*	Bowen ratio (flux)	–	5.2
γ	$\gamma = c_p/\lambda$	K^{-1}	A4
Γ_d	dry adiabatic lapse rate	Km^{-1}	2.3
$\delta(x)$	height of the IAL	m	2.1
δ_{ij}	Kronecker delta	–	2.3
ϵ	dissipation rate of turbulent kinetic energy	$m^2 s^{-3}$	3.5.1
ϵ^*	ratio of the molecular masses of water vapour and dry air	–	2.3
ϵ_{ijk}	permutation tensor (Levi Civita)	–	2.3
η	dimensionless height, $\eta = z/_o$	–	3.3.1
θ	(instantaneous) potential temperature, $\theta = \theta_r + \tilde{\theta}$	K	2.3
$\tilde{\theta}$	perturbation potential temperature, $\tilde{\theta} = \theta + \theta$	K	2.3
κ	constant in the approximation of τ	–	A5
κ	ratio, $\kappa = R_d/c_{pd}$	–	2.3
κ_H	thermal diffusivity, $\kappa_H = k/\rho c_p$	$m^2 s^{-1}$	2.3
κ_v	diffusivity of water vapour	$m^2 s^{-1}$	2.3

Symbol	Description	S.I. unit	Introduced in:
λ	length scale used in Taylor's model	m	3.4.1
λ	latent heat of vaporization of water	$J\ kg^{-1}$	4.3.2
μ	molecular viscosity of air	$kg\ m^{-1}s^{-1}$	2.3
ν	kinematic viscosity of air	$m^2 s^{-1}$	2.3
ϱ	(instantaneous) density $\varrho = \rho_r + \tilde{\rho}$	$kg\ m^{-3}$	2.3
$\tilde{\rho}$	perturbation density	$kg\ m^{-3}$	2.3
σ_u	variance of the horizontal velocity fluctuation, $\sigma_u^2 = \overline{u^2}$	ms^{-1}	4.3.1
τ	shear stress	Nm^{-2}	3.2.1
τ	turbulent time scale	s	4.1.2
$\phi_{m,u,w}$	dimensionless functions in the atmosphere surface layer for momentum, heat and water vapour	$\sim$	3.2.3/5.2
ω	frequency	s^{-1}	2.3
Ω_i	earth rotation vector	s^{-1}	2.3

Abbreviations

ABL	Atmospheric Boundary Layer	2.1
ASL	Atmospheric Surface Layer	2.1
IAL	Internal Adapted Layer	2.1
IBL	Internal Boundary Layer	2.1
PBL	Planetary Boundary Layer	2.1
TKE	Turbulent Kinetic Energy	3.1

1 Introduction

1.1 SCOPE AND GOALS

This study deals with the problems which arise when one tries to
measure some of the components of the energy balance at the
earth's surface. A simplified picture of what happens at the
interface of the two distinctly different media air and earth is
the following. The net amount of energy supplied to the earth's
surface, after various physical processes (absorption, reflec-
tion, scattering etc.) have taken place, is used to heat the
ground and the atmosphere just above the surface and is also used
to evaporate the water at or near the surface. In this simplifi-
cation we have disregarded the energy absorbed by vegetation and
other, usually small, terms of the energy balance. Thus energy is
transported from the surface into the ground and the atmosphere.

The transport of a quantity per unit area and unit time is also
referred to as a flux density. Heating of the atmosphere and
evaporation are called the sensible and latent vertical heat flux
density, respectively. These flux densities can be directed up-
wards (into the atmosphere) or downwards (to the earth), depen-
ding on the stratification of the atmosphere just above the sur-
face. These two fluxes are always accompanied by a vertical flux
of horizontal momentum which is directed downwards.

The assessment of the magnitude of either three, or all of these
flux densities is of crucial importance to a number of practical
questions in meteorology, agriculture, hydrology and related
fields. In meteorology the energy supplied to the earth's sur-
face is one of the main processes driving the atmosphere. Because
of the large latent heat of vaporization of water, large amounts
of energy can be redistributed through the atmosphere. At a much
smaller scale the energy balance is an important boundary condi-
tion for models of the atmospheric boundary layer for air pollu-
tion models and studies of air-sea interaction. In hydrology the

fluxes of sensible and latent heat are important for the estimation of the water balance of inland lakes, the evaporation from vegetation systems etc.. For problems concerned with e.g. the water setup by wind in a network of channels the momentum flux must be known. Finally, in agriculture the estimation of the fluxes of momentum, latent and sensible heat are needed when one is interested in matters concerned with wind erosion, crop yield, plant diseases, pest control and the like.

Proper measurement of the flux densities is beset with many difficulties and uncertainties. It would of course be ideal if one is able to measure them directly at the surface using the conservation of mass principle and other conservation equations. Instruments performing these tasks have indeed been designed (drag plates, heat flux plates, lysimeters) and are in use, but they are not easily installed and cumbersome to use. The only possibility left is the indirect measurement in the atmosphere and in the ground. Net radiation is relatively easily and accurately measured but the other terms of the energy balance still provide some severe difficulties. Measurement of the soil heat flux density is difficult because of the large spatial variation of specific heat, water content and thermal conductivity of the soil. Also destillation processes and other latent heat fluxes in the soil are very difficult to assess quantitatively. Furthermore, the complexities introduced by water transport through the roots of vegetation makes this approach to flux measurement unattractive, thus forcing us to look at the only other alternative: flux measurements in the atmosphere.

In the atmosphere we are dealing with a medium that is highly turbulent most of the time and which will produce large fluctuations of the value of quantities measured in it. The fluctuating output of instruments placed in the turbulent atmosphere introduces the necessity of determining an average of that output over a given space or time interval. After establishing this average, the instantaneous value of a quantity consists of its average value plus the fluctuating part. Estimation of the

2

flux densities of momentum and those of sensible and latent heat can then roughly be divided into two methods.

The first possibility is the measurement of profiles of the mean values of wind speed, temperature and humidity. Using the concept of molecular diffusion, where the flux density of a quantity and its gradient are connected by means of a molecular diffusion coefficient, an analogy can be drawn between molecular and turbulent diffusion. Defining a so-called eddy diffusivity we relate the turbulent flux density of a quantity with the gradient of its mean value. This enables the estimation of the turbulent flux density, once we have a good approximation of both the eddy diffusivity distribution and the gradient of the mean value.

The second possibility is the direct measurement of turbulent quantities. If the proper turbulent quantities are correlated with each other the turbulent flux can be determined directly (eddy correlation technique) or indirectly (dissipation techniques).

The advantage of the profile method over the correlation and dissipation methods is that averages are relatively easy to obtain, while it is much more difficult to measure the correlation of two fluctuating quantities. Its disadvantage is that an accurate distribution of the eddy diffusivity is not easy to establish, or must be assumed, while it still remains questionable if gradient diffusion is a correct mechanism in all possible situations that may occur in the atmospheric boundary layer (see Corrsin, 1974). Recent and current research reveals that turbulent transport is not a smooth continuous process. It is a process which consists of relatively large periods of time with hardly any transport interspersed with relatively short periods of time with vigorous mixing and very large transport. Going down to molecular time and length scales we find that molecular diffusion is no continuous process either. We remedy this by considering only time and length scales which are several orders of magnitude larger than the molecular scales, in this way ensuring the validity of the continuum hypothesis. Turbulent diffusion in the

atmosphere comprises time and length scales which are very much larger than the molecular ones. In fact they are large enough to make an analogy with molecular diffusion hazardous, especially when large spatial and/or time variations occur.

The direct measurement of correlations of turbulent quantities avoids the use and the problems of the eddy diffusivity concept. But a serious disadvantage of this method is that the fluctuation measurement sensors require a fast response. Because all frequencies occurring in the spectrum of turbulence contribute to the turbulent flux, sensors have to be fast enough to register even the highest of those frequencies. This poses a very high demand on sensor performance, especially when installed close to the surface. Finally, a difficulty connected with both methods is the problem of defining a proper length of time over which the average values should be determined.

All the above mentioned problems connected with the two methods have of course been studied extensively and considerable progress both in theoretical and technical respect has been made. But there are a few basic assumptions which form the corner-stone of both methods, and which also need careful consideration. These assumptions may all be condensed in the following crucial starting point of the theories underlying the two methods just described. We assume that the surface layer of the atmosphere is in equilibrium with the underlying surface. Equilibrium means that all the characteristic variables of the atmospheric surface layer will not change when the flow continues its course over the earth's surface.

Amongst other things, which will be disregarded for the moment, equilibrium implies that fluxes will be constant with height in the atmospheric surface layer and are equal to the fluxes at the surface. This means that instruments may be placed at any height in this layer, excluding the demands on sensor performance from our consideration for the time being. Equilibrium also implies that a relationship between the vertical distribution of the

4

average value of a quantity and its vertical flux density can be established, which means that the fluxes can be derived from measured profiles. Finally, equilibrium also implies that several terms in the equations for the second moments are small enough to be neglected, which implies that production and dissipation (or destruction) terms balance each other. This is a necessary condition for the application of the dissipation technique.

It is obvious from the definition of equilibrium given above that true equilibrium will never occur in practice because external conditions will change both in time and space. But in some cases a reasonable approximation of the state of equilibrium can be reached. This is possible if weather conditions do not change during the averaging period and if the measuring site is chosen in such a way to ensure a large upstream fetch of uniform terrain. It is not surprising therefore, that for the well-known experiments performed in Kansas (Izumi, 1971) and Minnesota (Izumi and Caughey, 1976) great care was taken in choosing the location for measurements in order to avoid advection effects created by a non-uniform upstream fetch as much as possible. These are the experiments, amongst others, that have provided the data from which numerous empirical flux-profile relations have been determined and from which many empirical constants have been established in the theory of atmospheric turbulence. This means that existing formulae for the determination of turbulent fluxes are, strictly speaking, only valid in equilibrium situations. A proper choice of the measuring period and of the averaging time will ensure almost constant weather conditions, but extensive homogeneous terrains are for most practical situations not easily available. So the question arises: how large are the errors introduced in the flux determination, using standard methods, by the non-uniformity of the upstream terrain, and is there a possibility to make corrections for the deviations generated by the inhomogeneities? These questions form the starting point of all that the present study encompasses.

1.2 METHODS

Any problem in physics can, generally speaking, be approached in
two distinctly different ways: theoretically and experimentally.
The first option is often beset with serious mathematical diffi-
culties. In the case of atmospheric physics and turbulence these
are very severe and drastic simplifications have to be made in
order to make the problem theoretically tractable. The question
then arises if enough of the essential processes and characteris-
tics of the system under consideration are preserved in order to
get sensible and non-trivial solutions. The second option is
beset with many practical difficulties such as the quality of
equipment, weather conditions, choice of location etc. Further-
more, it will lead to the setup of a measuring campaign which
generally is no mean feat, even when measuring only average
quantities, let alone turbulence quantities.

A separate branch of the theoretical treatment of problems in
science was developed with the introduction and large scale use
of fast digital computers and the application of numerical mathe-
matics in the fifties and early sixties. Modeling intricate phy-
sical processes and interactions using these computers belongs,
in principle, to the theoretical treatment option but is dis-
tinctly different from it in some respects. But on the other
hand it also has some characteristics which are typical features
of the experimental treatment option. It does not altogether be-
long to the theoretical analysis since the mathematical theory
for solving nonlinear partial differential equations is still in-
adequate and a complete solution of the Navier-Stokes equation
which describes the dynamics of turbulence, is a very long way off
indeed. The experimental character of the modeling option is gi-
ven by the fact that every run of the model on a computer looks
like the performance of a physical experiment. Thus modeling
forms a synthesis of the traditional two options and it soon
emerged as a powerful tool in solving problems in many fields in
science.

6

The advantages of this third option are obvious. No expensive measuring campaign is necessary, only a modern computer with its usual facilities is needed. With the theoretical analysis it shares the advantage of one being able to choose, within limits, parameters of, and variables in the atmospheric surface layer such as the Obukhov length, the wind direction, friction velocity, surface roughness length, temperature and humidity profiles. In contrast, for experiments performed in the atmosphere these quantities depend on large scale weather systems, terrain location, time of the season etc. Finally, the degree of simplification of the governing equations will often be less than the one necessary to obtain analytical solutions. Thus one is able to tackle a whole range of problems with numerical modeling techniques, which are far from being treated with analytical mathematical methods. But the third option still shares a number of disadvantages of the first option. It is e.g. not always trivial to see if all physical processes and interactions are properly described by the set of equations in use. Also, these equations have to be simplified in order to arrive at a numerically solvable set. It is difficult to assess how much information is lost by these simplifications. The system of equations also must form a closed set, i.e. the number of equations must equal the number of unknowns. This creates an enormous problem in atmospheric turbulence, generating a whole new field of science devoted to this subject.

There are also disadvantages typical for the third option which are almost absent in the other two options. E.g. the lesser the degree of simplification the larger the number of equations and, consequently the larger the number of closure assumptions. These assumptions each introduce a number of constants which have to be determined one way or another. Also, there will always be processes on scales smaller than the computational grid but which do interact with the larger features of the flow. These subgrid-scale processes have to be taken into account somehow, but more often than not they are simply neglected. Also, a numerical solution will never be able to provide the physical insight

7

into the problem as given by an analytical one, because it does not produce any functional relationship. This is the most important disadvantage.

The above considerations must be kept in mind when choosing a way to treat the aforementioned questions. But also factors like feasability must be taken into account. It was decided that the best strategy for this study was formed by the possibilities inherent to the third option.

Chapter 2 gives an analysis of the problem we are facing. It presents an outline of the basic laws of physics which are of interest here, as well as the simplifications which must be made. In Chapter 3 an account is given of the various models and methods which have been used in the past to study the effects created by a change in surface conditions, concentrating mainly on a change in surface roughness. In Chapter 4 a critical examination is made of the numerical model employed in the present study. It contains a summary of all the restrictions and drawbacks inherent to the use of this specific model. In Chapter 5 the standard flux profile methods are compared with flux profile relations derived from the modeled second moment equations for homogeneous situations. Chapter 6 treats the errors introduced by terrain inhomogeneities in the profile methods of flux determination. Chapter 7, finally, contains the conclusions of the present study. In it recommendations are given for further study and possible treatment of the problem with an experiment which, as usual, will have to give an answer to the question if all that is stated in this study has any truth in it.

2 Analysis of the problem

2.1 GENERAL FEATURES AND RELEVANCE FOR FLUX DETERMINATION TECHNIQUES

The thin layer of air (0.1 - 0.3% of the radius of the earth)
that envelops the surface of our planet is called the atmosphere.
It is kept in motion primarily by the differences in local hea-
ting of the earth's surface by the sun. At or near the interface
of the atmosphere and the surface of the earth a continuous in-
teraction takes place. This interaction ranges from the large
scales (oceans, continents, mountain ranges) to the very small
scales (pebbles, leaves of grass, grains of sand), in fact down
to the molecular scale. As a consequence, the atmospheric motions
comprise a large spectrum of length and time scales (Figure 2.1).
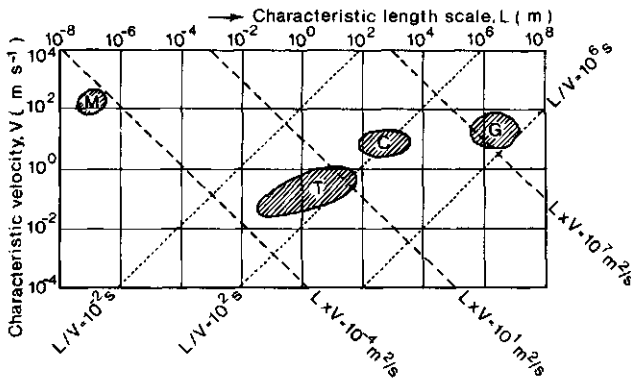

Figure 2.1   Classification of length and time scales of
             atmospheric motions

The lowest layer of the atmosphere is affected directly by the
nature and properties of the surface itself. In this part of the
atmosphere which is called the atmospheric boundary layer (ABL)
turbulence plays an important role.

In the upper part of the ABL the Coriolis force contributes substantially to the dynamics of it. The lowest part of the ABL is called the atmosphere surface layer (ASL) (Figure 2.2). Within this layer the turbulent fluxes do not change significantly with height if the surface of the earth is horizontally homogeneous.
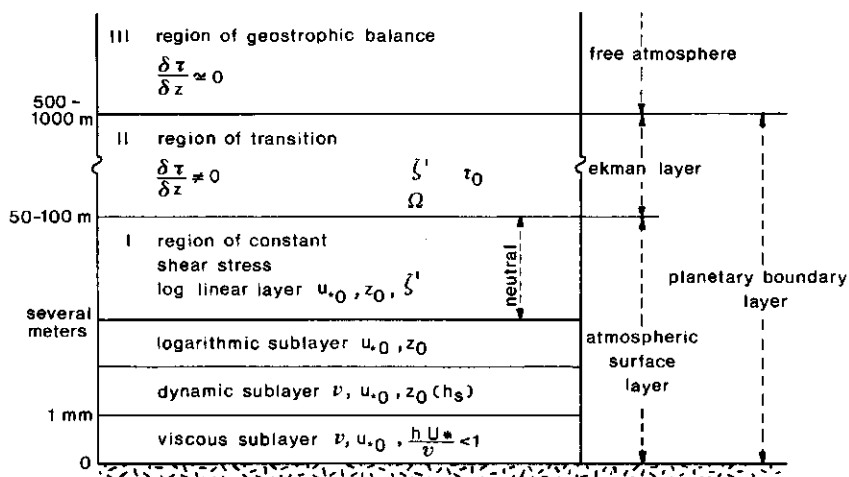

Figure 2.2   Vertical structure of the atmospheric boundary
            layer (after: Huang and Nickerson, 1972)

Within the ASL also the influence of the Coriolis force is negligible. For that reason the direction of the wind remains approximately constant with height. This means that our analysis of the surface layer is a two-dimensional one. We align the horizontal axis of the coordinate system along the direction of the mean wind vector.

In its course over the surface of the earth the ASL interacts, as was mentioned above, with the underlying surface of the earth. This interaction process is maintained by means of the turbulent fluxes of momentum, heat, water vapour and other, usually negligible, constituents of the atmosphere. If the surface is homo-

10

geneous over a sufficiently large distance and if external
weather conditions (e.g. the overall pressure gradient, the sta-
tic stability etc.) are constant, a state of equilibrium in the
ASL will be reached. Disregarding other possibilities, the state
of equilibrium of the ASL will be defined here as that situation
where mean turbulent fluxes are constant with height, or very
nearly so, and the profiles of mean quantities such as tempera-
ture do not change downstream (see also section 1.1).

If an air mass in such an equilibrium encounters a stepwise
change in surface conditions it will have to adjust to these new
conditions. Eventually, under the same restrictions as mentioned
before, the surface layer will reach a new state of equilibrium,
determined by the new surface conditions. This problem belongs to
a class of problems in turbulent shear flow theory, viz. that of
relaxing flows. We state that a relaxing flow is one in which a
turbulent shear flow changes from one state of equilibrium to an-
other state of equilibrium by virtue of changes in external con-
ditions. These changes in external conditions are represented by
changes in boundary conditions of the theoretical models that
describe the physics of the atmosphere subjected to these discon-
tinuities. The change may be limited to a single quantity such as
surface temperature (e.g. Johnson,1955; Vugts and Businger,1977),
surface humidity (Weisman,1975; McNaughton,1976), surface heat
flux (Antonia et al.,1977), surface roughness (Elliott,1958; etc.)
or surface topography (de Bray,1973; Bowen and Lindley,1977;
Dawkins and Davies,1981). But, usually two or more of these quan-
tities will change simultaneously (Rider et al.,1963; Dyer and
Crawford 1965; Tieleman and Derrington,1977).

The ASL which is subjected to a stepwise change in surface condi-
tions will be transformed. As was pointed out in the previous
chapter, this transformation need not be a smooth continuous pro-
cess. In fact, experiments show that turbulent transport for the
greater part results from the action of turbulent structures.
These turbulent structures represent elongated, spatially cohe-
rent, organized flow motions (Schols, 1984). Keeping this in
mind we merely hope that with the practice of using averages
the effects of the individual turbulent structures will be

11

smoothed by the averaging procedure. On the average, the surface
layer will start to adjust to the new surface conditions in
its lowest layers close to the ground. Through turbulent trans-
port the change in surface conditions will affect layers of in-
creasing height as the air travels downstream. Thus at a given
horizontal distance (x) downstream of the discontinuity this in-
fluence will change the atmospheric surface layer up to a certain
height $(d(x))$. This height increases with x. Above this height no
change will be noticeable. The region of the atmospheric surface
layer between $z = 0$ and $z = d(x)$ is called the Internal Boundary
Layer (IBL) (Figure 2.3). Below $z = d(x)$ the profile of every
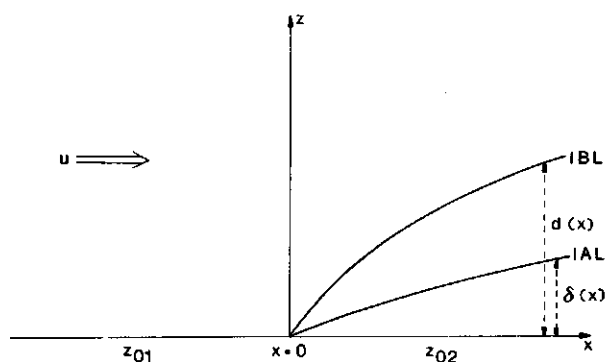

Figure 2.3 Definition sketch of a change in surface conditions

variable will deviate from its original equilibrium distribution.
Above $z = d(x)$ every profile remains unchanged. Of course, the
definition of these layers is not rigorous for it results from
the use of statistical methods. There are large eddies and turbu-
lent structures in the ASL which momentarily are able to transport
parcels of air already affected by the new surface to heights far
greater than d.

As the air travels further along, the lowest part of the IBL will
become locally adapted to the new surface. This means that up to
a certain height $z = \delta(x) < d(x)$ fluxes will be constant with
height though they are still changing with downstream distance.
Thus no new equilibrium has yet been reached, but the local flux-
12

es in the lowest part of the IBL are constant up to $z = \delta(x)$. We will call the region the Internal Adapted Layer (IAL) (Figure 2.3).

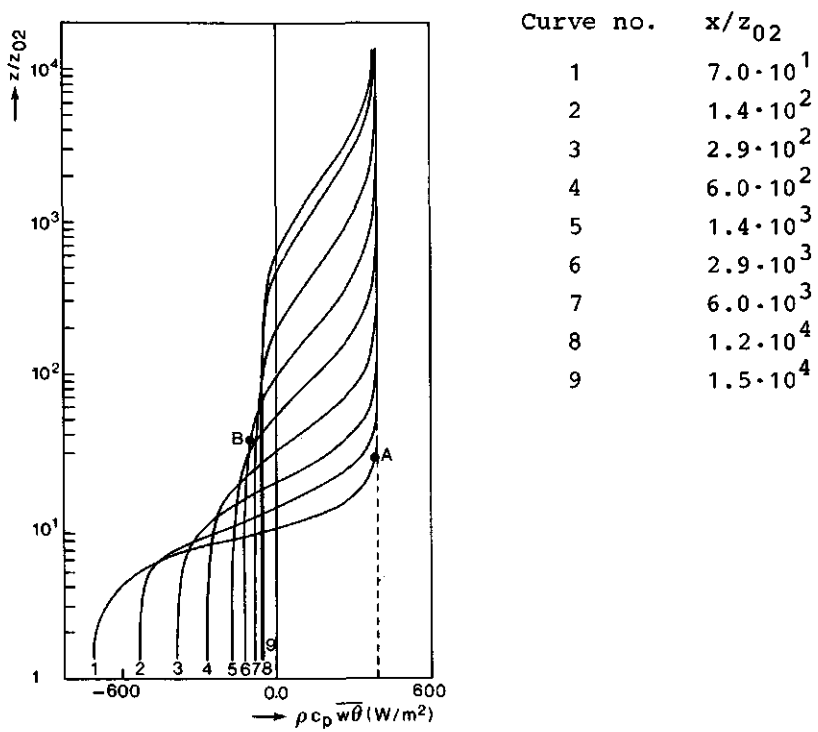| Curve no.	x/z_{02}
1	$7.0 \cdot 10^1$
2	$1.4 \cdot 10^2$
3	$2.9 \cdot 10^2$
4	$6.0 \cdot 10^2$
5	$1.4 \cdot 10^3$
6	$2.9 \cdot 10^3$
7	$6.0 \cdot 10^3$
8	$1.2 \cdot 10^4$
9	$1.5 \cdot 10^4$

Figure 2.4   Profiles of the vertical heat flux
             after a change in surface conditions

Figure 2.4 serves to illustrate the above. It presents the stream-
wise variation of the turbulent heat flux profile $\rho c_p \overline{w\theta}(x,z)$ af-
ter a change from a hot, dry, smooth surface to a cool, wet, rough
surface as calculated with the model of Rao et al.(1974b).Starting
from a surface layer which is completely in equilibrium with the
underlying terrain, we see that in that case (indicated by the
dashed line) the vertical turbulent heat flux is constant with
height. The value of $\rho c_p \overline{w\theta}$ is positive, denoting an upward heat
flux. The other curves represent the heat flux profile for va-
rious distances downstream. Just after the step change the tem-
perature of the surface drops, generating a downward, negative

heat flux. Only the lowest region of the surface layer is affec-
ted up to e.g. point A of curve 1. This point A corresponds to
the local height of the IBL. Gradually a region develops where
$\rho c_p \overline{w\theta}$ is constant with height (e.g. up to point B of curve 6)
though $\rho c_p \overline{w\theta}$ still depends on the horizontal distance (x).
Point B corresponds to the local height of the IAL.

Figure 2.4 clearly shows that the magnitude of the vertical heat
flux critically depends on the location. Thus the determination
of flux densities above a non-homogeneous terrain is beset with
many difficulties and uncertainties. Depending on the method one
uses to determine those flux densities, this may lead to consi-
derable errors. In practice, one is usually interested in the
flux density from a given stretch of nearly homogeneous field ir-
respective of the characteristics of the surrounding terrains. As
the horizontal dimensions of the field of interest are always
finite, problems often arise concerning the use of flux determi-
nation formulae, interpretation of the results of measurements,
sensor location etc.

2.2 GOAL OF THE PRESENT STUDY

In this study it is our intention to analyse the effects created
by one, or more, changes in surface conditions on the structure
of the atmospheric surface layer in order to:
1. estimate the error introduced in the standard flux determina-
   tion techniques when they are applied in these conditions, and
2. provide simple techniques for estimating these errors using
   a minimum number of data concerning sensor location, surroun-
   ding terrain(s) etc.

To achieve these goals we use the data provided by the model des-
cribed in Chapter 4, as if they were actually determined by expe-
riment. We implicitly assume that the model represents the actual
situation fairly well. Using the data from the model we are able
to perform the above mentioned analyses and draw our conclusions
on the performance of the standard flux determination techniques
in non-homogeneous situations.

2.3 GOVERNING EQUATIONS

Whatever happens to the air above the changing surface conditions, it will always have to obey the conservation equations of mass, momentum and specific entropy. These equations have been derived many times (e.g. Hinze, 1959; Lumley and Panofsky, 1964; Monin and Yaglom, 1971; Tennekes and Lumley, 1972), hence we confine ourselves to the main lines. For details we refer to the textbooks mentioned. Notice will be taken, however, of the approximations and assumptions involved in this derivation.

We start with the conservation equations for an ideal, viscous, compressible, Newtonian fluid in a uniform gravitational field and in a rotating system

$$\rho\left(\frac{\partial u_i}{\partial t} + u_j\frac{\partial u_i}{\partial x_j}\right) = -\frac{\partial P}{\partial x_i} - \rho g_i + \frac{\partial}{\partial x_j}\left[\mu\left(\frac{\partial u_i}{\partial x_j} + \frac{\partial u_j}{\partial x_i}\right) + \right.$$

$$\left. -\frac{2}{3}\mu\frac{\partial u_k}{\partial x_k}\delta_{ij}\right] - 2\Omega_j\varepsilon_{ijk}u_k\rho, \tag{2.1}$$

$$\frac{\partial\rho}{\partial t} + \rho\frac{\partial u_i}{\partial x_i} + u_i\frac{\partial\rho}{\partial x_i} = 0, \tag{2.2}$$

$$\rho T\left(\frac{\partial S}{\partial t} + u_j\frac{\partial S}{\partial x_j}\right) = \frac{\partial u_i}{\partial x_j}\left[\mu\left(\frac{\partial u_i}{\partial x_j} + \frac{\partial u_j}{\partial x_i}\right) - \frac{2}{3}\mu\frac{\partial u_k}{\partial x_k}\delta_{ij}\right] + \frac{\partial}{\partial x_j}\left(k\frac{\partial T}{\partial x_j}\right), \tag{2.3}$$

$$P = \rho R_d T. \tag{2.4}$$

These equations represent the conservation equations of momentum, mass and specific entropy, respectively and the equation of state. S is specific entropy, ρ density, T temperature, u_i velocity, μ viscosity, k thermal conductivity, δ_{ij} is Kronecker's delta and ε_{ijk} is the alternating tensor (Levi Civita). In addition Einstein's summation convention is used. We assume that the gradients of P, ρ and T are small enough to ensure that μ and k are approximately constant throughout the fluid. We define a refer-

ence state of the atmosphere, denoted by the subscript "r" such that the instantaneous value m of the variable $m(m = \rho, T, P$ or $u_i)$ is decomposed in

$$\underset{\sim}{\rho} = \rho_r + \tilde{\rho} \quad , \quad \underset{\sim}{P} = P_r + \tilde{P} \quad , \quad \underset{\sim}{T} = T_r + \tilde{T}, \quad \underset{\sim}{u_i} = u_{i,r} + \tilde{u}_i \quad , \qquad (2.5)$$

where $\tilde{m}$ is a perturbation of this reference state.

Following e.g. Dutton and Fichtl (1969) the equation of state is expanded around this reference state, this yields

$$\frac{\rho - \rho_r}{\rho_r} = \frac{P - P_r}{P_r} - \frac{T - T_r}{T_r} \quad \text{or} \quad \frac{\tilde{\rho}}{\rho_r} = \frac{\tilde{P}}{P_r} - \frac{\tilde{T}}{T_r} \quad , \qquad (2.6)$$

where higher order derivatives are ignored. This is only permissible if the deviations $\tilde{\rho}$, $\tilde{T}$ and $\tilde{P}$ are small in comparison with their respective reference state value,

hence $|\frac{\tilde{\rho}}{\rho_r}| \ll 1 \quad , \quad |\frac{\tilde{P}}{P_r}| \ll 1$ and $|\frac{\tilde{T}}{T_r}| \ll 1.$

If for the reference state, we assume that the effects of radiation, viscosity and heat conduction are not important and that the fluid is in steady motion, hence e.g. $u_{i,r} = U_r(z)$, the equations of motion (2.1) imply that

$$\frac{\partial P_r}{\partial x} + \frac{\partial P_r}{\partial y} = 0 \quad \text{and} \quad \frac{\partial P_r}{\partial z} = -\rho_r g \qquad (2.7)$$

which, after some manipulation gives

$$\frac{\partial T_r}{\partial x} + \frac{\partial T_r}{\partial y} = 0. \qquad (2.8)$$

This means that the vertical variation of $U_r(z)$, $\rho_r(z)$ and $T_r(z)$ is still free to choose.

In the reference state the atmosphere is supposed to have an

16

adiabatic temperature profile

$$\frac{\partial T_r}{\partial z} = -\frac{g}{c_{pd}} = -\Gamma_d \ . \tag{2.9}$$

Now, Eqs. (2.7) and (2.9) together with the equation of state

$$P_r = R_d T_r \rho_r \ , \tag{2.10}$$

completely determine the vertical distribution of P_r, T_r and ρ_r.

The continuity equation (2.2) may be expanded in the form

$$\frac{\partial \tilde{\rho}}{\partial t} + (\tilde{u}\frac{\partial \tilde{\rho}}{\partial x} + \tilde{v}\frac{\partial \tilde{\rho}}{\partial y}) + \tilde{w}\frac{\partial \tilde{\rho}}{\partial z} + \tilde{w}\frac{\partial \rho_r}{\partial z} = -\frac{1}{\rho_r}(\frac{\partial \tilde{u}}{\partial x} + \frac{\partial \tilde{v}}{\partial y}) - \frac{1}{\rho_r}\frac{\partial \tilde{w}}{\partial z} \ , \tag{2.11}$$

where $|\tilde{\rho}/\rho_r| \ll 1$ has been used on the right hand side. Replacing all variables by a Fourier representation and estimating the orders of magnitude of all variables and their derivatives Dutton and Fichtl (1969) were able to show that in Eq. (2.11) only the terms on the right hand side remain, hence

$$\frac{\partial \tilde{u}_i}{\partial x_i} = 0 \ , \tag{2.12}$$

if the following conditions are met

(i) $\omega^2 \ll g/\ell_w$,
(ii) $|\hat{v}_H/\hat{w}| \leq \ell_H/2\pi\ell_w$,
(iii) $\ell_w \ll H_\alpha$,
(iv) $\ell_w \sim \ell_\alpha$. $\tag{2.13}$

Here ω is the frequency in the time dependent part of the Fourier representation ℓ_w, ℓ_H and ℓ_α are length scales for the vertical and horizontal motion and the vertical variation of specific volume ($\alpha = \rho^{-1}$) respectively. H_α is a scale height defined by

17

$H_\alpha^{-1} = \frac{1}{\alpha_r} \frac{\partial \alpha_r}{\partial z}$. Because (2.13) restricts the permissible vertical scales to heights much smaller than H_α this case is known as "shallow convection". For shallow convection, this approximation allows the fluid to be treated as incompressible.

Moreover, using condition (iii) of Eq. (2.13), it is possible to show that the pressure perturbation term in Eq. (2.6) can be ignored in the case of shallow convection, hence this equation reduces to

$$\frac{\tilde{\rho}}{\rho_r} = - \frac{\tilde{T}}{T_r} \ . \tag{2.14}$$

Next we turn to the equations of motion (2.1). We divide (2.1) by ρ and substitute the perturbation forms (2.5). The nonviscous vertical component terms on the right hand side of (2.1) then read

$$- \frac{1}{\rho} \frac{\partial P}{\partial z} - g = - \frac{1}{\rho_r} \frac{\partial \tilde{P}}{\partial z} - \frac{\tilde{\rho}}{\rho_r} g \ ,$$

where $\left| \frac{\tilde{\rho}}{\rho_r} \right| \ll 1$ has been used, except in the gravitation term, where it cannot be ignored (Boussinesq approximation). The kinematic viscosity is defined by $\nu = \nu_r = \mu / \rho_r$. If we furthermore use (2.12) and (2.15) the equations of motion become

$$\frac{\partial \tilde{u}_i}{\partial t} + \tilde{u}_j \frac{\partial \tilde{u}_i}{\partial x_j} = - \frac{1}{\rho_r} \frac{\partial \tilde{P}}{\partial x_i} + \frac{\tilde{T}}{T_r} g_i + \nu \frac{\partial^2 \tilde{u}_i}{\partial x_j \partial x_j} - 2\Omega_j \, \varepsilon_{ijk} \, \tilde{u}_k \ . \tag{2.15}$$

The entropy equation (2.3) can be transformed in an equation in terms of the temperature (see Appendix 1):

$$\frac{\partial \tilde{T}}{\partial t} + \tilde{u}_j \frac{\partial \tilde{T}}{\partial x_j} = \kappa_H \frac{\partial^2 \tilde{T}}{\partial x_j \partial x_j} \ , \tag{2.16}$$

where $\kappa_H = k / \rho_r c_p$ is the thermal diffusivity.

As the latent heat flux will also play an important role in the

18

present study we must supplement the above equations with one representing the variation of specific humidity. To a good approximation, water vapour can be considered as a passive contaminant. We find, analogous to (2.16)

$$\frac{\partial \tilde{q}}{\partial t} + \tilde{u}_j \frac{\partial \tilde{q}}{\partial x_j} = \kappa_v \frac{\partial^2 \tilde{q}}{\partial x_j \partial x_j} \quad , \tag{2.17}$$

where $\tilde{q}$ is the specific humidity and κ_v is the diffusivity of water vapour. To account for the effect of the variable water vapour contents of the atmosphere on the density, we introduce the virtual temperature T_v which is defined by

$$T_v = \{1 + q(\frac{1}{\epsilon^*} - 1)\} T \sim (1 + 0.608q)T. \tag{2.18}$$

This correction for moisture is of importance only in the buoyancy term in the equations of motion. In the reference state of the atmosphere we assume that no water vapour is present hence

$$\underset{\sim}{T}_v = T_{vr} + \tilde{T}_v = T_r + \tilde{T}_v. \tag{2.19}$$

Finally, we introduce the potential temperature which will be used from now on instead of the real temperature

$$\underset{\sim}{\theta} = \underset{\sim}{T}(P_o/\underset{\sim}{P})^\kappa \quad , \tag{2.20}$$

where P_o usually is taken equal to $1,0 \cdot 10^5$ Pa and $\kappa = R_d (1 - 0.23 q)/c_{pd}$ which may be simplified to $\kappa = R_d/c_{pd}$. We split $\underset{\sim}{\theta}$ into

$$\underset{\sim}{\theta} = \theta_r + \tilde{\theta} \quad , \tag{2.21}$$

where, according to (2.9) $\partial\theta_r/\partial z = 0$. In the atmospheric surface layer we may assume to a good approximation (within 1% at sea level) $\underset{\sim}{\theta} \cong \underset{\sim}{T}$ and $\tilde{\theta} \cong \tilde{T}$.

19

The set of equations now consists of Eqs. (2.12), (2.17) and

$$\frac{\partial \tilde{u}_i}{\partial t} + \tilde{u}_j \frac{\partial \tilde{u}_i}{\partial x_j} = - \frac{1}{\rho_r} \frac{\partial \tilde{P}}{\partial x_i} + \frac{\tilde{\Theta}_v}{T_r} g_i + \nu \frac{\partial^2 \tilde{u}_i}{\partial x_j \partial x_j} - 2\Omega_j \epsilon_{ijk} \tilde{u}_k \quad , \qquad (2.22)$$

$$\frac{\partial \tilde{\Theta}}{\partial t} + \tilde{u}_j \frac{\partial \tilde{\Theta}}{\partial x_j} = \kappa_H \frac{\partial^2 \tilde{\Theta}}{\partial x_j \partial x_j} \quad . \qquad (2.23)$$

Next we assume that the air motions can be separated into a slow-ly varying mean flow and a rapidly varying turbulent component. Furthermore we assume that the flow is ergodic, which means that ensemble averages may be replaced by time averages. Thus we arrive at Reynolds' convention,

$$\tilde{u}_i = U_i + u_i \quad , \quad \tilde{\Theta} = \Theta + \theta \quad , \quad \tilde{P} = P + p \quad , \quad \tilde{q} = Q + q \quad , \qquad (2.24a)$$

where $\overline{u}_i = 0$, $\overline{p} = 0$ etc., $\overline{\tilde{u}_i \tilde{\Theta}} = \Theta U_i + \overline{\theta u_i}$ etc. and

$$\overline{\Theta \tilde{u}_i} = \Theta U_i \text{ etc.} \qquad (2.24b)$$

Applying (2.24a) and (2.24b) to Eqs. (2.12), (2.17), (2.22) and (2.23) and averaging these equations (see Appendix 1) the equations for the mean flow read

$$\frac{\partial U_i}{\partial x_i} = 0 \quad , \qquad (2.25)$$

$$U_j \frac{\partial U_i}{\partial x_j} = - \frac{1}{\rho_r} \frac{\partial P}{\partial x_i} + g_i \frac{\Theta_v}{T_r} - 2\Omega_j \epsilon_{ijk} U_k + \nu \frac{\partial^2 U_i}{\partial x_k \partial x_k} +$$

$$- \frac{\partial}{\partial x_j} (\overline{u_i u_j}) \quad , \qquad (2.26)$$

$$U_j \frac{\partial \Theta}{\partial x_j} = \kappa_H \frac{\partial^2 \Theta}{\partial x_k \partial x_k} - \frac{\partial}{\partial x_j} (\overline{u_j \theta}) \quad , \qquad (2.27)$$

20

$$U_j \frac{\partial Q}{\partial x_j} = \kappa_v \frac{\partial^2 Q}{\partial x_k \partial x_k} - \frac{\partial}{\partial x_j} (\overline{u_j q}). \qquad (2.28)$$

As long as the viscous sublayer that coates the surface is excluded from our considerations, the molecular diffusion terms in (2.26)-(2.28) can be neglected. We furthermore consider the situation where a fully turbulent steady air flow is at right angles to the surface discontinuity. This means that a restriction is made to a two-dimensional case. These simplifications of Eqs. (2.25)-(2.28) result in the following set of equations,

$$\frac{\partial U}{\partial x} + \frac{\partial W}{\partial z} = 0 , \qquad (2.29)$$

$$U\frac{\partial U}{\partial x} + W\frac{\partial U}{\partial z} = - \frac{1}{\rho_r} \frac{\partial P}{\partial x} - \left[\frac{\partial}{\partial x} \overline{u^2} + \frac{\partial}{\partial z} \overline{uw} \right] , \qquad (2.30)$$

$$U\frac{\partial W}{\partial x} + W\frac{\partial W}{\partial z} = - \frac{1}{\rho_r} \frac{\partial P}{\partial z} - \frac{\Theta_v}{T_r}g - \left[\frac{\partial}{\partial x} \overline{uw} + \frac{\partial}{\partial z} \overline{w^2} \right] , \qquad (2.31)$$

$$U\frac{\partial \Theta}{\partial x} + W\frac{\partial \Theta}{\partial z} = - \left[\frac{\partial}{\partial x} \overline{u\theta} + \frac{\partial}{\partial z} \overline{u\theta} \right] , \qquad (2.32)$$

$$U\frac{\partial Q}{\partial x} + W\frac{\partial Q}{\partial t} = - \left[\frac{\partial}{\partial x} \overline{uq} + \frac{\partial}{\partial z} \overline{wq} \right] , \qquad (2.33)$$

where the terms containing the effect of the Coriolis force have been neglected.

Careful consideration of the terms on the right hand side of (2.30)-(2.33) (Yeh and Brutsaert, 1970; Plate, 1971; Peterson, 1972) led to the conclusion that the first term between the brackets, as well as the pressure term in (2.30), are negligible in comparison with the second term between the brackets, at least for fetches larger than, say, 1 m. This implies that Eq. (2.31) can be omitted, while Eqs. (2.30) (2.32) and (2.33) reduce to

$$U\frac{\partial U}{\partial x} + W\frac{\partial U}{\partial z} = -\frac{\partial}{\partial z}\,\overline{uw}\quad,\tag{2.34}$$

$$U\frac{\partial \Theta}{\partial x} + W\frac{\partial \Theta}{\partial z} = -\frac{\partial}{\partial z}\,\overline{w\theta}\quad,\tag{2.35}$$

$$U\frac{\partial Q}{\partial x} + W\frac{\partial Q}{\partial z} = -\frac{\partial}{\partial z}\,\overline{wq}.\tag{2.36}$$

The four equations (2.29) and (2.34)-(2.36) contain seven unknowns: U, W, Θ, Q, $\overline{uw}$, $\overline{w\theta}$ and $\overline{wq}$, hence they do not form a closed system and cannot be solved. This is the well-known closure problem. This problem can only be tackled if a closed system of equations is obtained. Two possibilities now arise:

(i) decrease the number of unknowns by expressing the quantities on the right hand side of Eqs. (2.34)-(2.36) as a combination of the other dependent variables on the left hand side. This is called first order modeling.

(ii) increase the number of equations by introducing conservation equations for the quantities on the right hand side of Eqs. (2.34)-(2.36). This is called second order modeling.

If the first possibility is used a relatively simple model will emerge which can often be treated analytically. If we use the second possibility the problems turn out to be aggravated. By devising additional equations for the variables on the right hand side new unknowns appear which make the difference between the number of equations and the number of unknowns even larger. So in this case one is again forced to use the first option: reducing the amount of unknowns. The modeling of the unknowns in the second moment equations often cannot be done rigorously on sound physical grounds, and in that case it must be constructed rather artificially.

In the next Chapter models will be encountered which have been constructed using either one of the two mentioned closure techniques. There, the benefits and drawbacks of both types of models will be analysed.

22

3 Models for the description of the internal boundary layer

3.1 INTRODUCTION

In this Chapter a review will be given of existing models con-
cerned with turbulent shear flows adjusting to suddenly altered
lower boundary conditions. In this review of theoretical models
we will focus our attention primarily on models dealing with a
change in surface roughness.

Ever since 1958 (Elliott) and 1952 (Gandin) (for the English,
respectively Russian literature) a lot of work has been dedica-
ted to the problem under consideration. A tremendous number of
articles concerning models of ever increasing sophistication has
appeared. In some of these articles the growth rate of the IBL
is predicted, while in others a more detailed description of the
flow within this region is given. The results of the first group
of articles can be applied directly to estimate the constraints
posed upon the maximum height at which instruments may be loca-
ted when measuring e.g. profile derived fluxes. The second group
of papers allows the prediction of the velocity-and shear stress
profiles within the IBL as well as the variation of the surface
shear stress downstream of the discontinuity. Not until the more
advanced second order models appeared in the late sixties was it
possible to give a more complete description in terms of the be-
haviour of other turbulent quantities which were neglected or
parameterized in the older models.

Apart from some early methods in which the roughness change pro-
blem is treated as a diffusion problem (Philip, 1959; Dyer, 1963)
the bulk of theoretical models will be divided into three classes
of increasing order of complexity:
1. First order closure (i)   Integral models
                        (ii)   Models based on self preservation
                        (iii) Numerical models
2. "One and a half" order closure (also called $k - \varepsilon$ or turbulent

kinetic energy (TKE) models)

3. Second order closure.

In the following we will discuss these types of models.

3.2 INTEGRAL MODELS

3.2.1 Description

One of the first attempts to treat the effect of a step change in roughness length theoretically was carried out by Elliott (1958).

Elliott postulated that there is a region in which the changes of the flow occur and he called this the internal boundary layer (IBL). Within the IBL he assumed that the shear stress is independent of the height (z), while the surface shear stress is a function of the downstream distance (x). All other models in this class make the same assumptions but only differ in the assumed form of the shear stress profile within the IBL (Panofsky and Townsend 1964, Taylor 1969).

To close the set of equations formed by (2.29) and (2.34), Elliott used the relationship between the turbulent flux of momentum $\overline{uw}$ and the gradient of the mean wind U, which is valid in horizontally homogeneous situations, assuming that it also holds in advective situations:

$$- \overline{uw} = \ell^2 \left(\frac{\partial U}{\partial z} \right)^2 , \tag{3.1}$$

or

$$\tau = - \rho \, \overline{uw} = \rho \, K_m \frac{\partial U}{\partial z} , \tag{3.2}$$

which means that

$$K_m = \ell^2 \left| \frac{\partial U}{\partial z} \right| , \tag{3.3}$$

where ℓ is the mixing length, usually taken as

$$\ell = kz . \tag{3.4}$$

24

The equations (2.29), (2.34), (3.1) and (3.4) form a closed sys-
tem which can be solved. In accordance with the von Kármán-Pohl-
hausen technique the equations are integrated over the height of
the IBL resulting in an equation relating U, d and u_{*2}. By inser-
ting a prescribed velocity profile in that equation and combining
it with the necessary condition of velocity continuity at
$z = d(x)$, Elliott obtained a differential equation which can be
solved to give $d(x)$. After this quantity has been established it
is possible to obtain $u_{*2}(x)$, $U(x,z)$ and $\overline{uw}(x,z)$ respectively by
the scheme outlined in Appendix 2.

After Elliott's publication a number of authors have sought to
improve his model. Panofsky and Townsend (1964) removed the dis-
continuity in shear stress in Elliott's model by assuming a
linear variation of the shear stress with height within the IBL,
instead of a constant stress. A few years later Taylor (1969)
constructed a model in which even the shear stress gradient was
continuous at the interface at $z = d$. For a comparison of these
shear stress profiles the reader is referred to Taylor (1969).
Both theories are refinements of the model of Elliott and their
results consequently do not considerably differ from the original
model. A somewhat deviating approach was presented by Plate and
Hidy (1967) who integrated the momentum equation between $x = 0$
and a given value of x, while they also incorporated a streamline
displacement in their model. The advantage of this model, as poin-
ted out by Plate (1971), is the possibility of incorporating pres-
sure gradients and a gradual change in roughness downstream of
$x = 0$. Plate and Hidy developed this model to predict the beha-
viour of a wind blowing from a smooth solid surface to a water
surface with small waves of increasing waveheight.

3.2.2 Results

Because in the models of Elliott, Panofsky and Townsend and
Taylor the shear stress- and velocity profiles are prescribed,
their main merit lies in the prediction of the growth rate of
the IBL height $d(x)$. Elliott approximated this rate by

25

$$d(x) = a \cdot z_{02} \left(\frac{x}{z_{01}}\right)^{0.8}, \text{ where } a = 0.75 - 0.03 \ln\left(\frac{z_{02}}{z_{01}}\right) \quad (3.5a,b)$$

The $d \sim x^{0.8}$ growth rate appears to be a very good estimate. Panofsky and Townsend (P&T) used a somewhat different definition of d resulting in d-values that are larger than those predicted by (3.5), but the growth rate is essentially the same.

Note that in this type of model also the variation of the surface shear stress for x>0 can be computed. By equating the horizontal velocity at z=d, an equation is obtained that gives u_{*2} as a function of x, z_{02} and m, where

$$m = z_{01}/z_{02} \quad \text{and} \quad M = \ln(m) \quad (3.6a,b)$$

This is not mentioned by the authors themselves.

For both the Elliott and the Panofsky and Townsend models these curves are given in Figure 3.1 for rough-to-smooth(RS) as well as smooth-to-rough (SR) changes. A typical feature of these curves is the over(under)-shoot followed by a gradual return to a new equilibrium value. This behaviour of the surface shear stress was confirmed by experiments (e.g. Bradley, 1968).

3.2.3 Discussion

The main shortcoming of integral models is the a priori assumption of the profiles of velocity and shear stress within the IBL, which pose a severe restriction to the possible types of flow for x > 0. Just downstream of x = 0 the flow is developing towards a new equilibrium, hence it is very doubtful that an equilibrium logarithmic profile will exist there.

Furthermore the concept of the mixing length is assumed, where only depends on local, averaged quantities. This assumption ignores all history of the turbulent flow upstream, which is not realistic.
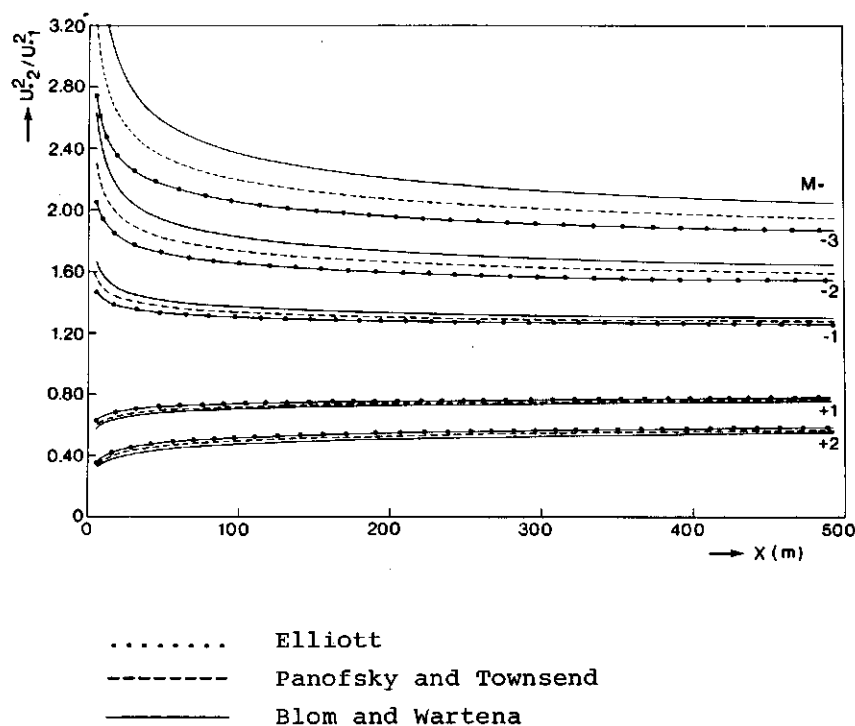
26

Figure 3.1 Variation of surface shear stress with downstream
            distance for various models

As was mentioned by Antonia and Luxton (1972) and also by Plate
and Hidy (1967) the integral models require a limited depth of
the disturbed boundary layer compared with the whole of the PBL.
This means that integral models are only applicable within a
limited distance downstream of x = 0.

Finally, Peterson (1969) states that the prescribed form of the
shear stress profile is only true if the nondimensional windshear

27

$\phi_m = \dfrac{kz}{u_*} \dfrac{\partial U}{\partial z}$ equals unity in the transition region in nonequilibrium flow conditions, which is often not the case. The prescription of this profile is in fact a fourth equation which creates a model where the number of equations exceeds the number of unknowns. It should be possible to calculate shear stress distributions by solving the horizontal equation of motion, given the velocity profile and the equation of continuity. But, as Taylor (1969) noticed, the variation of the wind profile downstream and the behaviour of the surface shear stress might be obtained without the use of the mixing length hypothesis. The vertical distribution of shear stress, however, can not be obtained without this hypothesis.

3.3 MODELS BASED ON SELF PRESERVATION OF PROFILES

3.3.1 Description

The first and most important attempt to treat the problem of a step change in roughness based on arguments of self preservation was undertaken by Townsend (1965a,b; 1966).

Assuming the profile of a given quantity to be "self preserving" is equivalent to saying that the functional form for the vertical distribution of this quantity is invariant with fetch and that the scale is a function of fetch only.

Townsend assumed that upstream of the step the velocity is given by the usual logarithmic profile, i.e. $\dfrac{kz}{u_*} \dfrac{\partial U}{\partial z} = 1$, while downstream of x = 0 he distinguished three regions:
region I   : only vertical displacement of streamlines
region II   : transition layer
region III   : velocity and shear stress locally adapted to the new roughness.
The velocity within the IBL (region II and III) consists of three parts:
1/ the original velocity profile for x < 0
2/ a contribution due to flow acceleration

28

3/ the velocity change due to the vertical displacement of the
   streamlines.

Using the condition of incompressibility, Townsend showed that
the change in velocity due to the streamline displacement is
smaller than the change due to the acceleration of the flow, so
part 3/ was neglected within the IBL. For a change of roughness
Townsend assumed self preservation of the shear stress and of the
acceleration term of the velocity change:

$$V(z) = \frac{u_o}{k} f(\frac{z}{\ell_o}) \tag{3.7}$$

$$\tau_2(z) = u_*^2 + (u_{*2}^2 - u_{*1}^2) F(\frac{z}{\ell_o}) \tag{3.8}$$

where V is the contribution part 2/.

$\ell_o(x)$ is a length scale denoting the thickness of the
           accelerated region

$u_o(x)$ is the scale of the change in mean velocity

f,F   are universal functions, independent of x because of
       the assumed self preservation.

Substituting these expressions in the equation of motion (2.34)
gives a relation between f and F:

$$- \eta(\frac{df}{d\eta}) = \frac{dF}{d\eta} \tag{3.9}$$

where $\eta = z/\ell_o$

A second relation between f and F is obtained by using the mixing
length hypothesis (Eq.(3.2)):

$$\frac{df}{d\eta} = \eta^{-1}F. \tag{3.10}$$

Solving (3.9) and (3.10) for f and F yields

$$F(\eta) = e^{-\eta} \tag{3.11}$$

$$f(\eta) = - \int_\eta^\infty \frac{e^{-x}}{x}dx = Ei(-\eta) = - E_1(\eta) \tag{3.12}$$

29

To obtain expressions for $u_o(x)$ and $\ell_o(x)$ Townsend used the assumption that for small values of z the velocity profile within the IBL is adapted to the new roughness length and friction velocity i.e.

$$U = \frac{u_{*2}}{k} \ln\left(\frac{z}{z_{02}}\right)$$
(3.13)

This is the so-called inner boundary condition. Together with the forms derived for $f(\eta)$ and $F(\eta)$, Townsend arrived at expressions for $u_o(x)$ and $\ell_o(x)$.

It was shown by Blom and Wartena (1969) that for small values of z the expression for u_o did not approach the inner boundary condition. They were able to remove this inconsistency of Townsend's theory, giving a slightly different expression for $u_o(x)$. Blom and Wartena also applied Townsend's theory to two subsequent changes in surface roughness. They found expressions analogous to those calculated by Townsend. A consequence of multiple roughness changes, however, is an increasing number of layers generated by every new roughness change, which are all influenced by different regions of the upstream surface. The number of analytical solutions then grows rapidly and soon becomes unattractive.

Self preservation of wind and shear stress profiles was used by Logan and Fichtl (1975) who assumed that the velocity defect and shear stress difference functions were self preserving. They derived analytical forms for these functions, which agree reasonably well with the experimental results of Bradley (1968).

The latest attempt, using arguments of self preservation of profiles has been made by Mulhearn (1977), who considered the changes in surface fluxes and mean profiles of velocity, temperature and concentration of a scalar quantity after a roughness change. Mulhearn notices that z_o is a quantity primarily connected with the flow and not with the underlying surface. Only in equilibrium flows can a connection be made between z_o and the surface bounding the flow. Thus near the transition we may not, strictly

30

speaking, use an equilibrium value of z_o to describe the flow. Mulhearn's model is very similar to the one of Townsend: he assumed that the velocity within the IBL consists of three parts identical to the expressions used by Townsend, hence he also used the relations (3.7) and (3.8). Mulhearn showed that self preservation is possible if $u_o \sim (\ell_o)^a$ which leads to a relation between f and F resembling eq. (3.9):

$$af - \eta (\frac{df}{d\eta}) = \frac{dF}{d\eta} \tag{3.14}$$

A second relation between f and F is derived from a perturbed form of the upstream mixing length equation, resulting in eq. (3.10). In practice

$$u_o^{-1} \frac{du_o}{dx} << \ell_o^{-1} \frac{d\ell_o}{dx}$$

which implies that $|a| << 1$, then eq. (3.14) transforms to eq. (3.9) and the same solutions eqs. (3.11) and (3.12) are obtained. Mulhearn distinguished two regions in his analysis:
1. the region just downstream of the roughness change, where z_o can not be used to specify the underlying surface
2. the region where the fetch is large enough to use z_o.

Using the argument of self preservation and imposing the 'law of the wall' on the velocity profile close to the surface, he was able to derive expressions for both the velocity and length scales u_o and ℓ_o in these regions. Finally, Mulhearn extended his analysis to changes in a scalar quantity (concentration of a passive contaminant or temperature) but excluded stability effects. He obtained expressions for g and G which describe the change in scalar concentration and scalar flux respectively, and are identical to those for f and F.

3.3.2 Results

The self preserving profiles for the velocity and shear stress viz. eqs. (2.11) and (2.12) are identical in the theories of

31

Townsend, Blom and Wartena and Mulhearn, only Logan and Fichtl obtained different forms.

A comparison of the velocity profiles of Blom and Wartena (1969) with the corresponding ones of Elliott (1958) and Panofsky and Townsend (1964) is presented in Figure 3.2. It shows that the different models give very similar results as far as velocity changes are concerned, a fact already noticed by Taylor (1969). This means that the horizontal velocity U is not a proper quantity to distinguish between the performance of different models or to compare theoretical results with experimental data. Because the wind profile within the IBL is prescribed or subjected to severe restrictions, it is more useful to consider e.g. d(x) for which these models were originally devised. Nevertheless some authors

1: Revised Townsend profile (x = 15500 m)
2: Elliott profile (x = 413 m)
3: Panofsky & Townsend profile (x = 413 m)
4: Revised Townsend profile (x = 413 m)
5: Revised Townsend profile (x = 26.9 m)
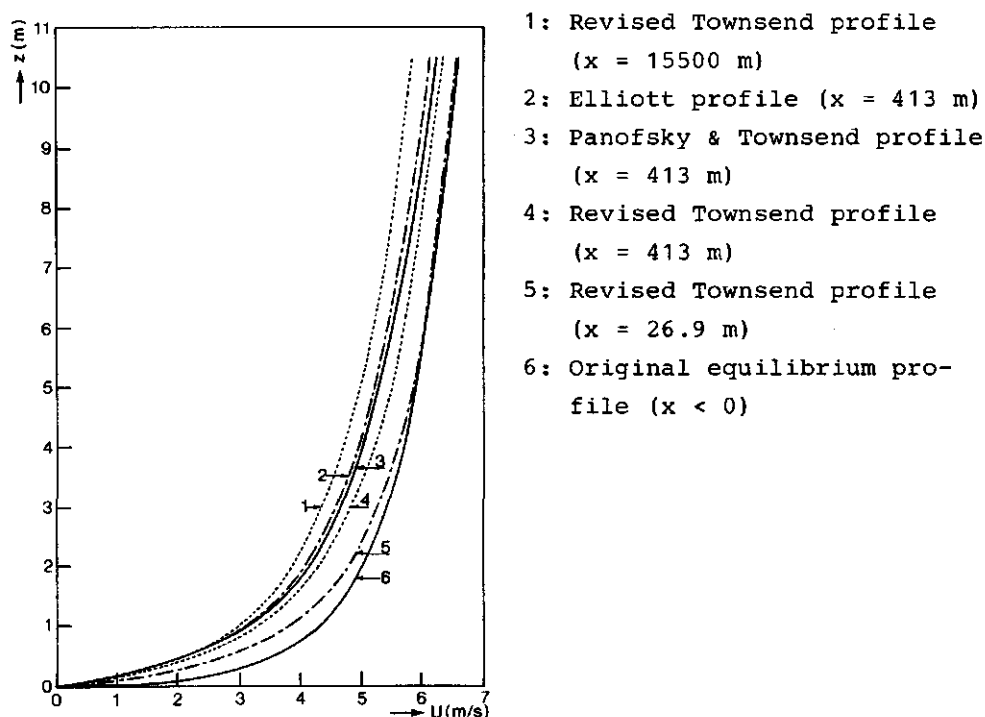6: Original equilibrium profile (x < 0)

Figure 3.2   Velocity profiles after a change in surface roughness. (After Blom and Wartena, 1969).

(e.g. Panofsky and Townsend, 1964; Blackadar et al., 1967) do not
use this quantity to examine the results of certain models with
experiments. This is understandable because mean velocity mea-
surements are relatively easy to make, while turbulent quantities
such as shear stress are much harder to measure. As a consequence
the number of mean velocity measurements after a change in sur-
face roughness cited in the literature far exceeds that of all
other quantities.

In Figure 3.1 the downstream variation of the surface shear
stress from the model of Blom and Wartena is compared with the
variation predicted by some integral models. Apparently there
is a close agreement between these sets of curves. The difference
in the surface shear stress values of the various models is lar-
ger for the SR than for the RS change. Furthermore this differ-
ence decreases with increasing downstream distance and, especial-
ly for the SR case, it also decreases with decreasing roughness
difference. Both phenomena are a consequence of the fact that
firstly, u_{*2} approaches u_{*1} when $x \to \infty$, though only theore-
tically for an infinitely deep boundary layer, and secondly, a
smaller difference $z_{02}-z_{01}$ naturally will cause a smaller distur-
bance of the flow field. The growth rate of ℓ_o is similar to the
one of d predicted by Elliott, exponents ranging between 0.71 and
0.88 for $-3 < M < 3$.

A puzzling fact remains the independence of ℓ_o on the downstream
surface roughness (z_{02}), which can be detected on inspecting
Blom and Wartena's eq. (12), which can be written as

$$\ell_o [\ln(\frac{\ell_o}{z_{01}}) - 1] = 2k^2 x.$$

In Figure 3.3 shear stress profiles within the IBL of several mo-
dels are compared. Figure 3.3b uses the true vertical distance and
hence it also shows the height of the IBL of the different models.
If we nondimensionalize the vertical coordinate by means of the
appropriate IBL height of the model Figure 3.3a is obtained. It
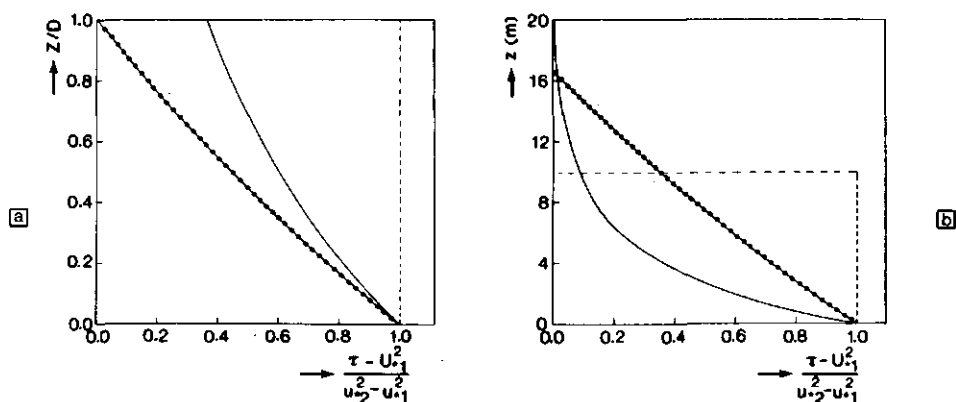shows that for the three models in question, the profiles of the

Figure 3.3 Shear stress profiles for various models for a smooth to rough transition ($M = -3$). ---- Elliott, ... Panofsky and Townsend , —— Blom and Wartena.

shear stress do not resemble each other, in contrast with the close agreement between the velocity profiles and the downstream variation of the surface shear stress.

3.3.3 Discussion

One of the main shortcomings of the self preservation models is the mixing length assumption (also discussed in 3.2.3) which they have in common with all other first order closure models. All self preservation models neglect the influence of the induced pressure field which makes the analysis only applicable to distances relatively far from the step change i.e. $d/z_{o2} >> 1$, (see e.g. Tani (1968) and Antonia and Luxton (1972)).

The models of Townsend and Blom and Wartena result in a small value of the adapted layer height $\delta \cong 0.1$. ℓ_o giving a height to fetch ratio of $1/300$. This is considerably smaller than predicted by other theories.

Finally, another limitation of the self preservation models is that the prediction of the surface shear stress and the IBL

34

thickness is only justified for small changes of the roughness length. This limits their applicability.

3.4 NUMERICAL MODELS WITH FIRST ORDER CLOSURE

3.4.1 Description

Further development in the analysis of the effects occurring after a change in surface characteristics is made primarily with the aid of numerical models. After writing the governing equations in a finite difference form and specifying the boundary conditions, the spatial distribution of each dependent variable can be computed. The set of equations always include the continuity equation and the horizontal momentum equation. To these equations one may add one or more terms to incorporate additional effects e.g. buoyancy. Several authors include the vertical momentum equation in their model, and hence are able to calculate the pressure field generated by the surface discontinuity. Also, other equations may be added to analyse more than one change in surface conditions simultaneously.

All models mentioned in this section still use the mixing length assumption to close the set of equations, hence they all have the same deficiencies connected with this particular assumption. Most of them consider flows in neutral stability only. It is not necessary to give a detailed description of each and every first order model ever constructed, rather a survey of the most important characteristics of them is worth mentioning. These details are summarized in Table 3.1.

3.4.2 Results

To present the results of every first order model would be rather exhaustive, so only the most interesting features are briefly reviewed here, and comparisons are made with the results of earlier models.

The governing equations of Taylor's first model (1969a) are

35

Table 3.1 Summary of first order models

MODEL	ADDITIONAL TERMS IN EQ. (2.34)	ADDITIONAL EQS. TO (2.29) and (2.34)	MIXING LENGTH DISTRIBUTION	REMARKS
Taylor (1969[a])	none	none	$l = k\ (z + z_{oi})$	abrupt change in mixing length throughout IBL
Taylor (1969[b])	pressure and Coriolis force	Y-momentum	$l = \dfrac{k(z + z_{oi})}{1 + kz/\lambda}$ $\lambda = \dfrac{G}{f}(0.0004)$	description of Ekman layer
Wagner (1966)	time derivative and Coriolis force	Y-momentum (2.29) and (2.34) combined, incl. energy, eq. of state	$l = \dfrac{k(z + z_o)}{1 + k(z + z0)/\lambda}$ $\lambda = 0.00027(U_g^2 + V_g^2)/f$	see above + non-steady state
Nickerson (1968)	none	none	$l = kz$	change in u_* instead of z_0
Onishi and Estoque (1968)	pressure	z-momentum[1]	$l = kz$	gradual change of z_0 coincident with change in l
Huang and Nickerson (1974)	pressure	z-momentum[1]	$l = kz\phi$ ϕ = stability factor	also for unstable situations and change in surface temperature
Taylor (1970)/ (1971)	none	heat flow eq.	$l = \dfrac{k(z + z0)}{\phi}$ ϕ = stability factor	also for change in surface temperature or heat flux. For (un)stable situation

(1) The z-momentum equation is transformed into an elliptic equation for the pressure, by taking the divergence of the vector momentum equation.

36

identical with the ones used by Panofsky and Townsend (1964). It is therefore not surprising that the results of his numerical model show good agreement with their results. But where P&T assumed a linear variation of $\tau^{\frac{1}{2}}-u_{*1}$ with z/d, Taylor found the distributions given in Figure 3.4. This result indicates that (i) shear stress profiles are a much better quantity for comparing different models than the velocity profiles and (ii) these shear stress profiles are almost self preserving as assumed by Townsend (1965, 1966). On the other hand self preservation of shear stress profiles was not found by Wagner (1966), Onishi and Estoque (1968) and Huang and Nickerson (1974). The shear stress profiles of these last three models closely resemble each other, which for the latter two is not surprising since Huang and Nickerson's model comprises only a slight extension of Onishi and Estoque's model. The upstream effect of the roughness change, as a conse-
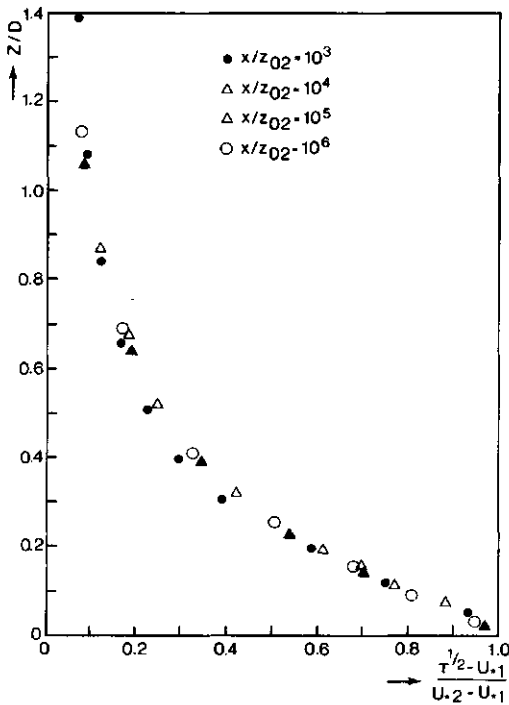

Figure 3.4
Shear stress profiles after a change in surface rough-ness (M = +2).
(After: Taylor, 1969a)

quence of the introduction of a pressure term in the horizontal
momentum equation, is clearly visible in the results of Onishi
and Estoque (1968) and Huang and Nickerson (1974). It is absent
in Wagner's results, although Wagner did detect a slight effect
in the upstream horizontal velocity distribution.

The inclusion of a pressure term and, consequently, the vertical
momentum equation gives an opportunity to study the generated
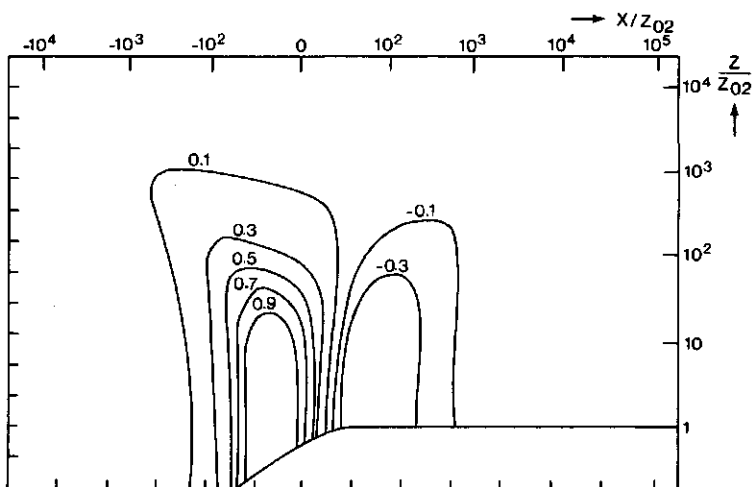pressure field (Figure 3.5). As observed by Onishi and Estoque

Figure 3.5   Nondimensional pressure field (deviation from the
              hydrostatic pressure) for a smooth to rough transi-
              tion with M = -5. (After Huang and Nickerson, 1974a).

this pressure field "... acts as if it were a smoothing function,
causing the change in wind speed to occur over a larger horizon-
tal distance". At larger downstream distances no net pressure
effect is noticeable. The effect of the pressure is thus con-
fined to a small distance before and after the roughness change.
Here it also affects the distribution of the vertical velocity,
shifting the place of maximum velocity and decreasing absolute
values compared to the vertical velocity field obtained without
the pressure term extension.

38

There is a close agreement in the growth rate of the IBL height
between the different models, all confirming Elliott's power law.
However, the absolute value of the IBL height is just a matter of
definition. Taylor (1969) defined it as the height where $\tau^{\frac{1}{2}} - u_{*1}$
has been reduced to 10% of its surface value of $u_{*2} - u_{*1}$, whereas
Wagner (1966) defines this height by a 0.2% change in horizontal
velocity. A slight difference in the growth rate between the RS
and SR changes was noticed by Huang and Nickerson (1974). They
found the growth rate for a RS change to be approximately $\sim x^{0.7}$
instead of $\sim x^{0.8}$. This was attributed to the fact that the ad-
justment of the flow to the new z_o value is faster above a rela-
tively rough surface than above a smooth surface, a feature also
noticed by Wagner (1966).

The effects of stratification were incorporated in the models of
Huang and Nickerson (1974) and Taylor (1970, 1971). The former
authors also considered a change in surface temperature coinci-
dent with a change in surface roughness. The presence of an un-
stable upstream flow, they concluded, only results in small de-
viations from the neutral upstream flow case. Unfortunately, the
effects created by the instability of the upstream flow and those
created by the change in surface temperature are difficult to
distinguish. Taylor (1970, 1971), in an extension of his model
of 1969, also considered the effect of a change in roughness with
or without either a change in surface heat flux or temperature.
When only a step change in surface temperature without a change
in roughness was considered, solutions became unstable for large
distances downstream. Taylor attributed this to the particular
form used for the mixing length. In the case of a step change in
heat flux similar problems arised. The extension of his model to
include the stable case Taylor (1971) resulted in the peaking of
the shear stress profiles near the outer edge of the IBL in the
case of a step in surface heat flux. Taylor's model results indi-
cate that roughness change effects are greatest near the leading
edge, while further downstream thermal stability effects will
play a dominant role.

Finally, the effects of a roughness change in a deeper layer

39

than the constant flux layer were examined in the models by
Taylor (1969b,c) and Wagner (1966). Both considered these changes
in the Ekman layer at neutral stability. This extension could be
made by incorporating the Coriolis force effect in the equations
of motion. At the same time the length scale distribution has to
be specified in the Ekman layer.

Taylor was able to show that a roughness change has an effect on
the wind direction noticeable up to a rather large value of
$x/z_{02} \cong 10^7$.

3.4.3 Discussion

The first advantage of numerical models over analytical methods
is the possibility of deriving the profiles of the velocity and
the shear stress instead of prescribing them (integral models) or
making restricting assumptions (self preservation models). Fur-
thermore, numerical models do not need an a priori assumption
about an internal boundary layer required for earlier models. The
second advantage of numerical models is the relative ease with
which they can be modified or extended to include various addi-
tional terms in the governing equations to account for additional
effects e.g. pressure, buoyancy etc.

In general, the disadvantage of numerical models is that in order
to get computationally stable solutions sometimes additional sim-
plifications in the terms of the governing equations have to be
introduced which may affect the final solutions. The effects of
these simplifications are difficult to estimate. Moreover, any
numerical model usually contains a large number of numerical con-
stants, the values of which are subject to limitations posed by
modeling assumptions. These values may range quite arbitrarily
between those limits. A fundamental objection against the use of
first order models (numerical as well as analytical) is, again,
the closure using the mixing length hypothesis (Plate, 1971).

Peterson (1969) points out that in some models the value of the

nondimensional wind shear is put equal to unity (e.g. Onishi and Estoque (1968)) while this is in disagreement with experimental data and the results of higher order models. This simplification, Peterson asserts, results in smooth velocity profiles without a point of inflection. Huang and Nickerson (1974b) notice that mixing length models do not contain advection and diffusion terms of the turbulent kinetic energy. This manifests itself in an overestimation of the surface shear stress in case of a SR change. The most essential difference, they maintain, is the much faster increase of the surface shear stress in higher order models after a RS change. As indicated by their results and those of others (Peterson, 1969) a mixing length model reasonably describes the flow structure only when the production of turbulent kinetic energy (TKE) equals its dissipation, which is not the case in the non-equilibrium part of the flow just downstream of the surface roughness change, and in the transition region between the adapted layer and the edge of the IBL.

3.5 NUMERICAL MODELS WITH A HIGHER ORDER CLOSURE

3.5.1 Description

As was pointed out before, closing the horizontal momentum equation by means of correlating the Reynolds stress with the gradient of the mean velocity is beset with many theoretical and practical objections. To overcome these objections, many other ways have been tried to model the Reynolds stress terms. Reviews of several methods to obtain the desired closure are presented e.g. by Launder and Spalding (1972), Mellor and Herring (1973), Harsha (1977), Rodi (1979) and Zeman (1981). For the roughness change problem, comparisons between higher order closure models and integral and first order closure models were presented by Taylor (1973) and Wood (1978).

The models which use a higher order closure scheme to analyse the effects of a change of surface conditions can be devided into two groups:

(i) Turbulent kinetic energy models (one and a half order
    closure).
This group contains the models of Bradshaw, Ferriss and Atwell
(1967), Peterson (1969), Shir (1972) and Huang and Nickerson
(1974b). The basic assumption is: $\tau \sim \overline{e^2}$, hence the Reynolds stress
depends on the turbulent kinetic energy (TKE):

$$k = \overline{e^2} = \overline{u_i u_i}^{(*)}$$. Hence a transport equation for $\overline{e^2}$ must be added.

This type of model can be extended to include also a transport
equation for the mixing length (k-ϵ models). Although k-ϵ models
appear to be very promising for boundary layer analysis, little
use of them for roughness change modelling has so far been made,
only one attempt was briefly described by Wood (1978).

(ii) Second order closure models.
This group consists mainly of different versions of the model of
Wyngaard, Coté and Rao (1974): viz. those of Rao et al. (1974a)
for a change in surface roughness, Rao (1975) the same model but
extended for diabatic situations, Rao et al. (1974b) for a change
in surface roughness, temperature and humidity, and Wyngaard and
Coté (1974) for the evolution of a convective planetary boundary
layer. In 2nd order modeling an explicit transport equation is
written for every second moment. For the two-dimensional case
this requires equations for: $\overline{uw}$, $\overline{u^2}$, $\overline{v^2}$, $\overline{w^2}$ and $\overline{\epsilon}$. For diabatic
conditions those are completed with equations for: θ, $\overline{w\theta}$, $\overline{u\theta}$ and
$\overline{\theta^2}$. Finally these can also be extended with equations for:
Q, $\overline{wq}$, $\overline{uq}$ and $\overline{q^2}$ if a change of surface humidity is coincident
with the roughness change. However, the problem of closure is
getting more difficult with every equation which is added to the
list.

ad (i) <u>Kinetic energy models</u>
An attempt to model turbulence was undertaken in 1967 by Bradshaw,
Ferries and Atwell (1967). Apart from the equations (2.29) and

(*)Some authors define the TKE to be equal to $\frac{1}{2} \overline{e^2}$.

42

(2.34) with the momentum equation modified with the boundary
layer approximation to account for the pressure gradient force,
an equation is added which accounts for the transport of TKE:

$$\tfrac{1}{2}\rho\,(U\frac{\partial \overline{e^2}}{\partial x} + W\frac{\partial \overline{e^2}}{\partial z}) - \tau\frac{\partial U}{\partial z} + \frac{\partial}{\partial z}(\overline{pw} + \tfrac{1}{2}\rho\,\overline{e^2 w}) + \rho\,\overline{\varepsilon} = 0 \qquad (3.15)$$

where $\overline{e^2} = \overline{u_i u_i}$ is the TKE

$\overline{\varepsilon} = \nu\,\overline{(\partial u_i/\partial x_j)^2}$ is the viscous dissipation rate.

Closure of this equation is obtained by defining:

$$a_1 = \tau/\rho\,\overline{e^2} \qquad (3.16a)$$

$$L = \frac{(\tau/\rho)^{3/2}}{\overline{\varepsilon}} \qquad (3.16b)$$

$$G = (\frac{\overline{pw}}{\rho} + \tfrac{1}{2}\,\overline{e^2 w})/(\frac{\tau_{max}}{\rho})^{\tfrac{1}{2}}\cdot\frac{\tau}{\rho} \qquad (3.16c)$$

where $\tau_{max} = \tau(z = \tfrac{1}{4}d)$

Bradshaw et al. used $a_1 = 0.15$ and assumed that L and G are
functions of z/d and depend on the shear stress profile. With
the asumptions (3.16) Equation (3.15) is transformed into a
transport equation for the Reynolds stress $\overline{uw}$. After defining
suitable boundary conditions, Bradshaw et al. (1967) were able
to show that their model proved to be satisfactory in correlating
model predictions with experimental results. However, the authors
did not apply their model to the roughness change problem. This
extension of their model was made by Schols (1979) and Douwes
(1980).

Peterson (1969) and Shir (1972) also used an equation similar to
Eq. (3.15) to close their set of equations, the latter making
use of a vorticity equation instead of the usual horizontal mo-
mentum equation. A slight modification to these Bradshaw-type
models was introduced by Huang and Nickerson (1974b). Referring

43

to the experiments performed by Yeh and Nickerson (1970) the relationship between τ and $\overline{e^2}$ was transformed into:

$$\tau = -\overline{uw} = (\overline{e^2})^{\frac{1}{2}} \ell_1 \frac{\partial U}{\partial z} \tag{3.17}$$

The diffusion term and the dissipation term were approximated by respectively:

$$\overline{pw} + \frac{\overline{we^2}}{2} = -K_m \frac{\partial}{\partial z} (\frac{\overline{e^2}}{2}), \tag{3.18a}$$

where $K_m = (\overline{e^2})^{\frac{1}{2}} \ell_1$

and $\overline{\varepsilon} = (\frac{\overline{e^2}}{2})^{3/2} \frac{1}{\ell_\varepsilon}$ $\qquad$ (3.18b)

After deriving equations for the length scales ℓ_1 and ℓ_ε, the TKE equation, the continuity equation and the two momentum equations (including the pressure term) form a closed set.

A discussion on the relative importance of the terms in the TKE equation and the momentum equation was given by Peterson (1972). He applied his analysis to a more extended TKE equation than the one used in his model of 1969. In his analysis he used the same approximations for the diffusion and dissipation terms as in his earlier model. With the given set of equations 7 different models are constructed depending on the inclusion or rejection of one or more terms of interest in the model and comparisons are made between the predictive qualities of each model.

ad (ii) Second order closure models
As is discussed e.g. by Zeman (1981) many attempts have been made in turbulence modeling by means of 2nd order closure techniques. But the application of these techniques to the roughness change problem is restricted to a small number of cases.
The only models described so far, with explicit equations for the second moments are the ones developed by Rao, Wyngaard and Coté They were summarized at the beginning of this section. The horizontal momentum equation (2.30) was used without the pressure term.
44

The equation for the Reynolds stress tensor $\overline{u_i u_j}$ is derived from the Navier-Stokes equation resulting in:

$$U_j \frac{\partial}{\partial x_j} \overline{u_i u_k} + \overline{u_j u_k} \frac{\partial U_i}{\partial x_j} + \overline{u_j u_i} \frac{\partial U_k}{\partial x_j} = - \frac{\partial}{\partial x_j} (\overline{u_i u_k u_j}) +$$

$$- (\overline{u_k \frac{\partial p}{\partial x_i}} + \overline{u_i \frac{\partial p}{\partial x_k}}) - 2\overline{\epsilon} \frac{\delta_{ik}}{3} \tag{3.19}$$

where $\overline{\epsilon}$ is the viscous dissipation rate of TKE, and the summation convention applies. The third order terms on the right hand side of Eq. (3.19) have to be modeled. To achieve this, use has been made of the closure techniques devised by Lumley and Khajeh-Nouri (1974). This procedure is described by Wyngaard, Coté and Rao (1974). The resulting equations for $\overline{uw}$, $\overline{u^2}$, $\overline{v^2}$ and $\overline{w^2}$ ($\overline{uv}$ = $\overline{vw}$ = 0) together with the modified Eq. (2.30), the continuity equation (2.29) and an equation for $\overline{\epsilon}$:

$$U_j \frac{\partial \overline{\epsilon}}{\partial x_j} + \frac{\partial}{\partial x_j} (\overline{u_j \epsilon}) = - 4 \frac{\overline{\epsilon}^2}{\overline{e}^2} + 4a \overline{\epsilon} \frac{P}{\overline{e}^2} \tag{3.20}$$

where a = 0.5 and P is the production rate of TKE, form the basic set of equations. After modeling the third order terms in Eqs. (3.19) and (3.20) the problem is solved numerically. In Chapter 4 we will give a more detailed description of the extended form of this model, which also contains temperature and humidity variables.

3.5.2 Results

It is interesting to know how much is gained by extending the numerical models with higher moment equations. Therefore we will concentrate our attention in this section on the differences in the results of 1st and higher order models.

The velocity profile downstream of x = 0, which in 1st order theories was a monotonic function of ln(z) demonstrates a different behaviour in the higher order models. Peterson (1969) was the first to notice that velocity profiles within the IBL, as

predicted by a higher order model, contain a point of inflection both for the RS and SR changes i.e. a local minimum, respectively maximum of the velocity gradient. This observation was confirmed by the results of Shir's model (1972) as well as those of Huang and Nickerson (1974b) and Rao et al. (1974a). If the nondimensional wind shear is defined by:

$$\phi_m = \frac{k\dot{z}}{u_{*2}} \cdot \frac{\partial U}{\partial z} \qquad (3.21)$$

then it follows from Eqs. (3.1)-(3.4) and

$$\tau = \rho u_*^2 \qquad (3.22)$$

that ϕ_m was taken equal to unity in all models which use the mixing length assumption. Figure 3.6 shows the variation of ϕ_m in higher order models. It is clearly visible that $\phi_m > 1$ (< 1), for RS (SR) changes, over a major part of the IBL. For large
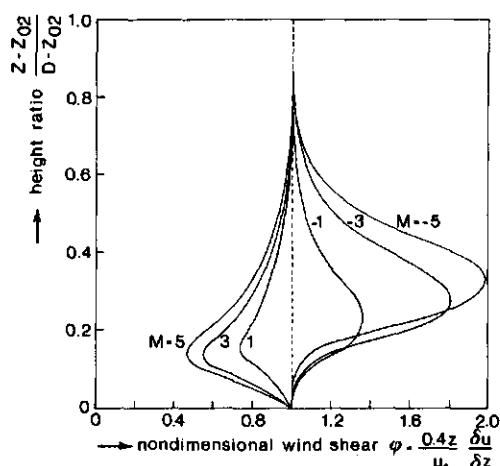

Figure 3.6   Comparative magnitudes of deviations of the nondimensional wind shear from unity for various roughness changes.

For M < 0, x/z_{02} = 10^2
            = + 1,   = 10^3
            = + 2,   = 10^4
            = + 3,   = 10^5

(After Peterson, 1969).

46

distances downstream the curves of ϕ_m tend to unity, indicating
that mixing length models will give more satisfactory results
there.

The shear stress profiles predicted by Peterson, Shir and Rao
et al. do not agree with each other. Both Peterson and Shir found
that, especially for the SR change, the shear stress profiles are
not self preserving. For the RS change their profiles are only
approximately self preserving. The model of Rao et al. on the
other hand produced shear stress profiles that possess self pre-
serving properties to a high degree, again especially for the RS
change and to a slightly lesser extend for the SR change (see
Figure 3.7). These last results agree very well with those of
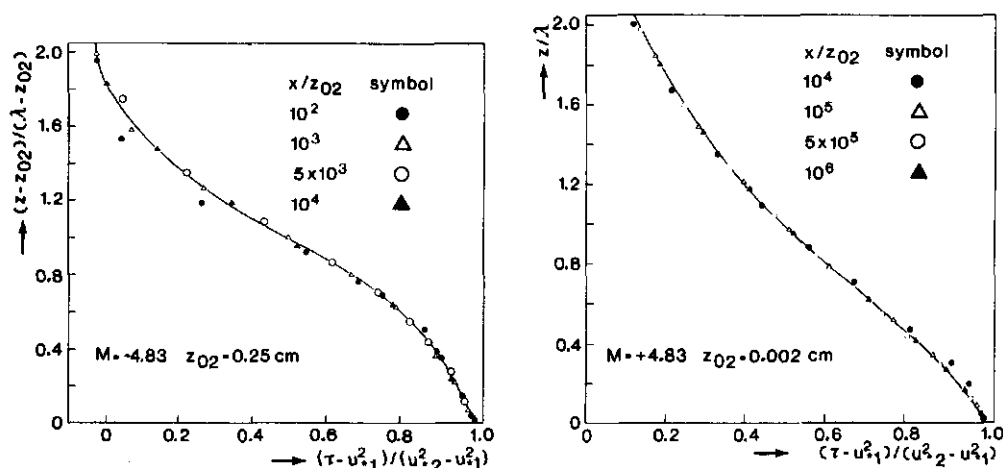Taylor's numerical model (see 3.4.2).

Figure 3.7   Nondimensional shear stress profiles for a smooth
to rough transition (left) and for a rough to smooth
transition (right). (After Rao, Wyngaard and Coté,
1974a).

The gain in accuracy of the prediction of the surface shear
stress variation as compared with 1st order and older models is
practically zero. A slightly faster response to the new surface
was detected by Huang and Nickerson (1974b), while Shir found a

47

peculiar behaviour in the SR change. Seemingly in agreement with the data of Bradley (1968) two oscillations occur close to x = 0 before the surface shear stress levels off to its asymptotic value. This pattern was not discernible in the RS case nor in any other model.

The prediction of the value of the height of the IBL is ambiguously because of the different definitions of d(x). Shir and Peterson introduce two IBL heights d_τ and d_u, defined with regard to the shear stress and velocity profiles respectively. All authors find, again, the same growth rate: $d(x) \sim x^{0.8}$, only Shir detects a small difference between the RS and SR changes. The influence of stratification on the growth rate was investigated by Rao (1975). He found that the growth rate exponent depends on the Obukhov length L but is approximately independent of M. He found that for neutral stability $d \sim x^{0.77}$ (both for RS and SR changes) while for unstable conditions exponents ranged from 0.9 (near neutral) to 1.4 (strongly unstable).

Finally, Rao et al. questioned the assumption of proportionality between shear stress and TKE as used by Bradshaw et al. (1967) and in other models in the nonequilibrium part of the flow. According to Rao's model results, the value of a_1 in Eq. (3.16a) varies considerably in this region. It approaches its equilibrium value only near the edge of the IBL. This is supported by the experimental results of Antonia and Luxton (1971).

3.5.3 Discussion

The need for second order models arose when "K-theory" or first order models appeared to fail in situations which are rapidly changing in space or time. The philosophy behind the application of second order models is: "if a crude assumption for second moments predicts first moments adequately, perhaps a crude assumption for third moments will predict second moments adequately". One implicitly assumes that in the latter case also the prediction of the first moments will be improved.

48

Hence second order models should provide a better tool for describing the effects after a change in surface conditions, in theory at least. In practice the results of second order models are only slightly better than the ones achieved by first order models as far as first moments are concerned. This is not surprising since there was hardly any room for improvement of the first moments anyway. The gain of second order models is largely confined to the description of the second moments, which are only crudely approximated by first order models or not at all. Unfortunately, measuring these second moments especially in the atmosphere, is at least very difficult (Reynolds stress components, turbulent fluxes) or even almost impossible (pressure strain correlations), so comparisons between theory and experiment are difficult to make. Also, it is important to notice that the reliability of a second order model depends on the modeling of the third moments as well as on the specification of the boundary conditions. Since the physical basis for this is weak, it is sometimes called an art (Wyngaard, 1982). This art of devising correct models for the higher order moments is still evolving rapidly, but a general basis to do so has already been constructed. Rotta (1951) and Lumley and his co-workers (Lumley, 1979), have developed the general lines for the modeling of the higher order terms, but no general agreement has yet been established. This is one of the disadvantages of the use of a second order model. Another one is the large number of modeling assumptions needed to close the system of equations. This unavoidably will bring along a great number of numerical constants the values of which are difficult to determine.

Second order models also have important advantages. First of all, they do not require the use of the mixing length assumption, which is the weak point of simpler models (Peterson, 1972; Huang and Nickerson, 1974b).

Finally , with higher order modeling one can easily incorporate advection and diffusion of TKE into the model as well as many other effects which can not be considered in first order models.

49

4 Examination of model performance

In this Chapter we will subject the model employed in this study to a close examination.

A physical model of nature helps us to understand the phenomena we are studying. It equips us with a framework of concepts and equations which will have to account for all the characteristics of the subject observed so far. With a model we should be able to interpret the information which experiments have given us, because it provides us with the interrelationships between the various properties of the observed phenomena.

Naturally, for our own sake, we try to keep a model as simple as possible, elegance lying in a simple model explaining a myriad of properties and even predicting phenomena heretofore not observed or even guessed at. However, as science progresses and observations are refined and extended, new matters may be brought to light which do not fit into the existing framework. We then either have to abandon the model altogether, devising a new one, or we have to alter and improve the existing one to incorporate the new facts.

An example of the latter course of science is the gradual sophistication of turbulence models presented in Chapter 3. But even the second order models mentioned there do possess a fair amount of simplifications and do neglect minor effects, just to keep things manageable. Some fundamental simplifications were already encountered in the derivation of Eqs. (2.26)-(2.28). The assumptions mentioned in that Chapter are commonly accepted and need no bother us here. We will concentrate therefore to the specific simplifications incorporated in the present model, some of which were discussed already in Chapter 3.

In section 4.1 a brief outline of the model is presented. By taking notice of the simplifications made beforehand one should be

able to appreciate the limitations inherent in the present model. In sections 4.2 and 4.3 the model's functioning will be analysed in homogeneous and inhomogeneous situations respectively.

4.1 DESCRIPTION OF THE MODEL

4.1.1 General

As we mentioned in Chapter 3 the model of Wyngaard, Coté and Rao (1974) was first used in 1974 (Rao et al., 1974a) to describe the structure of the IBL after a sudden change in surface roughness without any simultaneous change in surface temperature, heat flux etc. In the same year (Rao et al., 1974b) the extension in order to include these simultaneous changes was made. Model results compared favourably with the measurements of Rider et al. (1963). With a further extension (Wyngaard and Coté, 1974) comprising the whole of the ABL, results were obtained which agreed very well with the ones given by the 3-dimensional model of Deardorff (Deardorff, 1972). A detailed description of the model of Rao, Wyngaard and Coté was given by Wyngaard et al. (1974), who discussed the techniques used to close the equations for the second moments (Lumley and Khajeh-Nouri, 1974) as well as the boundary conditions and the numerical techniques. A brief summary of this model is presented in section 4.1.2.

In order to apply a model to a particular situation one usually has to modify certain parts of it. It is of course possible to change the closure assumptions using recently introduced ideas, but this is beyond the scope of the present study. Furthermore, as there is still no general agreement on the modeling of all the third order and pressure-strain terms, the modeling expressions of the original model were not fundamentally changed. The only changes were some buoyancy corrections as well as some boundary conditions and the constants of the model which are determined by these boundary values.

51

4.1.2 Model equations

Equations (2.29) and (2.34)-(2.36) are the equations of the steady state 2-dimensional mean field in the IBL. As was noticed in Chapter 2 they do not comprise a closed set of equations. In the second order modeling employed in the model of Wyngaard, Coté and Rao equations must be generated for the second moments: $\overline{uw}$, $\overline{w\theta}$ and $\overline{wq}$. The procedure to obtain these equations has been presented many times (e.g. Monin and Yaglom, 1971; Tennekes and Lumley, 1972) and hence an abridged version of this derivation will be presented here. We refer to the above mentioned litera-ture for details.

Equations (2.25)-(2.28) for the mean field variables U_i, θ and Q were obtained after subjecting the respective equations for the corresponding, instantaneous variables $\tilde{u}_i$, $\tilde{\theta}$ and $\tilde{q}$ (2.12), (2.17), (2.22) and (2.23) to the Reynolds' decomposition and averaging. Now if (2.25)-(2.28) are subtracted from (2.12), (2.17), (2.22) and (2.23) the equations for the turbulent field variables u_i, θ and q are obtained. We will not present these equations in this text for brevity, but they are derived and presented in Appendix 1. The equation for the Reynolds' stress tensor $\overline{u_i u_k}$ can be generated by multiplying the equation for u_i with u_k, adding the equation for u_k multiplied with u_i, and averaging the result. This proce-dure is outlined in Appendix 1. The resulting equation for steady state conditions reads

$$U_j \frac{\partial}{\partial x_j} \overline{u_i u_k} + \overline{u_j u_k} \frac{\partial U_i}{\partial x_j} + \overline{u_j u_i} \frac{\partial U_k}{\partial x_j} = - \frac{\partial}{\partial x_j} (\overline{u_i u_j u_k}) +$$
$$\qquad\quad \text{I} \qquad\qquad \text{II} \qquad\qquad \text{II} \qquad\qquad\qquad \text{IV}$$

$$- \frac{1}{\rho_r} (\overline{u_k \frac{\partial p}{\partial x_i}} + \overline{u_i \frac{\partial p}{\partial x_k}}) + \frac{1}{T_r} (g_i \overline{u_k \theta_v} + g_k \overline{u_i \theta_v}) - \frac{2}{3} \overline{\epsilon} \, \delta_{ik} +$$
$$\qquad\qquad\qquad \text{V} \qquad\qquad\qquad\qquad \text{III} \qquad\qquad\qquad \text{VI}$$

$$- 2\Omega_j (\epsilon_{ij1} \overline{u_1 u_k} + \epsilon_{kj1} \overline{u_1 u_i}). \tag{4.1}$$

This equation can also be obtained by first generating the equa-tion for the instantaneous Reynolds' stress $\tilde{u}_i \tilde{u}_k$, subtracting

52

Table 4.1. Scheme of interactions

equation \ variable	W	U	Θ	Q	$\overline{uw}$	$\overline{w\theta}$	$\overline{wq}$	$\overline{u^2}$	$\overline{v^2}$	$\overline{w^2}$	$\overline{u\theta}$	$\overline{uq}$	$\overline{\theta^2}$	$\overline{q^2}$	$\overline{q\theta}$	$\overline{\epsilon}$
(2.29) Cont.	x	x														
(2.34) U	x	⊗			x											
(2.35) Θ	x	x	⊗			x										
(2.36) Q	x	x		⊗			x									
(A3.15) $\overline{uw}$		x			⊗			x	x	x	x	⊠				x
(A3.12) $\overline{u^2}$		x			x			⊗	x	x						x
(A3.13) $\overline{v^2}$								x	⊗	x						x
(A3.14) $\overline{w^2}$						x		x	x	⊗						x
(A3.16) $\overline{u\theta}$		x	x	x	x	x	⊠	x	x	x	⊗					x
(A3.17) $\overline{w\theta}$			x	x		⊗		x	x	x			x		⊠	x
(A3.18) $\overline{uq}$ ▲					x		x	x	x	x		⊗				x
(A3.19) $\overline{wq}$							⊗	x	x	x				⊠	x	x
(A3.21) $\overline{\theta^2}$			x	x		x		x	x	x			⊗			x
(A3.22) $\overline{q^2}$ ▲				x			x	x	x	x				⊗		x
(A3.20) $\overline{q\theta}$			x			x	x	x	x	x					⊗	x
(A3.23) $\overline{\epsilon}$		x			x	x	x	x	x	x						⊗

o : variable in own equation

□ : introduced through moisture correction

▲ : equations that will vanish if no moisture correction is used (weak coupling).

53

from it the equation for $U_i U_k$, and subsequently averaging the result (see Monin and Yaglom, 1971).

The equation for $\overline{u_i \theta}$ can be derived by first multiplying the equation for θ with u_i, then multiplying the equation for u_i with θ, adding the two equations and averaging. Assuming stationarity again we obtain (see Appendix 1)

$$U_j \frac{\partial}{\partial x_j} \overline{u_i \theta} + \overline{u_i u_j} \frac{\partial \Theta}{\partial x_j} + \overline{u_j \theta} \frac{\partial U_i}{\partial x_j} = - \frac{\partial}{\partial x_j}(\overline{u_i u_j \theta}) - \frac{1}{\rho_r} \overline{\theta \frac{\partial p}{\partial x_i}} +$$

$$\underset{I}{} \qquad \underset{II}{} \qquad \underset{II}{} \qquad \underset{IV}{} \qquad \underset{V}{}$$

$$g_i \frac{\overline{\theta \theta_v}}{T_r} + -2\Omega_j \varepsilon_{ijk} \overline{u_k \theta} \ . \tag{4.2}$$

$$\underset{III}{}$$

An analogous procedure using the equation for q instead of θ yields the equation for $\overline{u_i q}$

$$U_j \frac{\partial}{\partial x_j} \overline{u_i q} + \overline{u_i u_j} \frac{\partial Q}{\partial x_j} + \overline{u_j q} \frac{\partial U_i}{\partial x_j} = - \frac{\partial}{\partial x_j}(\overline{u_i u_j q}) - \frac{1}{\rho_r} \overline{q \frac{\partial p}{\partial x_i}} +$$

$$\underset{I}{} \qquad \underset{II}{} \qquad \underset{II}{} \qquad \underset{IV}{} \qquad \underset{V}{}$$

$$g_i \frac{\overline{q \theta_v}}{T_r} + -2\Omega_j \varepsilon_{ijk} \overline{u_k q} \ . \tag{4.3}$$

$$\underset{III}{}$$

Equations (4.2) and (4.3) contain the second moments $\overline{\theta \theta_v}$ and $\overline{q \theta_v}$. Realizing that $\theta_v = (1 + 0.608q)\theta$ in accordance with Eq. (2.18) we see that we need three additional equations viz. those for the second moments $\overline{\theta^2}$, $\overline{q^2}$ and $\overline{q\theta}$ (see Table 4.1). They can be derived from the equations for q and θ (A1.12) and (A1.14) with the same method as employed before (see Appendix 1).

$$U_j \frac{\partial}{\partial x_j} \overline{\theta^2} + 2 \overline{u_j \theta} \frac{\partial \Theta}{\partial x_j} = - \frac{\partial}{\partial x_j}(\overline{u_j \theta^2}) - 2\overline{\varepsilon_\theta} \ , \tag{4.4}$$

$$\underset{I}{} \qquad \qquad \underset{II}{} \qquad \quad \underset{IV}{} \qquad \underset{VI}{}$$

$$U_j \frac{\partial}{\partial x_j} \overline{q^2} + 2 \overline{u_j q} \frac{\partial Q}{\partial x_j} = - \frac{\partial}{\partial x_j}(\overline{u_j q^2}) - 2\overline{\varepsilon_q} \ , \tag{4.5}$$

$$\underset{I}{} \qquad \qquad \underset{II}{} \qquad \quad \underset{IV}{} \qquad \underset{VI}{}$$

54

$$U_j \frac{\partial}{\partial x_j} \overline{q\theta} + \overline{u_j q} \frac{\partial \theta}{\partial x_j} + \overline{u_j \theta} \frac{\partial Q}{\partial x_j} = - \frac{\partial}{\partial x_j}(\overline{u_j q\theta}) - \overline{\varepsilon}_{q\theta} \qquad (4.6)$$

    I   II   II   IV   VI

As was mentioned in the previous chapter new unknowns appear in
Eqs. (4.1)-(4.6) which prevent us from obtaining a closed system
of equations. We will have to order all the terms of (4.1)-(4.6)
systematically and devise modeling assumptions for those terms
which contain unknown dependent variables. Inspection of (4.1)-
(4.6) shows that several corresponding terms can be distinguish-
ed. They will be briefly discussed.

Advection terms

All terms in (4.1)-(4.6) denoted by I read

$$U_j \frac{\partial}{\partial x_j} M = U \frac{\partial M}{\partial x} + V \frac{\partial M}{\partial g} + W \frac{\partial M}{\partial z} , \qquad (4.7)$$

where M is $\overline{u_i u_k}$, $\overline{u_i \theta}$, $\overline{u_i q}$, $\overline{\theta^2}$, $\overline{q^2}$ and $\overline{q\theta}$ respectively. These
terms represent the divergence of the transport $U_j M$ and thus the
net increase or decrease of the quantity M per unit volume and
unit time in stationary conditions for a fluid particle follow-
ing the flow. In that case the substantial derivative reads

$$\frac{dM}{dt} = \frac{\partial M}{\partial t} + U_j \frac{\partial M}{\partial x_j} = U_j \frac{\partial M}{\partial x_j} ,$$

because $\partial M/\partial t = 0$.

Shear production terms

In a manner analogous to the one we used to obtain (4.1)-(4.6)
for $\overline{u_i u_k}$, $\overline{u_i \theta}$ etc. equations for $u_i u_k$, $U_i \theta$ etc. can be derived
No derivation is given here, only the resulting equation for
$U_i U_k$ will be presented (see Monin and Yaglom, 1965)

55

$$U_j \frac{\partial}{\partial x_j} U_i U_k + \frac{\partial}{\partial x_j}\left[U_k \overline{u_i u_j} + U_i \overline{u_k u_j} \right] - \left[\overline{u_j u_k} \frac{\partial U_i}{\partial x_j} + \overline{u_j u_i} \frac{\partial U_k}{\partial x_j} \right] =$$

$$- \frac{1}{\rho_r}\left[U_k \frac{\partial P}{\partial x_i} + U_i \frac{\partial P}{\partial x_k} \right] + \frac{T_v}{T_{vr}}\left[g_i U_k + g_k U_i \right] - 2\Omega_j \left[\varepsilon_{ijk} U_l U_k + \right.$$

$$\left. + \varepsilon_{kjl} U_l U_i \right] + \nu \frac{\partial^2}{\partial x_j \partial x_j} U_i U_k - 2\nu \frac{\partial U_i}{\partial x_j} \frac{\partial U_k}{\partial x_j} . \tag{4.8}$$

If the equations for $\overline{u_i u_k}$ and $U_i U_k$ are compared we observe that
the terms

$$\overline{u_j u_k}\partial U_i / \partial x_j + \overline{u_j u_i}\partial U_k / \partial x_j$$

appear in both equations but with opposite signs. This leads to
the conclusion that these terms describe the exchange of
$\tilde{u}_i \tilde{u}_k$ between the mean and fluctuating motion. In a turbulent sur-
face layer these terms usually represent a gain for the turbulent
motion and consequently a loss for the mean motion. Hence they
are called the shear production terms. For the remaining terms
labelled II in the other equations, similar conclusions can be
drawn.

Buoyant production terms

When the atmosphere is neutrally stratified the term in the
u_i-equation (A2.7) containing g_i is equal to zero and hence the
terms in (4.1)-(4.3) labelled III are equal to zero. When
stratification is present however, these terms represent the
production or destruction (depending on the sign of the stabili-
ty) of a second moment.

Turbulent transport terms

Following e.g. Tennekes and Lumley (1972) we notice that the
terms labelled IV in (4.1)-(4.6) all have the form $\partial \overline{Mu}_j / \partial x_j$,
where M again is $\overline{u_i u_k}$, $\overline{u_i \theta}$, $\overline{u_i q}$ etc. Gauss' integral theorem
states that

$$\int \frac{\partial}{\partial x_j} (\overline{Mu_j})\, dV = \oint (\overline{Mu_j}) \cdot dS \ ,$$

where $\overline{Mu_j}$ is a vector field. This implies that the turbulent transport terms disappear when they are integrated over a volume on which surface the third order moments $\overline{Mu_j}$ are zero. Apparently these terms merely tend to redistribute the quantity M from one point inside the flow to another.

Modeling these terms with the technique of Lumley and Khajeh-Nouri (1974) would greatly complicate the present model, for Lumley's expressions relate several third order moments to each other. Hence we would be forced to calculate the third order terms, using a simple expression containing only second and lower order moments, and subsequently calculate all third order terms iteratively. To avoid an excessive growth of computer time only the original simple "ad hoc gradient diffusion" model as Wyngaard (1975) calls it was used i.e.

$$\overline{Mu_i} = -a_t \ \partial M/\partial x_j \ \overline{u_i u_j} \ \tau \ , \tag{4.9}$$

where a_t is a constant and $\tau = \overline{u_i u_i}/\varepsilon$ is a turbulent relaxation time. For $M = u_i u_k$ Eq. (4.9) is replaced by a more complex expression given in Appendix 3.

Pressure terms

Term V in (4.1) can be transformed as follows

$$\overline{u_k \frac{\partial p}{\partial x_i}} + \overline{u_i \frac{\partial p}{\partial x_k}} = \frac{\partial}{\partial x_i} \overline{pu_k} + \frac{\partial}{\partial x_k} \overline{pu_i} - (\overline{p \frac{\partial u_k}{\partial x_i}} + \overline{p \frac{\partial u_i}{\partial x_k}}) \ . \tag{4.10}$$

Its contribution to the turbulent kinetic energy budget can be obtained by letting i = k and summarizing. This yields

$$\text{pressure term} = 2 \frac{\partial}{\partial x_i} \overline{pu_i} - 2 \overline{p \frac{\partial u_i}{\partial x_i}} \ .$$

The second term on the right hand side of the last relation

equals zero by virtue of (A1.3). The first term, like the turbulent transport terms, is the divergence of a vector field and hence only redistributes the turbulent kinetic energy. No kinetic energy can be generated or destroyed by this pressure terms and its contribution to the turbulent kinetic energy equation is not important.

Next however we turn to the separate components $\overline{u_i^2}$ of the turbulent kinetic energy. Analysis of homogeneous two-dimensional flows shows that in that case the pressure terms tend to force the $\overline{u_i^2}$ - distributions towards isotropy and hence it plays an important role in the $\overline{u_i^2}$ - equations. Moreover it can be shown that the pressure terms destroy the off-diagonal components of the $\overline{u_i u_k}$ tensor (Hinze, 1959). We also have to consider the pressure terms in (4.2) and (4.3). Following Wyngaard (1982) (4.2) reduces to approximately

$$\overline{w^2} \frac{\partial \Theta}{\partial z} = - \frac{1}{\rho_r} \overline{\theta \frac{\partial p}{\partial z}} , \qquad (4.11)$$

in a horizontally homogeneous, near neutral surface layer in quasi steady state conditions. It shows that the pressure term must destroy the temperature flux at the same rate as it is produced by the temperature gradient. A similar behaviour of the pressure term in (4.3) can be expected.

The state of modeling the pressure terms in (4.1)-(4.3) is converging somewhat to generally accepted expressions, but no general agreement exists as yet. By the time the present model was developed no buoyancy and mean strain effects were incorporated in the pressure term model. Realization that these effects are necessary, especially in moderate to strong diabatic boundary layers ,soon emerged (Wyngaard and Coté, 1974 ; Wyngaard, 1975). The expressions used by Wyngaard (1975) are presented in Appendix 3 along with their forms used in the present model.

Dissipation terms

The dissipation terms labeled VI indicate the molecular smoothing of the structure of the turbulent correlations. Even in high-Re-

58

number flow, we expect viscous dissipation to be the major loss term for turbulent kinetic energy. When the Reynolds number is large one may assume that these terms are independent of the mean flow geometry. In Appendix 1 it was demonstrated that the dissipation terms only affect the variances $\overline{u^2}$, $\overline{v^2}$, $\overline{w^2}$, $\overline{q^2}$ and $\overline{\theta^2}$ and also the covariance $\overline{q\theta}$. The off-diagonal elements of the Reynolds stress tensor $\overline{u_i u_k}$ as well as the turbulent fluxes $\overline{u_i \theta}$ and $\overline{u_i q}$ are not affected at all. The dissipation terms play an important role in equations (4.1) and (4.4)-(4.6).

In the atmospheric turbulent flow, the Re-number is always high enough to justify that the breakup rate of the large eddies should be independent of ν. Hence it appears dimensionally correct to have

$$\overline{\varepsilon} = c \cdot \frac{\overline{u_i u_k}}{\tau} \delta_{ik} \ , \tag{4.12}$$

where the dissipation term is modeled as an isotropic term, because the viscous dissipation process is an isotropic process. The corresponding models for the destruction terms $\overline{\varepsilon_\theta}$, $\overline{\varepsilon_q}$ and $\overline{\varepsilon_{q\theta}}$ are

$$\overline{\varepsilon_\theta} = b \frac{\overline{\theta^2}}{\tau}, \quad \overline{\varepsilon_q} = b \frac{\overline{q^2}}{\tau}, \quad \overline{\varepsilon_q} = b \frac{\overline{q\theta}}{\tau}, \tag{4.13a,b,c}$$

where $b = 1.9$.

In the present model $\overline{\varepsilon}$ is not approximated by (4.12) but it is calculated from a dynamic equation obtained by modeling its governing equation. We will omit the derivation of this equation (Lumley and Khajeh-Nouri, 1974) and simply present their equation

$$U_j \frac{\partial \overline{\varepsilon}}{\partial x_j} = - \frac{\partial}{\partial x_j} (\overline{u_j \varepsilon}) - 4 \frac{\overline{\varepsilon}}{\overline{u_i u_i}} (\overline{\varepsilon} - aP) \ , \tag{4.14}$$

where P is the production rate of turbulent kinetic energy.

The turbulent transport term in (4.14) is modeled by the approxi-

mation given in equation (4.9).

Summarizing, we can say that the present model consists of four
mean flow equations (2.29) and (2.34)-(2.36), the equations for
the second moments (4.1)-(4.6) and one equation for the dissipa-
tion rate $\bar{\varepsilon}$ viz. (4.14), with all the modeling assumptions men-
tioned throughout the text. In all we have 16 coupled parabolic
partial differential equations for the 16 dependent variables
(see also Table 4.1): U, W, Θ, Q, $\overline{u^2}$, $\overline{v^2}$, $\overline{w^2}$, $\overline{uw}$, $\overline{w\theta}$, $\overline{u\theta}$, $\overline{wq}$, $\overline{uq}$,
$\overline{\theta^2}$, $\overline{q^2}$, $\overline{q\theta}$ and $\bar{\varepsilon}$. These equations are numerically integrated
using a Dufort-Frankel explicit finite-difference scheme (Dufort
and Frankel, 1953), with forward marching in the x-direction.

The model is divided in two parts. In part I the initial distri-
bution of all variables in the surface layer upstream of the dis-
continuity is calculated, using predetermined values of u_{*1}, T_{*1},
q_{*1}, z_{01}, Θ_{01}, Q_{01} and z_I (height of the ABL).

In part II the final distributions of all variables as calculated
in Part I are used as the initial values for the calculation of
these distributions downstream of the discontinuity. In part II
the surface value of every variable is a function of the down-
stream distance (x) and the only restriction at the surface is
imposed by the energy and water balance (see Appendix 3). Con-
trary to this the surface value of every variable in Part I re-
mains fixed.

4.1.3 Drawbacks

Because the present model contains a great number of equations
which describe many variables in detail, it necessarily must con-
tain a large number of modeling constants which are needed to
produce the desired characteristics of turbulence is the ASL.
The larger the number of constants in a given model the larger
the amount of empirical input needed to determine the values
of these "constants". This poses a limitation on the general
applicability of the model i.e. the values of the constants

60

have to be tuned to any change in characteristics which the user
of the model deems neccessary. Recently (Bradley, Antonia and
Chambers, 1982) doubts arised for instance on the model constant
involved in the approximation of the pressure term in the modeled
$\overline{u_i \theta}$ equation. Bradley et al. (1982) showed that the value of this
constant depends on the stability parameter z/L.

There are other simplifications in the present model which are
not mentioned by the designers, but which are important. The
first simplification incorporated in the model is that for a
SR change the lowest level of the numerical grid is placed at
the largest z_0-height. This means that the airflow below this
level for $x < 0$ does not influence the calculations for $x > 0$.
Consequently it implies that the momentum, energy and humidity
contents between z_{01} and z_{02} are neglected for the downstream
region. As the original model was applied to a SR change from
$z_{01} = 2 \cdot 10^{-5}$ m to $z_{02} = 1.4 \cdot 10^{-3}$ m, this approximation could
easily be made, but it certainly limits the applicability of the
model for roughness changes when $z_{02}-z_{01}$ is larger.

The second simplification is the omission of the pressure gra-
dient term in the equation of motion (2.34). This omission re-
sults in an important numerical simplification for it turns an
elliptical partial differential equation into a much easier to
handle parabolic one. This was pointed out by Rao et al. (1974a)
who based their decision to neglect the pressure field on results
obtained by Onishi and Estoque (1968). They demonstrated that the
omission of the pressure gradient term has no significant conse-
quences for great downstream distances. Only in the immediate
vicinity of the roughness change ($\frac{x}{z_{02}} < 10^3$) will it have any
effect. For greater distances downstream no pressure effect is
noticeable.

The lower boundary condition after the step change assumes the
independence of both the surface relative humidity R_{02} and the
difference R_n-G (Eqs. (A3.27) and (A3.25) of downstream dis-

tance. Rao et al. (1974a) commented on the latter assumption
argueing that this simplification is only a crude approximation
which in practice seems to be quite reasonable. They did not com-
ment on the former assumption of the constant value of R_{02} how -
ever. This parameter is, together with z_{02}, the only externally
imposed quantity which does not change after the step in surface
conditions. The assumption of a constant value of R_{02} can lead
to a non-physical behaviour of the solution when a change occurs
from a cold and humid surface to a warm and dry one, as will be
shown in section 4.3.2. For the reverse change this problem does
not arise (see also Appendix 4).

Also, it should be mentioned that in order to define the mean
horizontal wind speed throughout the entire flow it is necessary
to impose the logarithmic wind profile condition down to $z = z_0$,
which is very doubtful to say the least. On the other hand, it is
possible that this approximation will only give a minor deviation
limited to the lowest layers near $z = z_0$.

With regard to the various modeling assumptions employed in the
present model, we must realize that there is much that still has
to be learned about the distribution and dynamics of the third
moment-and pressure-strain terms. Until more insight is gained
in this matter we must accept the sometimes drastic simplifica-
tions and crude assumptions which need to be made in order to
arrive at manageable expressions. However, the closure approxi-
mation of the third moment (4.9) remains unsatisfactory.
Wyngaard et al. (1974) use "a rather simpler, ad hoc gradient
diffusion model", although Wyngaard (1975, 1982) does not fail
to notice that in the unstable surface layer this approximation
probably will fail. Even in Wyngaard's study of the convective
PBL (Wyngaard and Coté, 1974) and in a similar study of the sta-
ble PBL (Wyngaard, 1975) he stresses this obvious deficiency of
the modeling approximation, but no attempt has been made to
overcome this imperfection.

Finally, the arguments that are used by Rao et al. to compute
62

the step in surface heat flux at x = 0 remain rather vague. The authors refer to a comment made by Sibbons (Rider et al., 1965) in which he proposes a method to calculate the surface heat flux just after x = 0. It is unfortunate that Sibbons also does not clearly point out how he calculated this value. However, calculations made in the present study revealed that the value of the surface heat flux at x = 0 only determines a parameter which is used to nondimensionalize every variable.

4.2 HOMOGENEOUS SITUATIONS

Before applying the present model to inhomogeneous situations its capability to handle homogeneous situations should be tested. This means that results should be compared with experimental data and existing views on the structure of the atmospheric surface layer above homogeneous terrain. Only if the model is able to handle such a less complex situation reasonably well, it will be possible to have any faith in its performance in inhomogeneous situations.

In this section the performance of the model in homogeneous situations will be analysed in two ways. First the equilibrium distribution of the variables calculated in Part I of the model will be checked with experimental data. Second the contribution of every term in the equations for the second moments will be calculated and compared with experimentally determined budgets of the second moment equations.

4.2.1 Equilibrium distributions

Numerous experiments have been conducted in the past to establish the distribution of first and second moments in the atmospheric surface layer above homogeneous terrain. In Chapter 1 we mentioned the best efforts known today. These experiments provided the data which were needed to determine many of the constants in the formulae describing the equilibrium distributions in the Monin-

63

Obukhov similarity framework (Businger et al., 1971; Yaglom, 1977; Viswanadham, 1982).

Through the years, experimental methods and instrumentation improved, and a gradual convergence to the range of values of the empirical constants accepted today has taken place. These values and formulae were used to define the lower and upper boundary conditions in the present model (see Appendix 3). When the values of all variables at the upper and lower boundaries are fixed, it is expected that the calculated equilibrium profiles must agree with empirical curves. However, deviations from the empirical curves between the fixed boundary values might still occur. To avoid an exhaustive discussion of the equilibrium distribution of all the dependent variables in the present model, a restriction is made to those quantities which are commonly used to measure flux densities.

In part I of the model the vertical turbulent flux densities of momentum, heat and water vapour are calculated. According to equation (A3.24) their dimensionless value at the surface equals -1, while the value at the upper boundary (A3.28) agrees with their linear decrease with height to zero at z_I (i.e. the height of the ABL). As is evident from Figure 4.1 the distributions of the three dimensionless flux densities are identical and indeed vary linearly with height to a very good degree.

Figure 4.2 presents the variation of the dimensionless gradient of the horizontal wind speed $(\frac{kz}{u_{*1}} \frac{\partial U}{\partial z})$ and the temperature $(\frac{kz}{T_{*1}} \frac{\partial \theta}{\partial z})$ with height. The dimensionless gradient of the absolute humidity is omitted since it coincides with $\frac{kz}{T_{*1}} \partial\theta/\partial z$. This can be inferred from (A3.17) and (A3.19) and the equality of the $\overline{\theta\theta}_v/T_{*1}^2$ and $\overline{q\theta}_v/q_{*1}T_{*1}$ distributions. Figure 4.2 shows that in a moderately unstable atmosphere the curve of the dimensionless temperature gradient coincides with the empirical ϕ_h-curve to a very good degree. The dimensionless gradient of the horizontal
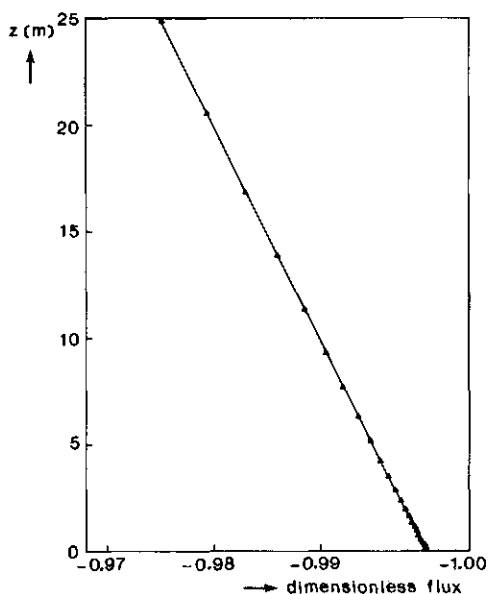
64

Figure 4.1   Vertical equilibrium distribution of the
            nondimensional turbulent fluxes of momentum,
            sensible and latent heat.

wind speed, however, deviates from the expected ϕ_m-curve, espe-
cially for large heights hence for large values of $|z/L|$. This
deviation points to two possible causes. Firstly, it indicates
that at least one of the modeling assumptions lacks a correction
for buoyancy effects. Indeed, if we look at the modeling expres-
sions used by Wyngaard and Coté (1974) and by Wyngaard (1975),
for an unstable and stable atmosphere respectively, we see that
they also had to add buoyancy and mean strain corrections in
order to arrive at physically realistic results. Though their
studies concentrated on the whole of the PBL, instead of only
the atmospheric surface layer, a fair amount of their grid levels
were situated in the latter layer because their vertical grid
spacings increased logarithmically with height. Efforts in the
present study to add similar corrections to the modeling expres-
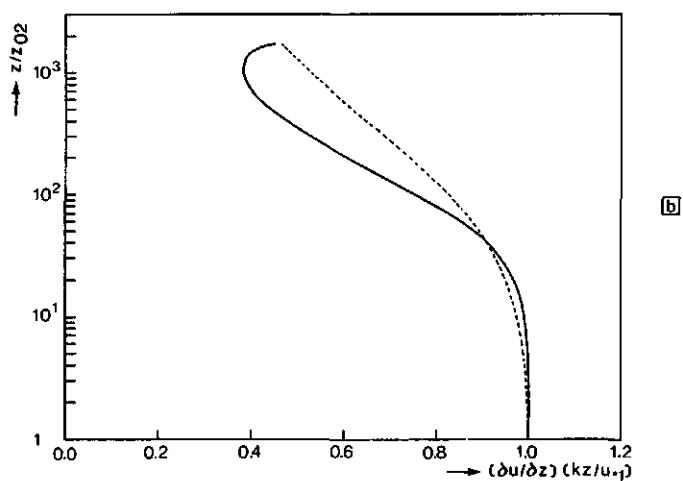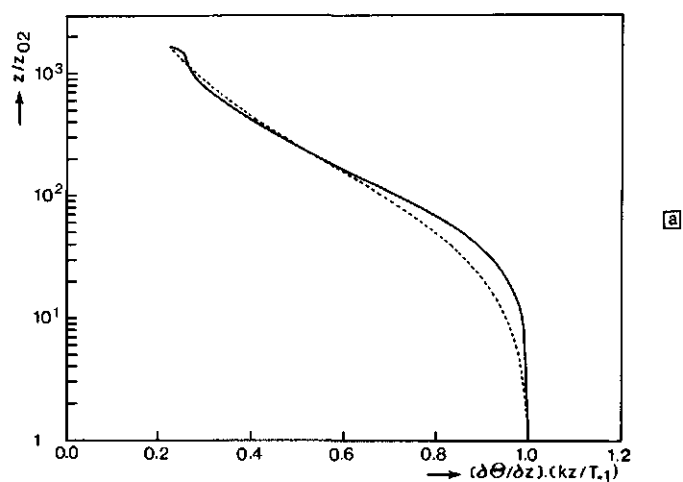sions employed in the present model have not yet produced

Figure 4.2   Distribution of the dimensionless gradient of
temperature (a) and horizontal wind speed (b).

a: ---- ϕ_h ,   —— $(\partial\Theta/\partial z).(kz/T_{*1})$

b: ---- ϕ_m ,   —— $(\partial U/\partial z).(kz/u_{*1})$

entirely satisfactory results.

The second possible cause is the definition of the upper boundary conditions. The model constants that appear as a factor in front of the dissipation and destruction terms have been determined by invoking the equality of both sides of the equations at the lower boundary. At the upper boundary, however, the equality of both sides of the equations need no longer be present, for the buoyancy terms are also important there. This inequality might force the gradient $\partial U/\partial z$ from its expected $\phi_m(z/L)$ distribution.

4.2.2 Assessment of budgets

To transform the set of equations (2.34)-(2.36) and (4.1)-(4.6) and (4.14) to the homogeneous case, it will simply suffice to put $\partial/\partial x = 0$, and by virtue of the equation of continuity (2.29) also $W = 0$. As a result the equations (2.34)-(2.36) read

$$\partial\overline{uw}/\partial z = 0, \qquad \partial\overline{w\theta}/\partial z = 0 \quad \text{and} \quad \partial\overline{wq}/\partial z = 0 . \qquad (4.15)$$

This indicates the existence of a constant flux layer. Applying these conditions to Eqs. (4.1)-(4.6) and (4.14), or rather to the same equations after modeling, the equations for the second moments and for $\overline{\varepsilon}$ in the homogeneous case are obtained. These equations are summarized in Appendix 3. Using the equilibrium profiles evaluated in the initialization program (Part I) we calculated the contribution of each term to the equation in which it is incorporated, thus enabling us to analyse the budgets of Eqs. (4.1)-(4.6) and (4.14) in homogeneous situations.

On inspecting (4.1)-(4.6) and (4.14) it appears that production, pressure gradient interaction, dissipation and/or molecular destruction terms are largest near the surface where all gradients are steepest and turbulent interaction is strongest. Going upwards into the atmosphere, most terms quickly diminish in magnitude as gradients are decreasing rapidly. This makes it difficult

67

to analyse them forthwith. When drawn on a linear height scale, it is next to impossible to gain any further information from the rapidly decreasing values of almost every term. To reveal the details of the budget also at higher levels, we multiply every term of a given equation with a properly chosen height dependent scale. We will adopt the approach of e.g. Wyngaard and Coté (1970), Wyngaard et al. (1971, 1978) and Bradley et al. (1981) who used kz divided by the proper combination of u_*, T_* and q_*.

Experimental determination of the budget of second moment equations is restricted to those of $\overline{\theta^2}$, $\overline{q\theta}$, $\overline{uw}$, $\overline{w\theta}$, $\overline{u\theta}$ and $\overline{e^2}$ = $\overline{u^2} + \overline{v^2} + \overline{w^2}$. This means that we can only examine the budgets of the corresponding equations from Eqs. (A2.19)-(A2.30). We will restrict ourselves to respectively: $\overline{\theta^2}$, $\overline{u\theta}$, $\overline{e^2}$ and $\overline{uw}$.

Temperature variance budget
Nondimensionalizing Eq. (A3.21) by multiplication with $kz/u_*T_*^2$ produces

$$\phi_m - \tfrac{1}{2} \frac{kz}{u_*T_*^2} a_t \frac{\partial}{\partial z}(\overline{w^2}\tau \frac{\partial \overline{\theta^2}}{\partial z}) + \frac{kz}{u_*T_*^2} b \frac{\overline{\theta^2}}{\tau} = 0 \quad . \qquad (4.16)$$
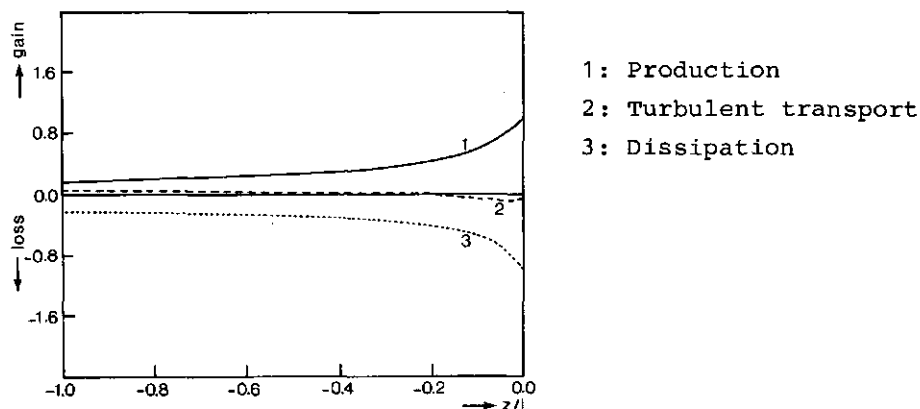

1: Production
2: Turbulent transport
3: Dissipation

Figure 4.3   Budget of the temperature variance equation.

In Figure 4.3 the magnitude of every term of this equation is given as a function of z/L. It is evident that there is an almost perfect balance between the production and dissipation term in moderately unstable and near neutral conditions. It means that the turbulent transport term is at least an order of magnitude smaller than both the production and the dissipation term. This agrees with experimental data from Bradley et al. (1981), Champagne et al. (1977) and Wyngaard and Coté (1971). If it has any significance at all, turbulent transport is a loss in near neutral situations and a gain in moderately unstable conditions. This was also noticed by Wyngaard and Coté (1971), although their data show much scatter and their observation might be considered tentative. For moderately to strong unstable conditions $(- z/L \cong 1)$ the ratio production/dissipation attains a value of 0.8 which is in accordance with the data of Champagne et al. (1977) but not with the data of Bradley et al. (1981).

Horizontal heat flux budget
Equation (A3.16) is nondimensionalized with $kz/u_*^2 T_*$ and reads

$$\phi_m + \phi_m + \frac{kz}{u_*^2 T_*} a_t \frac{\partial}{\partial z}(\overline{w^2}_\tau \frac{\partial \overline{u\theta}}{\partial z}) + \frac{kz}{u_*^2 T_*} d_1 \frac{\overline{u\theta}}{\tau} = 0 . \qquad (4.17)$$

Figure 4.4a shows the variation of every term of this equation with z/L. The turbulent transport is a small term representing a loss over the entire range of -z/L values considered here. This does not completely agree with the results of Bradley et al. (1981) and Wyngaard et al (1971). Although they also concluded that the turbulent transport term is very small in comparison with the remaining terms of the $\overline{u\theta}$-equation, they found a different behaviour of this term with -z/L. According to Bradley et al. turbulent transport is a loss for near neutral conditions (-z/L < 0.1) while beyond this value it represents a gain. Wyngaard et al. found a value of -z/L $\cong$ 0.3 for which this change in sign occurs. Figure 4.4 presents the $\overline{u\theta}$-budget found by Wyngaard et al. (1971) by comparison.
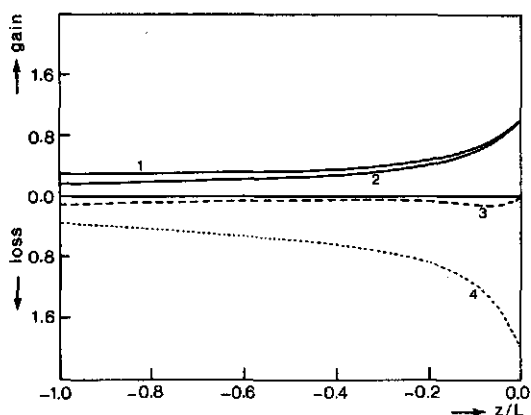
69
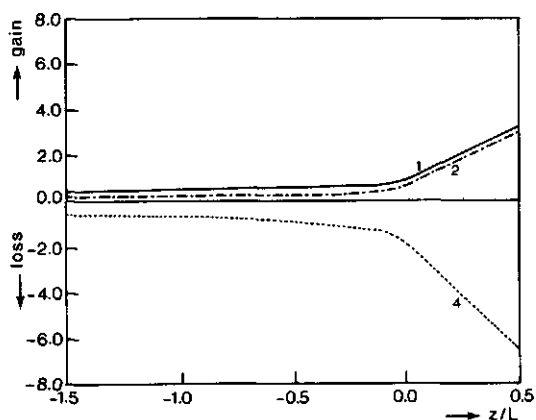
Figure 4.4   Budget of the horizontal heat flux equation;
a. present model, b. Wyngaard et al. (1971).

Turbulent kinetic energy budget
Adding Eqs. (A3.12)-(A3.14) and nondimensionalizing the result
with kz/u_*^3 yields

$$\phi_m - \frac{z}{L} + \frac{kz}{u_*^3} \, a_t \, \frac{\partial}{\partial z}(\overline{w^2} \tau \, \frac{\partial \overline{e^2}}{\partial z}) - \frac{kz}{u_*^3} \, \overline{\varepsilon} = 0 \ . \tag{4.18}$$

As a consequence of the modeling technique applied to the tur-
bulent transport and pressure transport terms (see Appendix 3)
it is not possible to separate the contribution of both terms to
the TKE budget. This means that the third term in Equation (4.18)

70

represents the contribution of both terms. The dependence of all terms on z/L is given in Figure 4.5a. An experimental determination of this budget was performed by Wyngaard and Coté (1971) and by Champagne et al. (1977). The results of Wyngaard and Coté are summarized in Figure 4.5b. To facilitate comparison, we have added the contributions of the imbalance term (= pressure transport term) and the turbulent transport term of their measurements. The sum of these contributions represents a gain for the given range of -z/L values. This implies that dissipation exceeds the total production in near neutral to moderately unstable situations. For increasing instability a balance between the total production and

1: Imbalance
2: Buoyancy production
3: Shear production
4: Turbulent transport
5: Dissipation
6: Imbalance + Turbulent transport
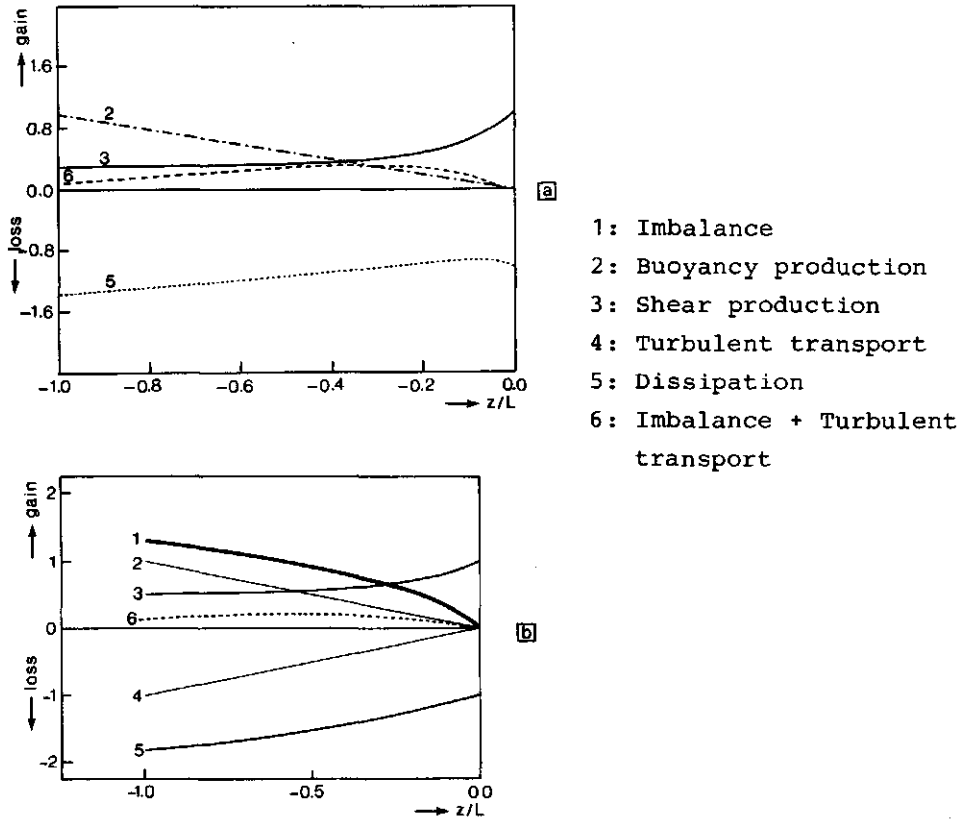
Figure 4.5   Budget of the turbulent kinetic energy equations;
             a. present model, b. Wyngaard and Coté (1971).

dissipation is approached for the total transport term diminishes in magnitude. This is consistent with the data from Wyngaard and Coté. Shear production deviates from $\phi_m(z/L)$ by the reasons mentioned before, while buoyancy production follows the expected $-z/L$ behaviour very well.
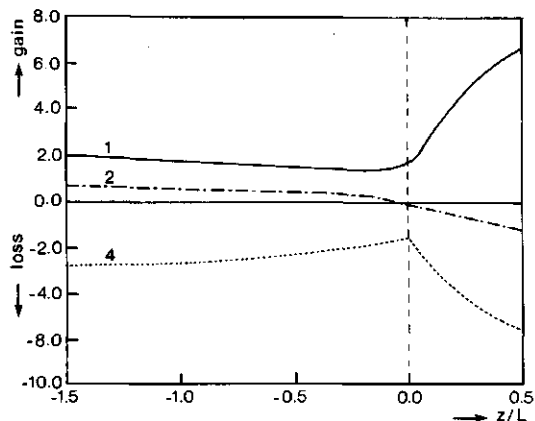
Shear stress budget
Multiplication of Equation (A3.15) with kz/u_*^3 yields

$$\frac{\overline{w^2}}{u_*^2} \phi_m + \frac{\overline{u\theta}}{\overline{w\theta}} \frac{z}{L} + \overline{uw} \frac{c}{\tau} \frac{kz}{u_*^2} = 0. \tag{4.19}$$
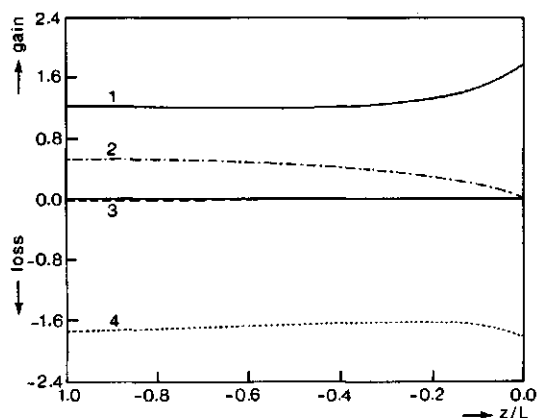
1: Shear production
2: Buoyancy production
3: Turbulent transport
4: Pressure gradient
   interaction

Figure 4.6   Budget of the shear stress equation;
a. present model, b. Wyngaard et al. (1971).

72

The first two terms represent shear production and buoyancy production respectively. The third term is the approximation for the pressure gradient interaction term, which always represents a loss in the atmospheric surface layer. Buoyancy production is a loss (gain) in stable (unstable) stratification. Shear production will always be a gain. Figure 4.6a presents the magnitude of these terms for unstable situations as calculated with the present model. It compares favourably with the experimental data obtained by Wyngaard et al. (1971) which are summarized in Figure 4.6b. The factor $\overline{u\theta}/\overline{w\theta}$ in the buoyancy production term reduces the importance of this term for increasing values of $-z/L$. Values of the factor $\overline{u\theta}/\overline{w\theta}$ were determined by Wyngaard et al. They found that the magnitude of this factor ranges from 3.4 to 0.6 for $-z/L$ ranging from 0 to 1.0. This agrees with the values calculated with the model viz. they range from 3.0 to 0.4 for the same $-z/L$ interval.

The factor $\overline{w^2}/u_*^2$ in the shear production term is always greater than unity. This implies that the shear production rate of shear stress exceeds the shear production rate of energy (eq. 4.18) over the entire stability range. Moreover, as $\overline{w^2}/u_*^2$ increases with increasing instability, it is obvious that the importance of this production term will not diminish as $-z/L$ increases. Wyngaard et al. actually found an increase of the shear production term for increasing instability, which does not agree with the results of our model, but this is a consequence, once again, of the deviations mentioned in 4.2.1.

4.2.3 Conclusions

The equilibrium profiles in the atmospheric surface layer generated by the present model agree with experimentally determined distributions. This is not surprising since both the upper and lower boundary conditions are chosen to ensure this. However, deviations still occur in moderate to strong unstably stratified boundary layers, where non-monotonic curves appear. These deviations are ascribed to the exclusion of buoyancy corrections in

the closure approximations for the higher order moments and to the inequality of the model equations when the upper boundary conditions are substituted.

The agreement of the budgets of the second moment equations with experimental data is satisfactory, although the scatter in some of the data is rather large and some terms are measured only indirectly. This makes several of our comparisons rather uncertain.

4.3   ANALYSIS OF INHOMOGENEOUS SITUATIONS

4.3.1   Single step in surface conditions

In order to get an appreciation of the quality of performance of the present theoretical model in inhomogeneous situations, a comparison should be made with experimentally obtained data. Model and experiment must of course be carefully tuned to each other. This means that external conditions (two-dimensionality, upstream and downstream roughness lengths, atmospheric stratification) should match as good as possible.

Many comparisons between the theory of relaxing flows and first moments such as the mean horizontal wind speed or the mean temperature have already been made in the past. Thus many times the usefulness of existing models that predict first moments has been demonstrated. We will not repeat such an analysis for the present model, as this would merely lead to the same conclusions drawn by Rao et al. (1974a) and the remarks made in Chapter 3. Furthermore, the gain in accuracy achieved by a second order closure model instead of a less complex first order closure model is primarily to be found in the prediction of the behaviour of the second moments (turbulent fluxes and other covariances). The first moments are already predicted with good accuracy even by the first order closure models.

The above considerations lead inevitably to the conclusion,

74

already made in section 3.5.3, that we must concentrate our
attention on the second moments when analyzing the performance
of the present model. In section 3.5.3 it was noticed that
reliable measurements of second order properties of turbulence
in the atmosphere above non-homogeneous terrain are very hard to
come by. In fact, the only data of second moments published till
today are the measurements performed by Peterson et al. (1979),
Højstrup (1981) and Lang et al. (1983). Figure 4.7 e.g. presents
the variation of the horizontal wind variance profile after a
SR change in surface roughness. The turbulent kinetic energy
model of Peterson (1969) seems to predict the behaviour of

$$\sigma_u = (\overline{u^2})^{\frac{1}{2}}$$

reasonably well, but this is one of the very few examples where
a direct comparison has ever been made.
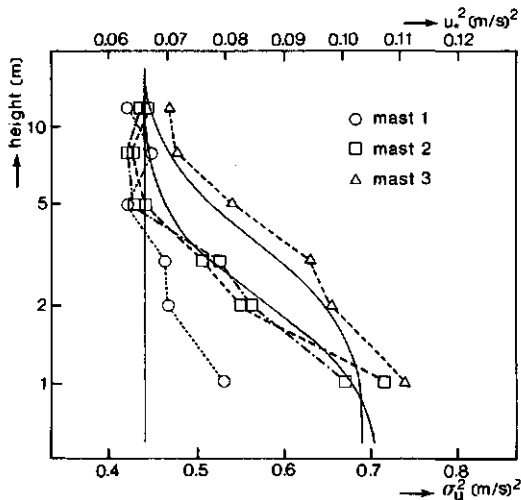

Figure 4.7   Variation of the horizontal wind variance profile
            after a smooth to rough transition.
            ——Peterson's 1969 model. (After Peterson et al., 1979).

Obviously, the scarcity of data of second moments in nonhomoge-
neous conditions, obtained by measurements in the atmosphere is
such that the comparison with model results will not lead to a

definite qualification of the performance of 2nd order models. This is what Bradshaw (1972) called the "fact gap": too many computers chasing too few facts.

This situation can partially be remedied by including windtunnel measurements in our consideration. The carefully designed experiments in a windtunnel often provide us with an abundance of mean and turbulence quantities suitable for model performance evaluation. But the difficulties and deficiencies inherent to the use of wind tunnel data for modeling atmospheric situations are not at all trivial, especially not when using these data for such goals as assessing the predictive qualities of numerical models designed for atmospheric situations.

4.3.2   Consistency of the present model

As experimental verification of the model results is not satisfactorily feasible and awaits the progress and development of experimental methods and instruments, we turn to another prerequisite of any model: it should be consistent with itself. This means that if a given initial equilibrium state of the atmospheric surface layer is subjected to two consecutive changes in surface conditions: the first change to a new set of surface characteristics and the second change back to the original set of surface characteristics, the atmosphere should ultimately return to its original equilibrium. It means that if an equilibrium surface boundary layer encounters a temporary disturbance, the deviations generated by this disturbance should die out as the flow progresses across its original surface.

To this end the distribution of every variable of the model was calculated when it was subjected to the set of boundary conditions presented in Figure 4.8. For x < 0 the equilibrium initial profiles were calculated using the predetermined surface parameters as discussed in section 4.1. At x = 0 the airflow encounters a surface which is rougher, warmer and dryer than the surface for x < 0. After an arbitrary distance of 21 meters the surface con-
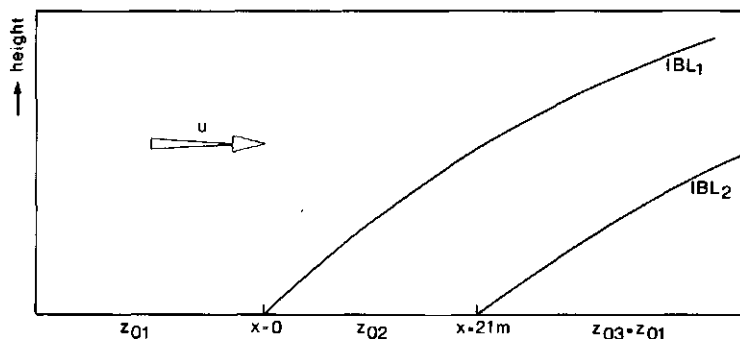
76

Figure 4.8   Definition sketch of two subsequent changes in
             surface conditions.

ditions change for the second time and regain their original
value. This applies to the surface roughness and the surface
relative humidity, the other surface parameters depend on the
downstream distance (x).

Two questions are interesting in the given situation. Firstly,
do the variable surface parameters (u_*, T_* and q_*) return to the
values they possessed at x < 0. And if so, how rapidly do these
values return. Secondly, what happens to the disturbances intro-
duced into the profile of every variable after the second step
change?

Figure 4.9a presents the variation of u_*, T_* and q_* with the
downstream distance (x) after the first step at x = 0 and after
the second step at x = 21 m. Along the vertical axis the ratios
$u_*(x)/u_{*1}$, $T_*(x)/T_{*1}$ and $q_*(x)/q_{*1}$ are plotted, where u_{*1}, T_{*1} and
q_{*1} are the original equilibrium values of the upstream surface
(x < 0). The three variables u_*, T_* and q_* determine the surface
fluxes of momentum, sensible heat and latent heat respectively by
virtue of

$$\tau(x) = -\rho \{u_*(x)\}^2 \tag{4.20}$$

$$H_0(x) = -\rho c_p\, u_*(x) T_*(x) \tag{4.21}$$

$$\lambda E_0(x) = -\rho\lambda\ u_*(x)q_*(x) \hspace{4cm} (4.22)$$

Starting with $u_*(x)/u_{*1} = 1$, $T_*(x)/T_{*1} = 1$ and $q_*(x)/q_{*1} = 1$ at $x = 0$, these variables are subjected to a change in surface conditions. After the first step at $x \simeq 0$ the variables over(under)shoot after which they gradually approach a new equilibrium value, which is different from the original one. This new equilibrium value is not reached however, because at $x \simeq 21$ m the second step generates a new over(under)shoot and the variables at the surface gradually adjust once again to the new surface.
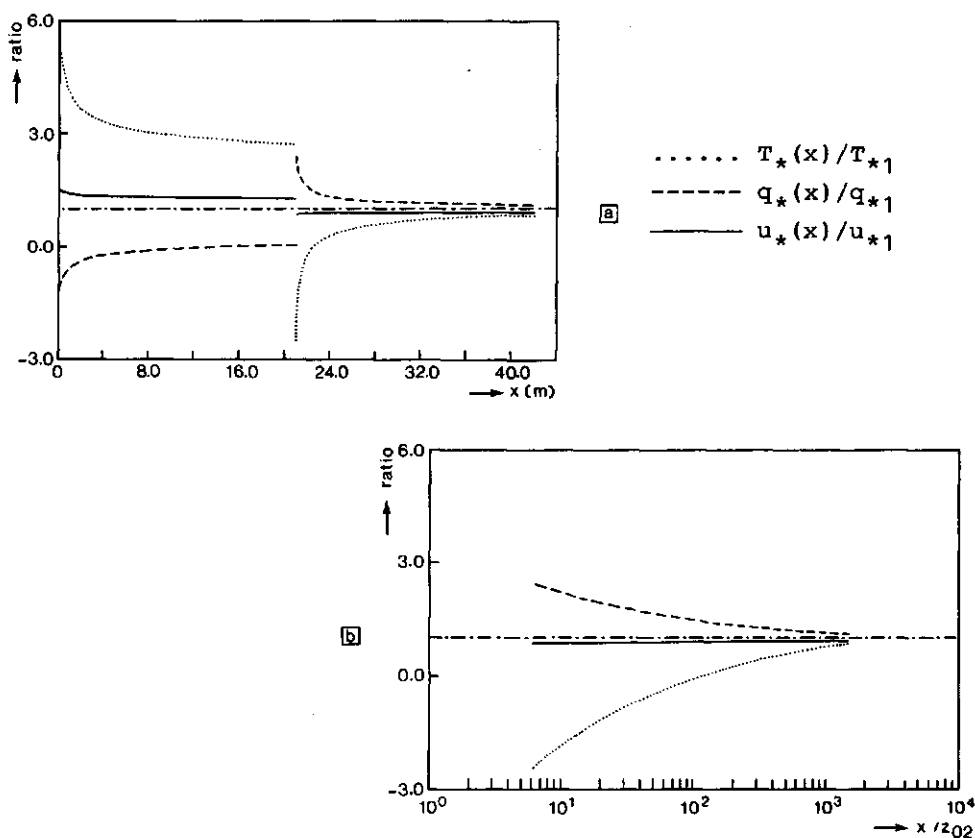

Figure 4.9   Variation of surface parameters for two
              subsequent changes in surface conditions.

The present model is consistent with itself if, after the second step change the dimensionless surface variables approach their equilibrium value of unity again. This happens indeed as can be seen in Figure 4.9b for x > 21 m. The logarithmic scale corresponds with the second part of Figure 4.9a.

The multitude of first and second moment variables in the current model makes a full description of every variable unattractive for reasons of brevity and readability. Therefore, a restriction is made in this section to the behaviour of the profiles of the mean temperature, absolute humidity and those of the vertical fluxes of humidity and heat.

Figures 4.10 and 4.11 present the profiles of the above mentioned variables for (i): the relaxation after the first surface discontinuity and (ii): the relaxation after the second surface discontinuity and the approach of the original equilibrium situation. Figure 4.10 gives the variation of the absolute humidity and the humidity flux for the two different situations. After the first transition the absolute humidity profile adjusts itself in the manner as shown in Figure 4.10a. Especially in the lowest layers the absolute humidity drops because the surface flux of water vapour has suddenly been reduced by the less humid surface. This decrease in absolute humidity gradually affects layers of greater height, and for $x/z_{02} = 1.5 \cdot 10^3$ the change in surface humidity is noticeable up to a height of 0.8 m. At this downstream distance no new equilibrium has yet been reached.

The last profile (curve no.8) in Figure 4.10a serves as the initial profile in Figure 4.10b, which gives the absolute humidity profiles after the second surface transition. At the lowest layers the absolute humidity increases again because of the humid surface. Again this increase diffuses upwards, though not to the highest layers where the decrease due to the first transition is still continuing. No new equilibrium is reached at $x/z_{02} = 3 \cdot 10^3$ but the original profile is approached and the disturbance damps

out as x increases.

From a physical point of view it is not possible to have a posi-
tive value of $\partial Q/\partial z$, indicating a negative (i.e. downward) tur-
bulent humidity flux adjacent to the surface. This would imply
that water vapour is transported downwards and is absorbed at the
surface. This is clearly impossible, for it means that condensa-
tion is taking place at the surface, while at the same time the
surface relative humidity remains unchanged at R_{02} < 100%. This
obvious model deficiency is attributed to the boundary conditions
(A3.25) and (A3.27) and was also discussed in section 4.1.3. A
more realistic boundary condition was suggested by McNaughton
(1984) on the basis of the Penman-Monteith equation, discarding
with Eq. (A3.27). This is discussed in Appendix 4.

The features encountered in the profiles of the absolute humidity
can also be understood in view of the profiles of the vertical
humidity flux (Figures 4.10c,d). The factor $u_{*1}q_{*2}$ is used to
nondimensionalize this flux. As q_{*2} < 0 and u_{*1} > 0 the dimen-
sional value of $\overline{wq}$ has a sign opposite from its dimensionless
value. Just after the first transition $\overline{wq}$ decreases from its
originally positive value to a negative, indicating a reversal
of the direction of the flux in the atmosphere just above the
surface, depleting these layers of water vapour. As $\overline{wq}$ increases
monotonically with z, a decrease of the absolute humidity at every
height occurs, in accordance with Figure 4.10a. After some dis-
tance downstream the surface value of $\overline{wq}$ becomes positive again
(curve no.8), which is reflected in the corresponding curve in
Figure 4.10a, where the vertical gradient of the absolute humi-
dity is negative at all heights.

After the second transition the $\overline{wq}$ curve is no longer monotoni-
cally increasing but exhibits a minimum value. The part of the
curve under this minimum represents an upward flux which decrea-
ses with height. At these levels the absolute humidity increases
with x, in accordance with Figure 4.10b. The part of the curve
above the minimum represents an upward flux which increases with

80
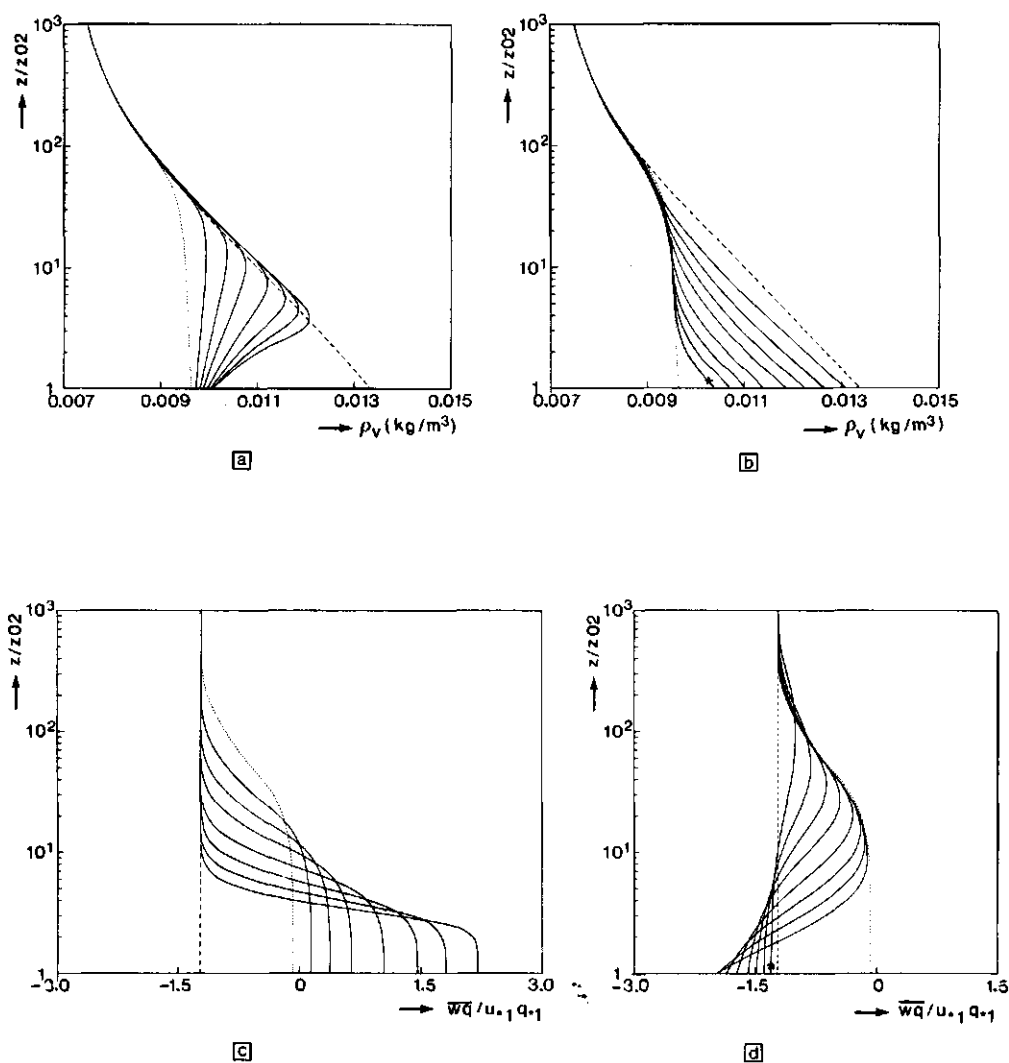
```
........    Profile at x = 21 m.
-------     Initial profile (x < 0).
   *        Profile at x = 42 m.
```
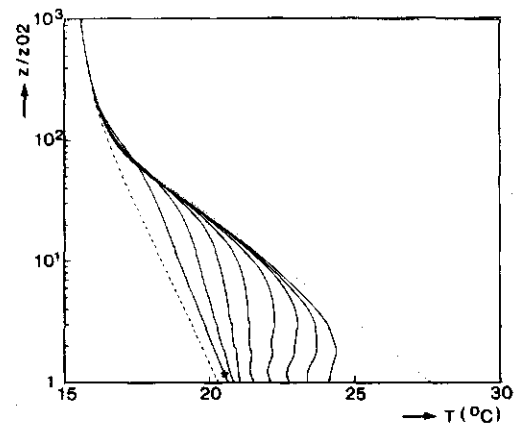
Figure 4.10   Profiles of the absolute humidity and the turbulent
               flux of water vapour after two subsequent changes in
               surface conditions for various distances downstream.
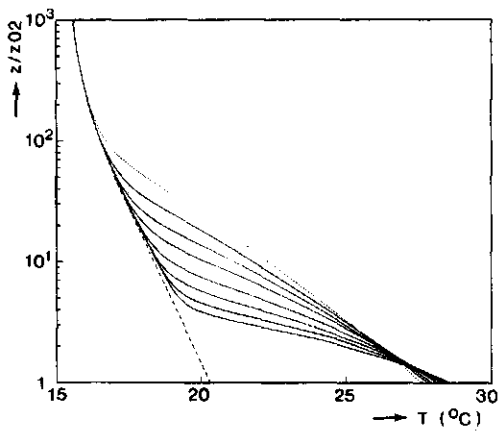
.... Profile at x = 21 m.
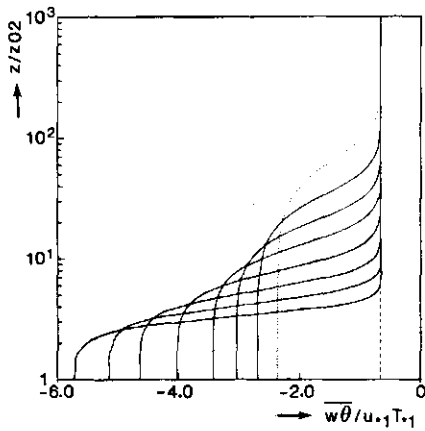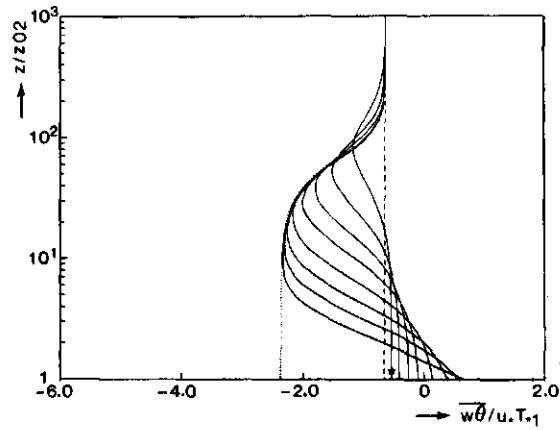
------ Initial profile (x < 0).

* Profile at x = 42 m.

Figure 4.11 Profiles of the temperature and the turbulent flux
of sensible heat after two subsequent changes in
surface conditions for various distances downstream.

height. At these levels the absolute humidity is still decreasing due to the former dryer surface. Further downstream, the $\overline{wq}$ profile returns to its equilibrium distribution where it is constant with height. The disturbance gradually damps out.

Observations, analogous to the ones just made on the absolute humidity and vertical humidity flux profiles can be made with respect to the mean temperature and vertical sensible heat flux profiles which are presented in Figure 4.11. We present this figure for completeness only and will not discuss it.

4.4 SUMMARY

Summarizing the results of the examination of the performance of the present model we can say that in its present state the model contains several imperfections which can be roughly divided into two classes:
(i)   imperfect modeling expressions and/or imperfect upper
      boundary conditions
(ii) unrealistic lower boundary conditions after the step change.

The flaws belonging to the first class betray their existence only in diabatic conditions when they produce deviations which are notably marked in the vertical gradient of the mean horizontal wind speed. Adjusting the modeling expressions for buoyancy and mean strain effects introduces a whole new set of numerical constants which must be tuned to obtain the desired results.

The imperfection which solely comprises the whole of the second class is the rather unrealistic assumption of a constant surface relative humidity after $x = 0$. This assumption is able to generate physically unrealistic results, and it certainly is subject to improvement.

5 Fluxes derived from the initial profiles

5.1 INTRODUCTION

Apart from the bulk methods the flux-profile methods, used to determine the surface flux densities, require the (relatively) least effort and (relatively) cheapest instruments. This was discussed in Chapter 1. It is therefore not surprising that this method, or rather this class of methods, has been used extensively and that it is still the most widely adopted method in many disciplines. It is for this reason that literature on this subject has proliferated enormously (for reviews see e.g. Brutsaert, 1982, de Bruin, 1982).

In Chapter 2 it was demonstrated that this method may only be applied if the upstream terrain is homogeneous for a considerable distance. In practice, this condition often is difficult to satisfy, which means that the flux-profile methods are often used in non-homogeneous situations.

As this method has been, and still is, applied so often, it is justifiable to concentrate the main effort in this study on the behaviour of the flux-profile method in non-homogeneous situations.

However, before that analysis can be made it must be known if, in the homogeneous case, the fluxes determined with the various standard methods are consistent with each other. Hence the standard flux-profile methods will be studied when they are applied to the equilibrium distributions of U, θ and Q generated by Part I of the model. In section 5.2 a brief review of the standard flux-profile relations is presented. Using the modeled equations for the turbulent fluxes $\overline{uw}$, $\overline{w\theta}$ and $\overline{wq}$ a set of so-called "second order flux-profile relations" is derived in section 5.3. This new set of relations is needed for the analysis of the flux profile relations above non-homogeneous terrains,

performed in Chapter 6. The second order flux-profile relations
are identical with the standard flux-profile relations if some
specific conditions are met. This will be discussed in section
5.4. In that section the results will be considered of the stan-
dard flux profile relations when these are applied to the equi-
librium profiles.

5.2 SUMMARY AND COMPARISON OF THE FLUX-PROFILE RELATIONS

Through the application of dimensional analysis, invoking
similarity, Obukhov (1946, 1971) has shown that the vertical
fluxes of momentum, sensible heat and water vapour are related
to the profiles of windspeed, temperature and humidity by:

$$I = - \rho k u_* z \frac{\partial U}{\partial z} / \phi_m (z/L) \quad , \tag{5.1}$$

$$H = - \rho c_p k u_* z \frac{\partial \Theta}{\partial z} / \phi_h (z/L) , \tag{5.2}$$

$$E = - \rho k u_* z \frac{\partial Q}{\partial z} / \phi_w (z/L) , \tag{5.3}$$

where ϕ_m, ϕ_h and ϕ_w are the dimensionless gradients of U,
Θ and Q respectively:

$$\phi_m (z/L) = \frac{\partial U}{\partial z} \cdot \frac{kz}{u_*} \quad , \tag{5.4}$$

$$\phi_h (z/L) = \frac{\partial \Theta}{\partial z} \cdot \frac{kz}{T_*} \quad , \tag{5.5}$$

$$\phi_w (z/L) = \frac{\partial Q}{\partial z} \cdot \frac{kz}{q_*} \quad . \tag{5.6}$$

These dimensionless gradients are universal functions of the
stability parameter z/L, where the Obukhov length (L) is defined
by:

$$L = - \frac{T_r}{gk} \cdot \frac{u_*^3}{(-u_* T_* - 0.61 \, T_r u_* q_*)} \cdot \tag{5.7}$$

The respective fluxes after substituting (5.4)-(5.6) into

(5.1)-(5.3) read:

$$I = - \rho u_*^2 , \tag{5.8}$$

$$H = - \rho c_p u_* T_* , \tag{5.9}$$

$$E = - \rho u_* q_* . \tag{5.10}$$

Equations (5.4)-(5.6) are referred to as the Monin-Obukhov similarity theory. These equations form the starting point of every flux-profile method applicable in the atmospheric surface layer. Equations (5.4)-(5.6) may only by employed when considering a horizontal, uniform surface under stationary conditions, and when we restrict ourselves to the atmospheric surface layer. As the functional form of the ϕ's is not predicted by the Monin-Obukhov similarity theory they have to be determined experimentally. Any experiment performed to achieve this objective must necessarily fulfill the above mentioned conditions. Thus the best sets of data were gathered above extensive, flat, homogeneous, featureless terrains (Kansas, Minnesota, Wangara). Many functional relationships were proposed during the last two decades, they were reviewed by Dyer (1974), Yaglom (1977) and Visnawadham (1982). In the present study the relations proposed by Dyer (1974) will be used:

$$\phi_m = \phi_h^{\frac{1}{2}} = (1 - 16 \ z/L)^{-\frac{1}{4}}; \text{ for } z/L < 0 \text{ (unstable case)} \tag{5.11}$$

$$\phi_m = \phi_h = 1 + 5 \ z/L \quad ; \text{ for } 0 < z/L < 1 \text{ (stable case)} \tag{5.12}$$

$$\phi_w = \phi_h \quad\quad\quad\quad ; \text{ for all } z/L \tag{5.13}$$

where $k = 0.41$.

If these relations are accepted, and $\partial U/\partial z$, $\partial\theta/\partial z$ and $\partial Q/\partial z$ are measured, Eqs. (5.4)-(5.6) constitute three coupled equations in three unknowns u_*, T_* and q_*. Usually Eqs. (5.4)-(5.6) are solved iteratively in their integrated form (Brutsaert, 1982;

86

de Bruin, 1982) but we will not elaborate on this point. The
three gradients are determined by measuring U, θ and Q at at
least two levels. Or either three at only one level, if respec-
tively the surface roughness length, the surface temperature or
the surface specific humidity is known. This standard flux
profile method is also known as the Aerodynamic Method (see
Table 5.1).

Table 5.1. Summary of input parameters for the application of
the various standard flux profile methods.

Method	R_n-G	U	θ	Q	Remarks
1. Aerodynamic method	− −	+ + + z_o	+ + + +	+ + + +	Iteratively; coupling by L
2. Bowen ratio method	+	−(+)−(+)	+ +	+ +	If I wanted: add U measurements
3. Combination method	+ + + +	+ + + z_o + + + z_o	+ + + + − − − −	− − − − + + + +	λE from energy balance (iteratively) H from energy balance (iteratively)

*N.B. +(++) measurements at 1 (2) level(s) required.

If the fluxes of heat and water vapour are coupled by means of
the energy balance equation, other possibilities arise. In its
simplest form (ignoring the smallest terms) the energy balance
equation reads:

$$R_n = H + \lambda E + G ,$$ (5.14)

where λ is the latent heat of vaporization.
Eq. (5.14) states that the net flux density of incoming radia-
tion energy (R_n) is distributed over the soil heat flux
density (G), the sensible heat flux density (H) and the latent

87

heat flux density (λE), counting all fluxes, except R_n, directed away from the surface positive. The quantities R_n and G are readily measured, which means that Eqs. (5.4)-(5.6) and (5.14) constitute four equations in three unknowns. The three possibilities that are presented to us are the three combinations consisting of Eq. (5.14) and two out of three equations from (5.4)-(5.6).

If Eq. (5.4) is excluded from the set of four equations we arrive at the "Bowen Ratio Method" (see Table 5.1). As $\partial U/\partial z$ is not determined no windspeed measurements need to be made. If the Bowen ratio is defined by

$$\beta = \frac{H}{\lambda E} \ , \tag{5.15}$$

and Eqs. (5.2) and (5.3) are substituted, we obtain

$$\beta = \frac{c_p}{\lambda} \cdot \frac{\partial \Theta/\partial z}{\partial Q/\partial z} \ , \tag{5.16}$$

where use has been made of Eq. (5.13).

Eq. (5.16) shows that the Bowen ratio can be determined by measuring temperature and humidity at two levels. The fluxes follow from

$$\lambda E = \frac{R_n - G}{1 + \beta} \ , \tag{5.17}$$

and

$$H = \beta \cdot \frac{R_n - G}{1 + \beta} \ . \tag{5.18}$$

The advantage of the Bowen ratio method is that it is independent of the functional form of ϕ_h and ϕ_w, as long as Eq. (5.13) applies. This method is also independent of the value of k, except for the determination of u_*, but it is not likely that u_* will be determined this way. Another advantage of this method is that it is not necessary to measure the exact height of the sen-

sors above the ground, as long as the two sets of sensors are mounted at the same heights. The disadvantage of the Bowen ratio method is that it does not apply when $R_n - G = 0$ (near sunrise and sunset) (Fuchs and Tanner, 1970; Sinclair et al., 1975; Revfeim and Jordan, 1976).

If either Eq. (5.5) or (5.6) is excluded from the set of equations (5.4)-(5.6) and (5.14), we refrain from temperature or humidity measurements respectively. As humidity measurements in the atmosphere are more difficult to perform than temperature measurements Eq. (5.6) usually will be the one that is excluded (see Table 5.1). This method, known as the "Combination Method", shares with the aerodynamic method the inherent uncertainties connected with the definition of the ϕ 's and the value of k. The advantage is that no humidity measurements are needed if Eq. (5.6) is excluded.

For comparison with the flux profile relations which will be derived from the modeled second order transport equations in 5.3 the flux densities are redefined in terms of eddy covariances:

$$I = \rho \; \overline{uw} \; , \tag{5.19}$$

$$H = \rho c_p \; \overline{w\theta} \; , \tag{5.20}$$

$$\lambda E = \rho \lambda \; \overline{wq} \; . \tag{5.21}$$

If Eqs. (5.1)-(5.3) are substituted into (5.19)-(5.21) respectively, we obtain:

$$\overline{uw} = - ku_* z \; \frac{\partial U}{\partial z} / \phi_m (z/L) = - K_m \frac{\partial U}{\partial z} \; , \tag{5.22}$$

$$\overline{w\theta} = - ku_* z \; \frac{\partial \Theta}{\partial z} / \phi_h (z/L) = - K_h \frac{\partial \Theta}{\partial z} \; , \tag{5.23}$$

$$\overline{wq} = - ku_* z \; \frac{\partial Q}{\partial z} / \phi_w (z/L) = - K_w \frac{\partial Q}{\partial z} \; . \tag{5.24}$$

89

The eddy diffusivity K of a property, introduced in these equations, is defined as the ratio of the property flux density to its concentration gradient, viz.

$$K_m = -I/(\rho \frac{\partial U}{\partial z}) = ku_* z/\phi_m(z/L) \quad , \tag{5.25}$$

$$K_h = -H/(\rho c_p \frac{\partial \Theta}{\partial z}) = ku_* z/\phi_h(z/L) \quad , \tag{5.26}$$

$$K_w = -\lambda E/(\rho \lambda \frac{\partial Q}{\partial z}) = ku_* z/\phi_w(z/L) \quad . \tag{5.27}$$

5.3 FLUX PROFILE RELATIONS DERIVED FROM THE MODELED TRANSPORT
      EQUATIONS

The modeled second order equations in the homogeneous case
(A3.12)-(A3.23) provide us with another possibility of deriving
flux profile relations. Rewriting the equations for the vertical
turbulent fluxes (A3.15), (A3.17) and (A3.19) for $\overline{uw}$, $\overline{w\theta}$ and $\overline{wq}$
respectively, we find after neglecting the turbulent transport
terms

$$\overline{uw} = -\frac{\overline{w^2}\tau}{c_{13}}(\frac{\partial U}{\partial z} - \frac{g}{T_r}\frac{\overline{u\theta_v}}{\overline{w^2}}) \quad , \tag{5.28}$$

$$\overline{w\theta} = -\frac{\overline{w^2}\tau}{d_3}(\frac{\partial \Theta}{\partial z} - \frac{g}{T_r}\cdot\frac{\overline{\theta\theta_v}}{\overline{w^2}}) \quad , \tag{5.29}$$

$$\overline{wq} = -\frac{w^2\tau}{d_3}(\frac{\partial Q}{\partial z} - \frac{g}{T_r}\cdot\frac{\overline{q\theta_v}}{\overline{w^2}}) \quad , \tag{5.30}$$

where $c_{13} = d_3 = 13.1$

These relations were already suggested by Deardorff (1966) and
were briefly discussed by Wyngaard (1982). If the turbulent
transport terms in Eqs. (A3.15), (A3.17) and (A3.19) are neglec-
ted, the production (shear and buoyancy) of the turbulent fluxes
is equal to the destruction. These counteracting processes do
balance each other to a very good degree. This can be inferred

90

e.g. from Fig. 4.6 which displays the balance of the terms in the $\overline{uw}$-equation. The balance of terms in the $\overline{w\theta}$ and $\overline{wq}$ equation, although not shown here, also indicates that the turbulent transport terms in those equations may be neglected.

5.4 COMPARISON IN HOMOGENEOUS SITUATIONS

Next, we could proceed with a direct comparison of the fluxes calculated with the standard flux-profile relations with the fluxes generated with the model. However, a better understanding will be obtained if a comparison is made of the standard flux profile relations and the "second order flux profile relations" (5.28)-(5.30). In 5.1 it was demonstrated that this is allowed in homogeneous situations.

5.4.1 Neutral stratification

In order to compare the standard flux-profile relations derived in 5.2 with Eqs. (5.28)-(5.30) the relatively simple case of a neutral atmosphere will be considered first. Equations (5.22) and (5.28) then reduce to respectively

$$\overline{uw} = - ku_* z \frac{\partial U}{\partial z} , \tag{5.31}$$

and

$$\overline{uw} = - \frac{\overline{w^2}\tau}{c_{13}} \cdot \frac{\partial U}{\partial z} . \tag{5.32}$$

These equations suggest that the factor $\overline{w^2}\tau/c_{13}$ may be identified with the eddy diffusivity $K_m = ku_* z$. This can also be demonstrated by substituting the lower- and upper boundary conditions for $\overline{w^2}$ and τ in $\overline{w^2}\tau/c_{13}$. We obtain then respectively:

$$\frac{\overline{w^2}\tau}{c_{13}} = ku_{*1} z_{01} \quad \text{at } z = z_{01} \text{ (lower boundary)} \tag{5.33}$$

and

$$\frac{\overline{w^2}\tau}{c_{13}} = ku_{*1}z_{max}(1 - \frac{z_{max} - z_{01}}{z_I})^{-1} \quad \text{at } z=z_{max} \text{ (upper boundary) (5.34)}$$

The factor $(1 - \frac{z_{max} - z_{01}}{z_I})^{-1}$ in equation (5.34) results from

the imposed linear decrease of $-\overline{uw}/\overline{u_{*1}^2}$ from unity near the sur-
face (lower boundary) to zero at the PBL-height (z_I). The value

of the factor $(1 - \frac{z_{max} - z_{01}}{z_I})$ ranges from 0.95 to 0.99 for

typical values of z_I and z_{max} for a well developed PBL. The
small variation of $\overline{uw}/u_{*1}^2$ with height thus introduced, results
in a gradually increasing deviation of $\overline{w^2}\tau/c_{13}$ from $K_m = ku_*z$
(Fig. 5.1). Similar remarks can be made on the water vapour
flux density $\overline{wq}$ and the gradient $\partial Q/\partial z$. In neutral conditions
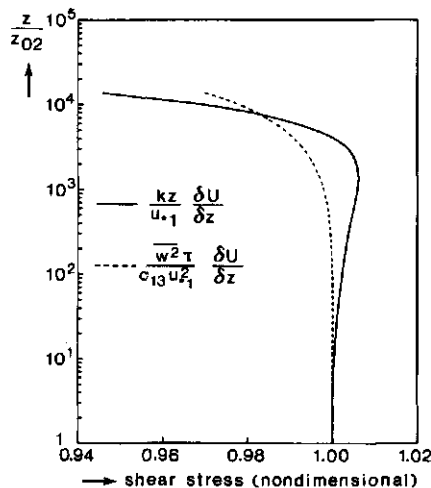these yield essentially the same results regarding the eddy dif-
fusivity of water vapour.

Figure 5.1   Nondimensional gradient of the windspeed in the
neutral case $(\frac{z}{L} = 0)$.

5.4.2 (Un)stable stratification

In the case of a diabatic atmosphere matters are more complicated. At first sight the term $\frac{g}{T_r} \overline{m\theta}_v / \overline{w^2}$ (m = u, θ or q) in Eqs. (5.28)-(5.30) seems to serve the same purpose as the inclusion of either ϕ_m, ϕ_h or ϕ_w in Eqs. (5.22)-(5.24) viz. a correction term for buoyancy. Why this apparently straightforward observation is not correct can be seen by inspecting the boundary conditions for the "eddy diffusivity" $\overline{w^2}\tau / c_{13}$. At the lower boundary minor changes occur in comparison with the neutral case, because buoyancy effects are of no importance there. Thus Eq. (5.28) e.g. again reduces to

$$\overline{uw} = - \frac{\overline{w^2}\tau}{c_{13}} \frac{\partial U}{\partial z} ,$$

which, after substituting the lower boundary conditions leads to (5.33). Analogous expressions apply for the $\overline{w\theta}$ - and $\overline{wq}$ equation.

At the upper boundary, however, buoyancy does have a noticeable effect. If the upper boundary conditions (A3.28) are substituted into $\overline{w^2}\tau / c_{13}$ it is at once obvious that the value of $\overline{w^2}\tau / c_{13}$ at the upper boundary and hence, also the value of $\overline{w^2}\tau / c_{13}$ at lower heights is influenced by stability. This means that buoyancy effects enter Eqs. (5.28)-(5.30) in two ways:
(i) through the generation of the term $\frac{g}{T_r} \overline{m\theta}_v / \overline{w^2}$ (m = u, θ or q) and
(ii) through the upper boundary conditions of $\overline{w^2}\tau / c_{13}$.
The combination of these two effects should equal the buoyancy correction introduced with ϕ_m, ϕ_h and ϕ_w in Eqs. (5.1)-(5.3). To investigate this assumption two possibilities can be explored. The first possibility is to transform Eqs. (5.28)-(5.30), rewriting terms containing $\frac{g}{T_r} \overline{m\theta}_v / \overline{w^2}$ as far as possible towards Eqs. (5.22)-(5.24). In doing so, we are able to show that the two sets of equations are very similar indeed. The second possibility lies in using both methods on the profiles of U, θ and Q generated with Part I of the model (homogeneous case).

The first possibility is explored in Appendix 5. The problem encountered there is the fact that the variables $\overline{w^2}$ and τ $(\tau = \overline{u_i u_i}/\overline{\epsilon})$ cannot be rewritten in terms of the first moments because calculation of the balance of the $\overline{u^2}$, $\overline{v^2}$ and $\overline{w^2}$ equations (A3.12)-(A3.14) shows that the turbulent transport terms occurring in those equations cannot be neglected. This deters us from obtaining a simple relation for $\overline{e^2}$ (U, Θ).

Figures (5.2) and (5.3) show the results of the calculations of the second possibility. Figures (5.2) and (5.3) represent the distribution of the momentum flux and the sensible heat flux, respectively. The latent heat flux curves are not presented as they coincide with the sensible heat flux curves if the horizontal axis is properly scaled.

In Fig. 5.2 the three curves represent the momentum flux obtained from: the aerodynamic method (curve 1), equation (5.28) (curve 2) and the model (curve 3). Comparison of curves 2 and 3
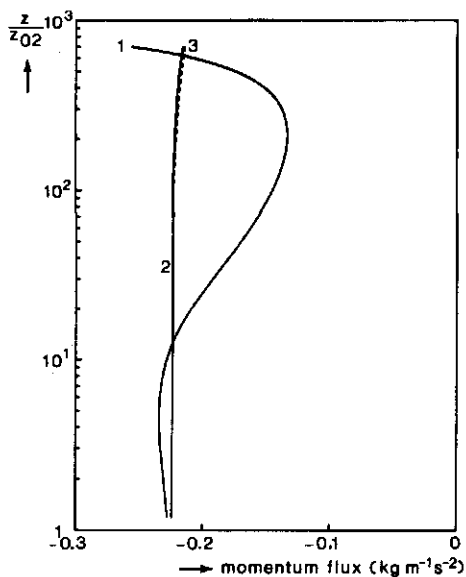

Figure 5.2   Profiles of the momentum flux calculated with: the aerodynamic method (curve 1), Eq. (5.28) (curve 2) and the present model (curve 3).
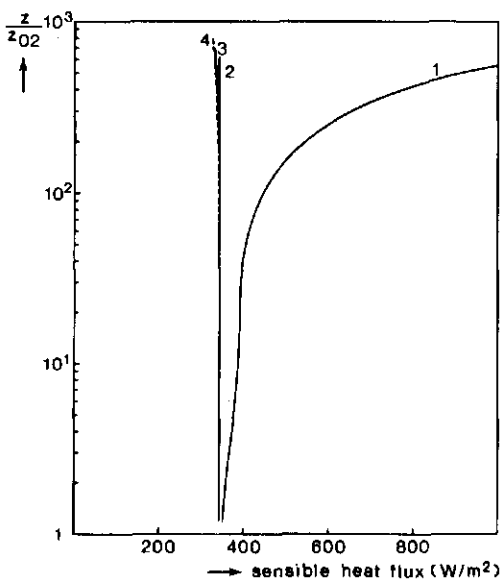
94

Figure 5.3   Profiles of the sensible heat flux calculated with:
the aerodynamic method (curve 1), the Bowen ratio
method (curve 2), Eq. (5.29) (curve 3) and the
present model (curve 4).

learns, once again, that the omission of the turbulent transport
term in Eq. (5.28) has no significant effect on the flux calcu-
lation. The deviation of curve 1 from the other two curves is of
more concern. This will be discussed further on.
The remarks made above, can be made on the curves in Fig. 5.3.
Here the four curves represent the sensible heat flux obtained
from: the aerodynamic method (curve 1), the Bowen ratio method
(curve 2), Eq. (5.29) (curve 3) and the model (curve 4). For the
sensible (and latent) heat flux the deviation of curve 1 from
the other curves is caused (just as in Fig. 5.2) by a deficiency
of the model. The problem in this case is the fact that Part I
of the model is not capable to produce profiles of the gradients
of U, θ and Q that obey Eqs. (5.22)-(5.24) exactly. This defi-
ciency of the model stems from the fact that the value of c_{13}
and d_3 in Eqs. (A3.15), (A3.17) and (A3.19) for $\overline{uw}$, $\overline{w\theta}$ and $\overline{wq}$
respectively, no longer suffices to ensure equality of both
sides of these equations when the upper boundary conditions are
substituted. This situation is notably prominent in very

95

(un) stable conditions when the buoyancy terms, which do not
influence the lower boundary conditions, enter the upper bounda-
ry conditions. Calculations show that in the $\overline{uw}$-equation (A3.15)
the discrepancy between both sides of the equation may be as
large as 10%, while for the $\overline{w\theta}$ and $\overline{wq}$ equations the discrepancy
is about 5%. This decrepancy at the upper boundary forces the
gradient $\partial U/\partial z$ to deviate from the expected $\phi_m(z/L)$ distribution,
and likewise for the $\partial\theta/\partial z$ and $\partial Q/\partial z$ distributions. This phenom-
enon is also visible in Fig. (4.2).

There is one other major assumption, though, in one of the
standard flux-profile techniques which bypasses the model's
deficiency mentioned above. This assumption, made in the Bowen
ratio method is

$$K_h = K_w . \tag{5.35}$$

Using the definition of the various K's (5.25)-(5.27) this
assumption reduces to Eq. (5.13):

$$\phi_w = \phi_h \quad ; \text{ for all } z/L.$$

To verify the validity of this assumption in the present model
we consider the correlation coefficient

$$r_{\theta q} = \frac{\overline{q\theta}}{(\overline{q^2})^{\frac{1}{2}}(\overline{\theta^2})^{\frac{1}{2}}} \tag{5.36}$$

It appears that in the equilibrium profiles this coefficient is
exactly equal to 1 everywhere. This implies that

$$\theta = - cQ + d , \tag{5.37}$$

which gives

$$\theta = cq \quad \text{and} \quad \frac{\partial\theta}{\partial x_i} = - c \frac{\partial Q}{\partial x_i} , \tag{5.38}$$

where c and d are constants. If (5.37), (5.38) and the defini-
tion of the K's (5.26)-(5.27) are used the condition $K_h = K_w$
is fulfilled exactly.

An alternative is to define a Bowen ratio (β^*) in terms of the
second order model flux profile relations (5.28)-(5.30)

$$\beta^* = \rho c_p \, \overline{w\theta}/\rho\lambda \, \overline{wq} \; . \tag{5.39}$$

Substitution from (5.28)-(5.30) yields

$$\beta^* = \frac{c_p}{\lambda}(\frac{\partial\theta}{\partial z} - \frac{g}{T_r} \frac{\overline{\theta\theta_v}}{\overline{w^2}})/(\frac{\partial Q}{\partial z} - \frac{g}{T_r} \frac{\overline{q\theta_v}}{\overline{w^2}}) \; . \tag{5.40}$$

This expression is compared with the standard Bowen ratio
formula

$$\beta = \frac{c_p}{\lambda} \frac{\partial\theta}{\partial z}/\frac{\partial Q}{\partial z} \; .$$

If the condition

$$\frac{\partial\theta}{\partial z}/\frac{\partial Q}{\partial z} = \frac{\overline{\theta\theta_v}}{\overline{q\theta_v}} \; , \tag{5.41}$$

is fulfilled, the expressions for β^* and β are identical.
Note that in Eq. (5.40) we still assumed that the turbulent
transport terms in Eqs. (5.28)-(5.30) can be ignored. But this
is not a necessary assumption for Eq. (5.38) to apply. When the
correlation coefficient $r_{\theta q}$ is considered again and (5.37)
and (5.38) are used in Eq. (5.41) this condition is fulfilled
exactly. Even if the turbulent transport terms in Eqs. (5.28)-
(5.30) and hence also in Eq. (5.40) are retained we would still
find that β^* and β are identical. Thus if the equilibrium dis-
tributions as generated by Part I of the model are substituted
in (5.41) an equivalence of both sides is obtained. As a result
of this equivalence, the fluxes of latent and sensible heat
calculated with the standard Bowen ratio method (5.16) are al-
most identical (within 5%) with the respective turbulent heat
fluxes as generated by the model (see Fig. 5.3). The small

difference of 5% follows, again, from the linear decrease of $\overline{w\theta}$ and $\overline{wq}$ with height to zero at the PBL height. As β is calculated by the ratio of these fluxes, the Bowen ratio method is not sensitive to this linear decrease and consequently yields heat fluxes which are essentially constant with height.

Finally, Figs. 5.2, 5.3 and 5.4 also contain the fluxes calculated with Eqs. (5.28)-(5.30). These fluxes do not deviate significantly from the fluxes generated by the model, by virtue of the good approximation of neglecting the very small turbulent transport terms.

5.5   CONCLUSIONS

In this chapter flux-profile relations were derived from (i) the "standard" or K-theory approach and (ii) the modeled transport equations of the turbulent fluxes in homogeneous situations. For both methods a number of approximations must be made. For the first class of relations (K-theory) these approximations are: (i) the profiles of U, Θ and Q above homogeneous terrain exhibit the well-known Monin-Obukhov similarity behaviour expressed by Eqs. (5.4)-(5.6) (the Aerodynamic and Combination methods) (ii) $K_h = K_w$ or rather $\phi_h = \phi_w$ (the Bowen ratio method). For the second class of relations (2nd order model) there is only one major approximation viz. (iii) the turbulent transport terms in the second moment equations may be neglected.

Of course there are other assumptions which are equally important e.g. the exact modeling expression for the pressure terms in the equations of the second moments, the assumption that $k = 0.41$ etc. The discussion of these assumptions lies beyond the scope of the present study.

From the comparison of the two classes of methods, performed in section 5.4, the following conclusions can be made. (i) The present model is not capable of reproducing the distribution

of the dimensionless gradients ϕ_m, ϕ_h and ϕ_w exactly. This is attributed to the discrepancy of the model equations where the upper boundary conditions are substituted. As a consequence, the results of the application of the aerodynamic method on the equilibrium profiles of U, Θ and Q show a large deviation from the fluxes calculated with the model. This deviation increases with $|z/L|$. (ii) An analytical treatment of the flux-profile relations from the second order transport equations (Appendix 5) in order to arrive at the standard flux-profile relations is only partly successful as the factor $\overline{w^2}\tau/c_{13}$ in Eqs. (5.28)- (5.30) cannot be rewritten in terms of the first moments (U, Θ and Q). (iii) The assumption $K_h = K_w$ is valid, by virtue of $r_{\theta q}$, defined in (5.36), equals 1. Thus in the equilibrium pro- files the application of the Bowen ratio method is allowed. It produces heat fluxes which are consistent with the heat fluxes generated by the model. (iv) The application of the Bowen ratio technique on the turbulent fluxes $\overline{w\theta}$ and $\overline{wq}$ from Eqs. (5.29) and (5.30) leads to an excellent agreement (within 5%) with the heat fluxes calculated with the "standard" Bowen ratio method. There is also a good agreement with the turbulent heat fluxes as cal- culated with the model.

Regarding (i) one must realize that in the example given in section 5.4 the instability was very strong (L = - 22 m). This, rather extreme, value of the Obukhov length was chosen delibera- tely to bring out the deviations of the two classes of methods more clearly. For moderate to weak unstable situations these deviations are smaller. The disadvantage of this choice of the Obukhov length is that it is questionable if the present and forthcoming analysis may be extended far beyond $|z/L| = 1$. Keeping this remark in mind, we may conclude that the analysis of the standard flux-profile methods in inhomogeneous situations with the aid of the second order model equations, which will be made in the next chapter, is very good feasible.

6 Flux-profile methods above inhomogeneous terrain

6.1 INTRODUCTION

From the moment the air flows over a different surface a relaxation towards a new equilibrium will occur (Ch. 2). Obviously, the indiscriminate use of standard flux-profile methods in these circumstances may lead to results which are unrealistic or which contain large errors. Confining the measurement heights to the IAL will probably exclude these problems as good as possible. However, it cannot be taken for granted that every flux-profile method will yield correct results there. In this chapter an analysis is made of the errors in the standard flux-profile methods when they are applied within the IAL.

In this chapter only one single change in surface conditions will be considered. Blom and Wartena (1969) showed that in the case of multiple changes in surface conditions a new IBL, and also a new IAL, will start to develop after every discontinuity of the surface. Thus the influence of former transitions in surface conditions will primarily influence the ASL above the newly developing IAL. This observation can also be inferred from the analysis of the double change in surface conditions in Ch. 4.

This chapter will mainly concentrate on two standard flux-profile methods: the Bowen ratio method (section 6.2) and the Aerodynamic method (section 6.3). The remaining combination method (see 5.2) merely combines, as the name indicates, some of the assumptions of both methods and no new viewpoints are expected from its analysis. From the two methods just mentioned, the Bowen ratio method will get the major part of the attention, for it has proven to be very consistent with both the second order flux-profile relations and with the fluxes as generated with the model in the homogeneous case (Ch. 5). The deviation of the results of the Aerodynamic method from the equilibrium model fluxes, primarily for large $|z/L|$ values, complicates the

application of this method in non-homogeneous conditions.

The fluxes of both standard methods after the change in surface
conditions (x > 0) will be compared with the fluxes calculated
with the model. The deviations encountered in this comparison
will be analyzed by considering the distribution of the terms in
the turbulent flux equations as well as some other important para-
meters of the ASL.

6.2   THE BOWEN RATIO METHOD

In the case which will be considered here, the air flows from a
smooth, hot and dry terrain to a rougher, cooler humid surface.
The upstream terrain is characterized by: z_{01} = 0.02 m, θ_{01} =
44.5°C, Q_{01} = 4.6 .10^{-3}, H_{01} = 336 W/m^2 and λE_{01} = 19 W/m^2,
resulting in L = -23 m. The parameters solely characterising the
downstream surface are: z_{02} = 0.06 m and R_{02} = 100%, all other
parameters are a function of the downstream distance (x).

From the situation described above, the latent heat flux is
expected to increase substantially just after the surface change,
while the sensible heat flux must decrease accordingly. The
dashed lines in Figs. 6.1 and 6.2 for the sensible and latent
heat flux respectively, represent the profiles of these quanti-
ties for various distances downstream of the surface change.
These fluxes, calculated with the model, will be indicated by
λE_{MD} and H_{MD}. As the air progresses over the humid surface its
absolute humidity increases and the vapour pressure deficit and
the latent heat flux near the surface decrease. For the sensible
heat flux the opposite occurs. The drawn lines in Figs. 6.1 and
6.2 represent the profiles of the sensible and latent heat flux
calculated with the Bowen ratio method, using the local profiles
of θ and Q. These fluxes will be denoted λE_{BR} and H_{BR}.

Several characteristic features can now be observed. For z > d
the profiles of θ and Q must, by definition, be unaffected by
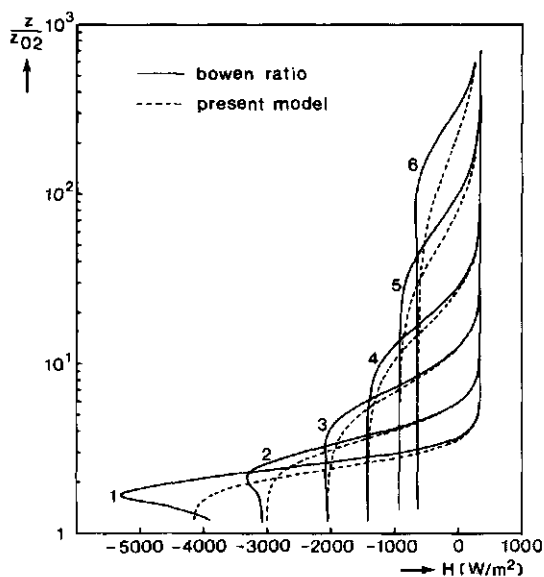
101

Figure 6.1

Figure 6.2

Figure 6.1   Profiles of the sensible heat flux density after a
change in surface conditions for various distances
downstream (z_{02} = 0.06 m).

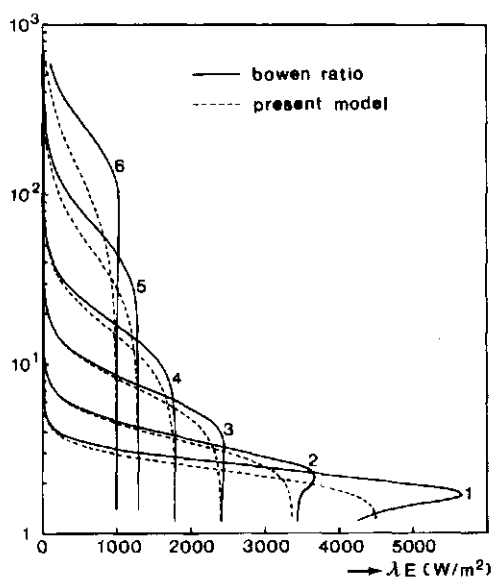| Curve	x/z_{02}	x (m)
1	1.7	0.1
2	8.5	0.5
3	$4.3 \cdot 10^1$	2.5
4	$1.7 \cdot 10^2$	10.0
5	$8.5 \cdot 10^2$	50.0
6	$3.4 \cdot 10^3$	200.0

Figure 6.2   Profiles of the latent heat flux density after a
change in surface conditions for various distances
downstream (curve numbers correspond to those of
Fig. 6.1).

102

the new surface. In this region the fluxes determined with the
Bowen ratio method are equal to the respective fluxes calculated
with the model. Only some small deviations, discussed in chap-
ter 5, can be observed. For $z \ll \delta$ the same observation can be
made. In this region the ASL is in local equilibrium with the
new surface and hence, the Bowen ratio method yields fluxes that
deviate less than a few percent from the fluxes calculated with
the model. Between these two layers the discrepancies are con-
fined.

Because the heat fluxes attain extremely high values just after
the surface change, Figs. 6.1 and 6.2 tend to obscure the rela-
tive differences between the fluxes of the two methods. Fig. 6.3
therefore presents the ratio of the latent heat fluxes of the
model and the Bowen ratio method $(\lambda E_{BR}/\lambda E_{MD})$. For the sensible
heat flux this ratio can attain unrealistic values, because both
H_{BR} and H_{MD} change sign at different heights. The ratio H_{BR}/H_{MD}
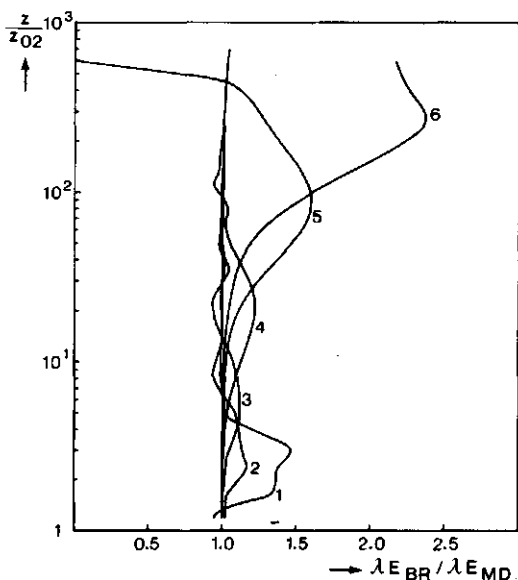

Figure 6.3   Ratio of the latent heat flux calculated with the
            Bowen ratio method (λE_{BR}) and the latent heat flux
            generated with the model (λE_{MD}) for various distan-
            ces downstream. (Curve numbers correspond to those
            of Fig. 6.1).

103

will not be considered. From Fig. 6.3 it can be seen that the
Bowen ratio method in the present case yields latent heat fluxes
within the IAL which are larger than the latent heat fluxes cal-
culated with the model. The error, however, nowhere exceeds 50%.
For distances just after the surface change (curves 1 - 3) this
error decreases with downstream distance, as expected. However,
the error increases again further downstream (curves 4 - 6).
This increase of the error can be explained as follows. As the
IBL height increases with downstream distance, the profiles of θ
and Q are affected at increasing heights. At these heights the
gradients of θ and Q are very small and even a minute perturba-
tion will cause a relatively large error in the flux-profile

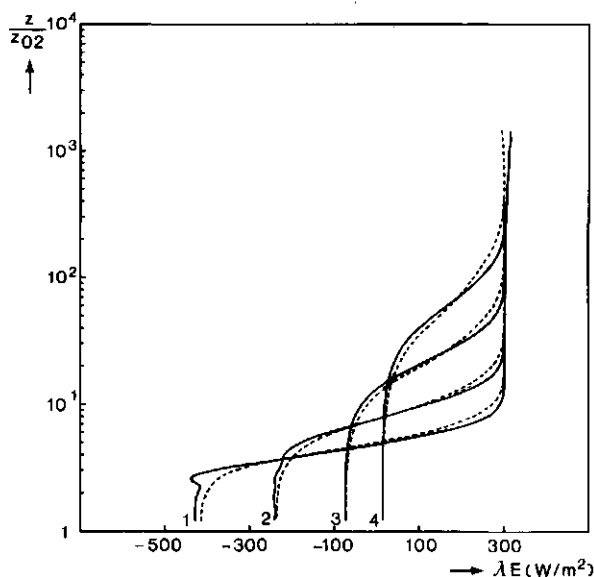Figure 6.4   Profiles of the latent heat flux density after a
              change in surface conditions for various distances
              downstream.

              Curve   x (m)
                1   0.25
                2   1.0
                3   5.0
                4   20.0

method. In the last two curves (5 and 6), where $d > z_{max}$ (upper grid level), the upper boundary conditions contaminate the solution in the upper IBL. We disregard this region from now on.

When a change takes place from a cool, humid terrain to a warm and dry surface the Bowen ratio method also yields heat fluxes which are larger than the heat fluxes produced by the model. This can be observed in Fig. 6.4 for λE.

In order to analyse the causes of the errors in the Bowen ratio method, the equation for the second moments must be considered. The reason for this is that we demonstrated in the previous chapter that the method in which the Bowen ratio $(\beta*)$ was defined with the mean turbulent heat fluxes $(\overline{w\theta}$ and $\overline{wq})$ from the model equations (5.40) yields results which are identical with the results of the standard Bowen ratio method (5.16). This agreement occurred if one condition was fulfilled viz. $r_{\theta q} = 1$, which also implied the condition (5.41). Application of the complete model equations for $\overline{wq}$ and $\overline{w\theta}$ in $\beta* = \frac{c_p}{\lambda} \overline{w\theta}/\overline{wq}$ will naturally yield latent and sensible heat fluxes which are exactly equal to λE_{MD} and H_{MD}. After the change in surface conditions, however, two effects will cause the inequality of β and $\beta*$. First, $r_{\theta q}$ no longer equals 1. And, second, the equations for $\overline{w\theta}$ and $\overline{wq}$ contain two new terms for the inhomogeneous part of the flow. The second effect will be considered first.

The modeled $\overline{wq}$ equation for $x > 0$ reads:

$$U \frac{\partial \overline{wq}}{\partial x} + W \frac{\partial \overline{wq}}{\partial z} + \overline{w^2} \frac{\partial Q}{\partial z} - \frac{g}{T_r} \overline{q\theta}_v - a_t \frac{\partial}{\partial z}(\overline{w^2}\tau \frac{\partial \overline{wq}}{\partial z}) = - d \frac{\overline{wq}}{\tau} \qquad (6.1)$$
$$\quad\text{I}\qquad\quad\text{II}\qquad\qquad\qquad\qquad\qquad\text{III}$$

A similar equation holds for $\overline{w\theta}$. Two advection terms (I and II) are added in the inhomogeneous situation. Note that after the surface change the turbulent transport term (III) no longer can be neglected forthwith. An assessment of the relative importance of the advection and turbulent transport terms together can be obtained by considering the ratio of the pressure term and the

sum of the production terms (shear and buoyancy). The distribu-
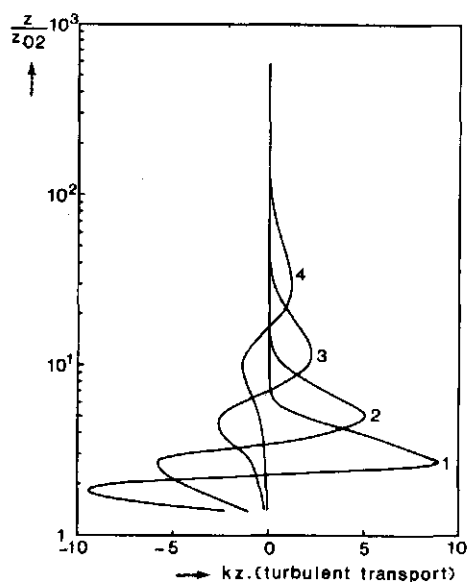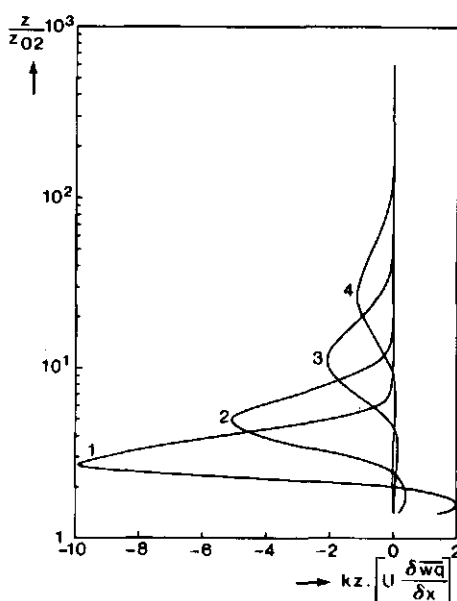tion of this ratio is given in Fig. 6.5a.
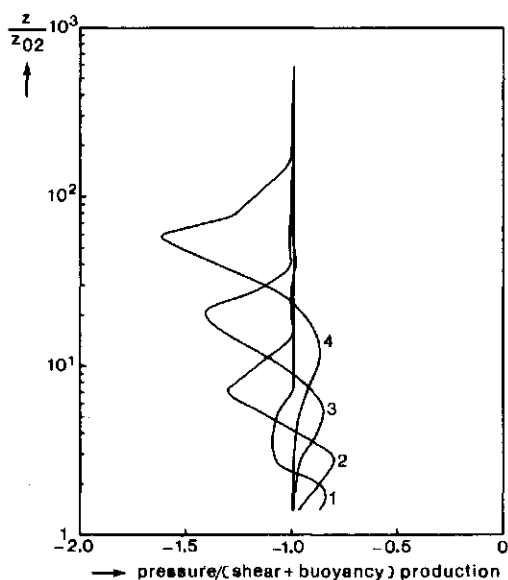
Figure 6.5a   Ratio of the pressure term of the $\overline{wq}$ equation
               (Eq. 6.1) and the sum of the buoyancy- and shear
               production terms of the same equation, for various
               distances downstream. (Curve numbers correspond to
               those of Fig. 6.1).

Fig. 6.5a shows that just downstream of x = 0 there is no region
adjacent to the surface where the production terms and the pres-
sure covariance term balance each other (curves 1,2). Approxi-
mately from curve 3 onwards (x = 2.5 m.) such a region does
exist. Note that as the IBL increases in height downstream, the
deviation of the ratio from the equilibrium value increases in
the upper part of the IBL. The reason, again, is the relatively
large sensitivity of the ratio for small perturbations in a
region where every term of the equation has become very small.

Calculation of the terms I, II and III learns that the vertical
advection term W $\partial\overline{wq}/\partial z$ (II) is much smaller than either of the
other two terms. It amounts to approximately 15% of either term

106

$$\frac{z}{z_{02}} 10^3$$

10^2

10^1

1

$-10 \quad -5 \quad 0 \quad 5 \quad 10$

⟶ kz.(turbulent transport)

4

3

2

1

$\boxed{b}$

$$\frac{z}{z_{02}} 10^3$$

10^2

10^1

1

$-10 \quad -8 \quad -6 \quad -4 \quad -2 \quad 0 \quad 2$

⟶ $kz.\left[U \dfrac{\delta \overline{wq}}{\delta x}\right]$

4

3

2

1

$\boxed{c}$

Figure 6.5b   Profiles of the turbulent transport term of the $\overline{wq}$-equation (eq. 6.1) for various distances downstream. (Curve numbers correspond to those of Fig. 6.1).

Figure 6.5c   Profiles of the horizontal advection term of the $\overline{wq}$-equation (eq. 6.1) for various distances downstream. (Curve numbers correspond to those of Fig. 6.1).

I or III. This does not imply that this vertical advection term is always insignificant. Figs. 6.5b and 6.5c show that the turbulent transport term (III) and the horizontal advection term (I) nearly cancel each other. Hence the vertical advection term (II), in which the roughness change information is contained, may be very important after all.

The effect of the "inhomogeneity term" i.e. the sum of the ad-
vection terms and the turbulent transport term in the $\overline{wq}$ (and
$\overline{w\theta}$) equations on the latent heat flux is presented in Figs. 6.6
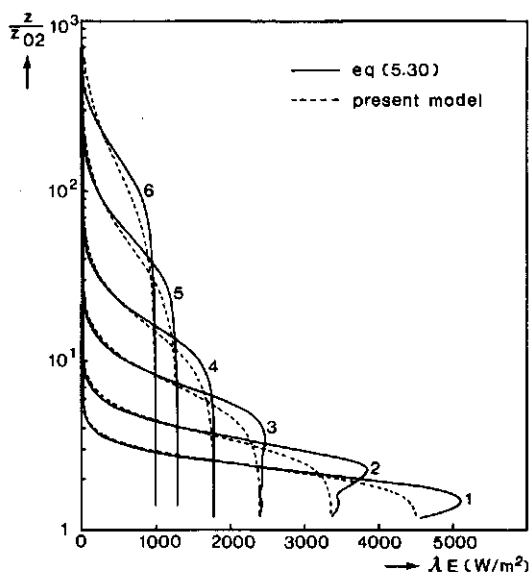and 6.7. In Figure 6.6 the dashed curves represent the model

Figure 6.6   Profiles of the latent heat flux density after a
change in surface conditions, for various distances
downstream. (Curve numbers correspond to those of
Fig. 6.1).

flux λE_{MD}, i.e. application of the full equation (6.1). The
drawn curves in Fig. 6.6 represent the latent heat fluxes ob-
tained by applying eq. (6.1) without the inhomogeneity term
(I + II + III). This flux will be denoted by λE_{HM}. The ratio
$\lambda E_{HM} / \lambda E_{MD}$ is given in Fig. 6.7.

If Figure 6.6 is compared with Fig. 6.2 it can be seen that the
errors in λE_{BR} for the greater part can be attributed to the
effects of the inhomogeneity term in the $\overline{wq}$ (and $\overline{w\theta}$) model
equations. This observation only applies, however, within the
IAL. Outside this layer, but well inside the IBL, the neglect
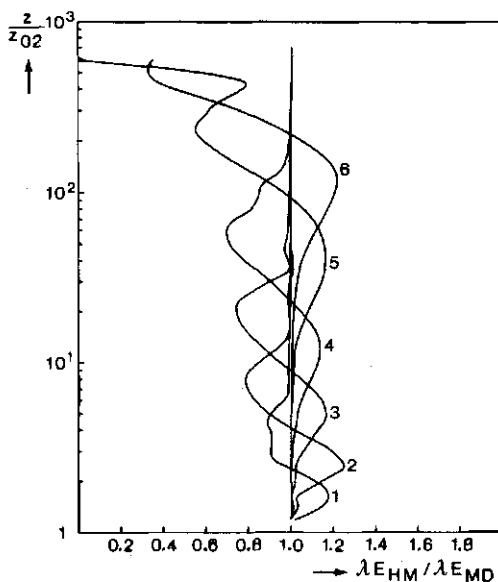of the "inhomogeneity term" causes the latent heat flux λE_{HM} to

108

Figure 6.7   Ratio of the latent heat flux calculated with
             eq. (5.30) (λE_{HM}) and the latent heat flux gene-
             rated with the model (λE_{MD}) for various distances
             downstream. (Curve numbers correspond to those of
             Fig. 6.1).

be smaller than λE_{MD}. This underestimation does not occur when
the standard Bowen ratio method is applied. As Fig. 6.5a indi-
cates, the contribution of the inhomogeneity term to the $\overline{wq}$-
equation in this part of the flow is reversed, hence it must be
expected that $\lambda E_{HM} < \lambda E_{MD}$. Therefore we conclude that there is
another effect which counteracts the effects of the reversed
contribution of the inhomogeneity term to eq. (6.1).

The agreement within the IAL of λE_{BR} and λE_{HM} is demonstrated
in Fig. 6.8. This figure presents the ratio $\lambda E_{BR}/\lambda E_{HM}$. Calcula-
tions show that within the IAL both fluxes agree within 3%. From
this figure it is immediately obvious, once more, that outside
the IAL the two methods strongly disagree.

Although the region above the IAL is of no direct concern for
the present study, it is still interesting to discuss the cause
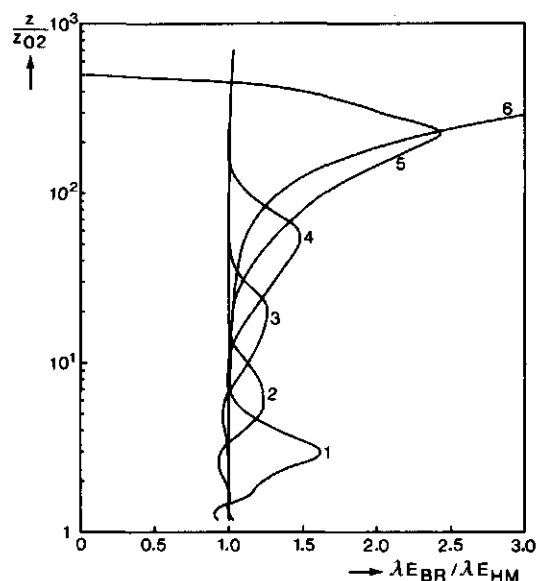of the above mentioned deviation. In chapter 5 it was shown that

109

Figure 6.8   Ratio of the latent heat flux calculated with the
Bowen ratio method (λE_{BR}) and the latent heat flux
calculated with eq. (5.30) (λE_{HM}) for various dis-
tances downstream. (Curve numbers correspond to
those of Fig. 6.1).

$\lambda E_{BR} = \lambda E_{HM}$ and $H_{BR} \simeq H_{HM}$ if condition (5.41) is fulfilled. In
Fig. 6.9 the ratio $[(\partial\theta/\partial z)/(\partial Q/\partial z)]/(\overline{\theta\theta}_v/\overline{q\theta}_v)$ is given for the
same downstream distances as the curves in Fig. 6.8. Comparison
of Figs. 6.8 and 6.9 learns that, especially for larger distan-
ces downstream (curves 3 and 4), the heights where $\lambda E_{BR}/\lambda E_{HM}$
showes a maximum coincide with the heights where the ratio of
Fig. 6.9 has a minimum. This coincidence of heights is not pre-
sent for small distances (curves 1 and 2). Hence, if distances
just downstream of the surface change (x < 1.m) are disregarded,
the disagreement of λE_{BR} and λE_{HM} above the IAL can be attribu-
ted to the differences in the transport of temperature and humi-
dity of which the ratio $[(\partial\theta/\partial z)/(\partial Q/\partial z)]/(\overline{\theta\theta}_v/\overline{q\theta}_v)$ is a measure.

Finally, one is usually interested in the value of the fluxes at
the surface (or at $z = z_o$). The Bowen ratio method inside the
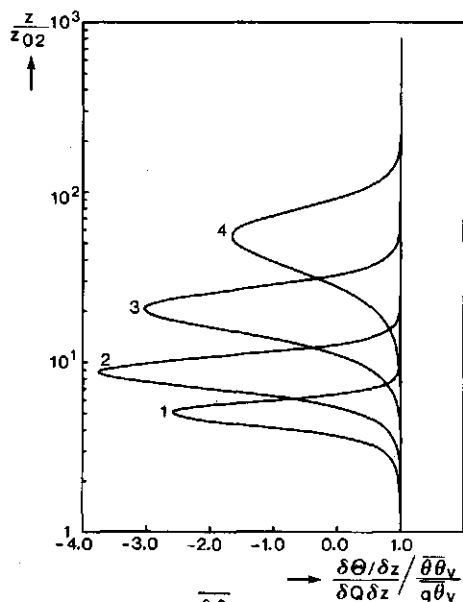IAL yields results which agree better with the surface flux than

110

Figure 6.9   Ratio $(\frac{\partial \Theta/\partial z}{\partial Q/\partial z})/\frac{\overline{\theta \theta_v}}{q\theta_v}$ for various distances downstream

(Curve numbers correspond to those of Fig. 6.1).

the model flux. This can be inferred from Figs. 6.1 and 6.2.
Thus as far as the surface fluxes are concerned, the Bowen ratio
method may even be applied above the IAL. As the accuracy of
present flux estimation techniques is approximately 10% (chap-
ter 5) a height (h_{BR}) can be defined below which the deviation
of λE_{BR} and H_{BR} is less than 10% of the respective surface
fluxes. The ratio h_{BR}/δ is approximately constant with down-
stream distance and amounts to 1.5.

Summarizing, in this section it was found that the Bowen ratio
method, applied above a wet, cool surface downstream of a dry,
hot terrain yields sensible- and latent heat fluxes in the IAL
of which the absolute values are larger than the respective heat
fluxes calculated with the model. If Bowen ratio measurements
are made within the IAL, the deviation of H_{BR} and λE_{BR} from the
fluxes calculated with the model (H_{MD} and λE_{MD}) does not exceed
10%, except for x < 1.0 m. This deviation within the IAL can
mainly be attributed to the neglect of the advection terms and
the turbulent transport term in the $\overline{wq}$ and $\overline{w\theta}$ equations. Outside

111

the IAL this neglect would result in latent heat fluxes which are up to 40% smaller than the model fluxes. In that part of the ASL, however, the differences in transport of water vapour and heat compensate for this underestimation.

6.3 THE AERODYNAMIC METHOD

Referring to the remarks made in sections 5.5 and 6.1 about the applicability of the Aerodynamic method, a quantitative discussion of this method cannot be made. Hence only a short qualitative review of the results of this method above non-homogeneous terrain is presented.

First of all, note that the Monin-Obukhov similarity theory formally cannot be used for $z < 10 h_o$ (Tennekes, 1973). Here h_o stands for the average height of the roughness elements and is related to z_o by $z_o \cong 0.14 h_o$. However, in the present model the calculations which use the Monin-Obukhov theory are performed down to $z = z_o$. We commented on this issue in section 4.1.3. For analytical purposes, this violation of the Monin-Obukhov theory has no serious consequences. Hence the discussion in this section may be performed. For practical purposes, however, only the region $z/z_{02} > 100$ must be considered. In the present situation $z = 100 z_{02}$ just about coincides with the height of the region above which the fluxes resulting from the aerodynamic method applied to the equilibrium profiles start to deviate considerably from the model fluxes (see Fig. 5.2). The qualitative results of the following, however, may be transposed to situations where those regions do not overlap.

Figure 6.10 shows the latent heat flux from the application of the aerodynamic method to the same situation as in the preceding section. Fig. 6.10 may be compared with Fig. 6.2 (note the difference in the scaling of the horizontal axes). From this comparison it is clear that the latent heat fluxes which result from the application of the aerodynamic method (λE_{AE}) show a
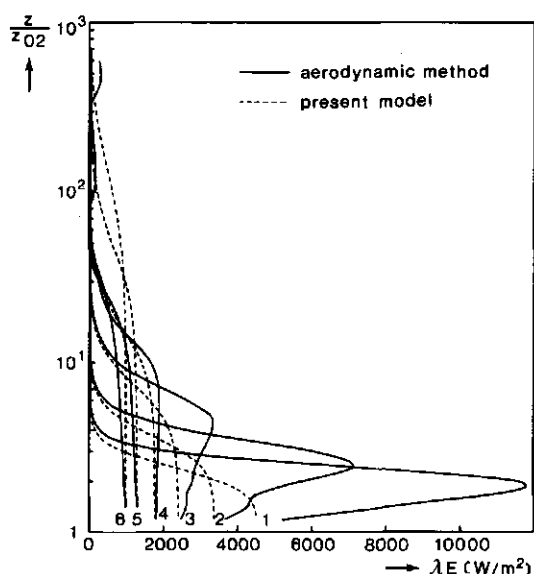
112

Figure 6.10   Profiles of the latent heat flux density after a change in surface conditions for various distances downstream. (Curve numbers correspond to those of Fig. 6.1).

much larger deviation from the model fluxes λE_{MD} than the fluxes λE_{BR}. Apparently the aerodynamic method has a larger sensibility for surface inhomogeneities than the Bowen ratio method. This stems from the more stringent conditions which the aerodynamic method has to satisfy (see section 5.2). Fig. 6.11 shows the ratio $\lambda E_{AE}/\lambda E_{MD}$. The upper part of this figure ($z/z_{02} > 30$) for curves 1 - 4 complies with Fig. 5.3: It shows the incapability of the present model to reproduce the theoretical $\phi_m(z/L)$ curves exactly. The lower part of this figure shows that the aero-dynamic method yields latent heat fluxes within the IAL, which are larger than the model fluxes λE_{MD}. The magnitude of the sensible heat flux is also overestimated by the aerodynamic method.

Comparison of Figs. 6.11 and 6.3 learns that the deviations of λE_{AE} from λE_{MD} are roughly 4 times as large as the deviations of λE_{BR} from λE_{MD}. It also shows that the aerodynamic method yields latent heat fluxes which are considerably smaller than
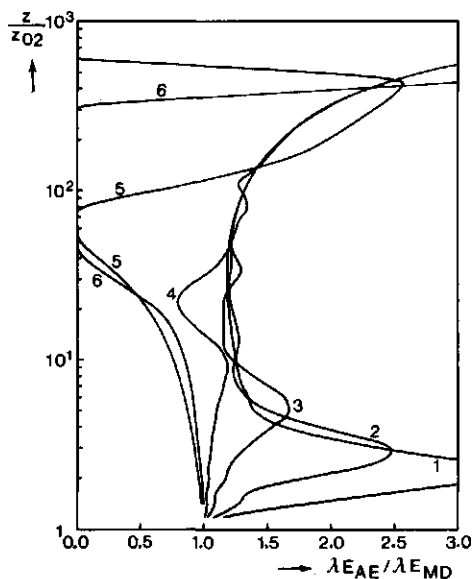
113

Figure 6.11   Ratio of the latent heat flux calculated with the
aerodynamic method (λE_{AE}) and the latent heat flux
generated with the model (λE_{MD}) for various dis-
tances downstream. (Curve numbers correspond to
those of Fig. 6.1).

λE_{MD} for larger distances downstream (curves 4 and 5) in the
upper part of the IBL. This is partly attributed to the deterio-
ration of the model results caused by the upper boundary condi-
tions discussed hereafter.

For very great distances downstream ($x/z_{02} \cong 2000$) the fluxes
from the aerodynamic method within the IAL, however, do not
converge towards the fluxes H_{MD} and λE_{MD}. This behaviour, which
was not present in the Bowen ratio results, is attributed to a
gradual deterioration of the quality of the model results as
the calculation is performed beyond $x = x_{max}$. At this distance
downstream the IBL height d equals $z = z_{max}$ (the upper calcula-
tion level). Especially the shear stress profiles are affected
by the errors which result from the application of the upper
boundary conditions for $x > x_{max}$. These errors gradually diffuse
downwards. The Bowen ratio method, by nature, is less suscep-
tible to perturbations in the shear stress profile. But, indi-

rectly, through the coupling of all the differential equations, also the Bowen ratio method is slightly in error in the upper part of the IBL (the last curve in Figs. 6.1 and 6.2). This is of no concern as yet.

7 Summary and conclusions

In Chapter 1 the goals of the present study were presented.
These goals are
(i)   the estimation and analysis of the errors introduced in the
      standard flux determination methods when they are applied
      above non-homogeneous terrain
(ii) providing simple techniques for estimating these errors,
      using a minimum number of data concerning sensor location,
      surrounding terrain(s) etc.
These goals suggested that a direct treatment of the flux-
profile methods above a non-homogeneous terrain, with the aid
of a second order model, was feasible. In the course of this
study, however, it turned out that a direct treatment was not
immediately possible. First of all, the performance of the model
had to be analyzed in order to tackle the posed problem. This
analysis was needed for the correct interpretation and apprecia-
tion of the results of the flux-profile methods above non-homo-
geneous terrain. Hence, the conclusions in this final chapter
can be separated in two groups: (i) those which concern the mo-
del used in the present study, and (ii) those which concern the
application of the model in order to study the flux-profile me-
thods.

In Chapter 2 the first simplifications were introduced. These
simplifications referred to the initial conditions as well as
the upper boundary conditions of the numerical model. E.g. the
present model is restricted to the atmospheric surface layer,
which in its initial state is supposed to be in equilibrium with
the surface. Also, the upper boundary value of every variable
(except W) remains fixed after the change in surface conditions.
This led to the conclusion that the model is only applicable to
a limited downstream distance (x_{max}). As soon as the flow per-
turbations, induced by the new surface, reach the highest grid
level (z_{max}) the fixed upper boundary values start to contami-
nate the solution. The deterioration of the solution subsequent-

116

ly diffuses downwards as the downstream distance increases beyond x_{max}. To avoid this problem the model should be extended to comprise the whole of the atmospheric boundary layer. This has already been accomplished (e.g. Wyngaard, 1975).

In Chapter 3 we concluded that second order models are superior to first order models, mainly when the second moments (fluxes and other (co)variances) are considered. However, the disadvantage of second order models is the difficulty related to the modeling of the third order terms and the pressure terms. Sometimes, mean strain and buoyancy terms have to be incorporated in the approximation of the 3rd order and pressure terms, in order to get physically realistic results. At present, there is no general agreement on the modeling of these terms. Usually the "engineering approach" is used, where model constants are tuned to obtain the desired results. The third order models which have recently appeared, merely shift the problem to the modeling of the fourth order terms. Obviously, much has still to be learned here.

The above conclusions hold for any 2nd order model. The present model was examined more closely in Chapter 4. It was found that flaws in the upper boundary conditions may be responsible for the deviation of the dimensionless gradients of U, Θ and Q from the expected universal ϕ-curves in diabatic equilibrium conditions. Efforts to overcome these imperfections were only partly successful. A comparison of the budgets of several 2nd moment equations with experimental results showed that the present model reproduces the equilibrium equation budgets quite accurately. A more serious problem was encountered in the statement of the lower boundary conditions downstream of the step change in surface characteristics. It was found that the condition of a constant surface relative humidity after the surface transition causes an unphysical solution for the change from a cool and humid terrain to a hot and dry one. A possible solution for this problem has been presented. Another problem, possibly related to the lower boundary conditions, emerged when the experimental

117

results of e.g. Lang et al. (1983) became available. It appears
that the model in its present state is not able to reproduce the
inequality of K_h and K_w in the IAL, found in the experiment. This
problem remains to be solved. In the same chapter the model was
modified and extended in order to be able to treat rough-to-
smooth transitions. It was then possible to demonstrate that,
when the ASL is subjected to a temporary change of the lower
boundary conditions, the solution will eventually approach its
original equilibrium.

The above results necessitated the analysis of the results of
the application of the standard flux-profile methods on the
equilibrium (or initial) profiles, generated with the initiali-
sation part (part I) of the model. Chapter 5 is devoted to this
subject. In Chapter 5 the so-called "second order flux-profile
relations" were derived from the modeled 2nd order equations.
This was done in order to be able to relate (in Chapter 6) the
distribution of every term of the modeled 2nd order equations
to the errors produced when applying the standard flux-profile
relations in inhomogeneous conditions. We demonstrated that the
2nd order flux-profile relations are identical with the standard
flux-profile relations in homogeneous and neutral conditions.
When the ASL above homogeneous terrain has a diabatic stratifi-
cation, the interpretation of the structure of the 2nd order
flux-profile relations is rather difficult. It was shown that
buoyancy effects enter these relations in two ways:
(i)   through the generation of an additional term in the rela-
      tions, and
(ii) through the modification of the factor in the relation which
      could be identified with the eddy diffusivity in neutral
      conditions.
It was found that the aerodynamic method yields fluxes which
deviate considerably from the fluxes generated with the model.
This is attributed to the disagreement between the dimensionless
profile of the wind shear ($\partial U/\partial z$) and the expected ϕ_m-curve.
This was discussed above and in Chapter 4. The Bowen ratio method
is not sensible for the exact definition of ϕ_h and ϕ_w as long as

118

these functions are equal. In Chapter 5 it was found that the dimensionless equilibrium profiles $\partial\Theta/\partial z$ and $\partial Q/\partial z$ are exactly equal. Hence, the application of the Bowen ratio method to the equilibrium profiles yields sensible- and latent heat fluxes which agree very well (within 5%) with the fluxes generated with the model.

In Chapter 6, both the Bowen ratio method and the aerodynamic method were applied to the relaxation profiles of U, Θ and Q after the surface change. Both methods yield heat fluxes in the IAL which are larger than the heat fluxes calculated with the model (λE_{MD}, H_{MD}). The difference of the Bowen ratio heat fluxes (λE_{BR}, H_{BR}) and the model fluxes within the IAL is less than 10% if the region just downstream of the surface change (x < 1 m.) is disregarded. This difference decreases as the downstream distance increases. The analysis of the various terms of the $\overline{wq}$-equation downstream of the surface change, showed that the two advection terms (U $\frac{\partial\overline{wq}}{\partial x}$ and W $\frac{\partial\overline{wq}}{\partial z}$) and the modeled turbulent transport term are responsible for the differences mentioned. Of these three terms the horizontal advection term and the turbulent transport term nearly cancel each other. Hence, the relatively small vertical advection term is important in this respect. Above the IAL the difference in transport of water vapour and heat partly compensates the deviation caused by the three above mentioned terms. The results of the Bowen ratio method also indicate that the determination of the value of the heat fluxes at the surface is quite accurate (within 10%) even when this method is applied just above the IAL (z $\leqslant$ 1.5 δ).

As was mentioned earlier (Chapter 4) the present model is not capable to reproduce the ϕ_m-curve exactly. Because the application of the aerodynamic method critically depends on the shape of this curve, the analysis of the aerodynamic method is rather complicated and uncertain. Nevertheless, it was found that the difference of the heat fluxes produced by the aerodynamic method (λE_{AE}, H_{AE}) and the model fluxes within the IAL is larger than the difference of $\lambda E_{BR}(H_{BR})$ and $\lambda E_{MD}(H_{MD})$. This is attributed

to the more stringent conditions which the aerodynamic method has to satisfy. At $x = x_{max}$ the IBL reaches the upper grid level. Beyond x_{max} the upper boundary conditions contaminate the solution. Especially the aerodynamic method is susceptible to these errors, and a proper analysis cannot be made for these large downstream distances.

The final conclusion is that the present state of the second order model used in this study is subject to improvement, both in the modeling of the pressure terms and in the lower boundary conditions. Until a substantial improvement has been achieved, the main merit of this (and similar) models lies primarily in the qualitative prediction of the structure of the ASL after a change in surface conditions. Used in this way, it is an excellent tool for the understanding of the various processes which take place above an inhomogeneous terrain. This possibility of the application of a 2nd order model has been explored in this thesis for one specific purpose: the analysis of flux-profile relations in inhomogeneous conditions. The application of this model for quantitative purposes turned out to be quite hazardous. This is the sole reason why the second goal of this study has not been achieved. This application awaits the progress in the modeling of the higher order- and pressure terms. The problems concerned with the definition of the lower boundary conditions must be approached experimentally. The performance of an experiment, designed for the precise measurement of the processes which take place near the lower boundary, logically is the next step to the ultimate solution of this problem.

Appendix 1

DERIVATION OF GOVERNING EQUATIONS

A1.1 Conservation of mass equation

With the assumptions mentioned in Chapter 2 it was shown that the mass-conservation equation (2.2) transforms in

$$\frac{\partial \tilde{u}_i}{\partial x_i} = 0 \ , \tag{A1.1}$$

which, after applying Reynolds' decomposition yields

$$\frac{\partial U_i}{\partial x_i} = 0 \ , \tag{A1.2}$$

and

$$\frac{\partial u_i}{\partial x_i} = 0 \tag{A1.3}$$

A1.2 The momentum equation

We start with the equations of motion (2.22)

$$\frac{\partial \tilde{u}_i}{\partial t} + \tilde{u}_j \frac{\partial \tilde{u}_i}{\partial x_j} = -\frac{1}{\rho_r} \frac{\partial \tilde{P}}{\partial x_i} + g_i \frac{\tilde{\Theta}_v}{T_r} + \nu \frac{\partial^2 \tilde{u}_i}{\partial x_j \partial x_j} - 2\Omega_j \varepsilon_{ijk} \tilde{u}_k \ , \tag{A1.4}$$

and introduce the Reynolds' decomposition (2.24a) into (A1.4)

$$\frac{\partial U_i}{\partial t} + \frac{\partial u_i}{\partial t} + U_j \frac{\partial U_i}{\partial x_j} + U_j \frac{\partial u_i}{\partial x_j} + u_j \frac{\partial U_i}{\partial x_j} + u_j \frac{\partial u_i}{\partial x_j} =$$

$$- \frac{1}{\rho_r}(\frac{\partial P}{\partial x_i} + \frac{\partial p}{\partial x_i}) + g_i(\frac{\Theta_v}{T_r} + \frac{\theta_v}{T_r}) + \nu \frac{\partial^2 U_i}{\partial x_j \partial x_j} + \nu \frac{\partial^2 u_i}{\partial x_j \partial x_j} +$$

$$- 2\Omega_j \varepsilon_{ijk} U_k - 2\Omega_j \varepsilon_{ijk} u_k \ . \tag{A1.5}$$

Averaging (A1.5) and using (A1.3) the equation for the mean field is obtained

$$\frac{\partial U_i}{\partial t} + U_j \frac{\partial U_i}{\partial x_j} = - \frac{1}{\rho_r} \frac{\partial P}{\partial x_i} + g_i \frac{\Theta_v}{T_r} - 2\Omega_j \varepsilon_{ijk} U_k + \nu \frac{\partial^2 U_i}{\partial x_k \partial x_k}$$

$$- \frac{\partial}{\partial x_j}(\overline{u_i u_j}) \ . \tag{A1.6}$$

Subtracting (A1.6) from (A1.5) yields the equation for the turbulent field

$$\frac{\partial u_i}{\partial t} + \frac{\partial}{\partial x_j} \overline{u_j U_i + U_j u_i + u_j u_i - \overline{u_i u_j}} = - \frac{1}{\rho_r} \frac{\partial p}{\partial x_i} + g_i \frac{\theta_v}{T_r} +$$

$$\nu \frac{\partial^2 u_i}{\partial x_k \partial x_k} - 2\Omega_j \varepsilon_{ijk} u_k \ , \tag{A1.7}$$

where (A1.2) and (A1.3) were used several times. Equation (A1.7) is needed for the derivation of the transport equations of $\overline{u_i u_j}$ $\overline{u_i \theta}$ and $\overline{u_i q}$ which will be done in section A1.4.

A1.3 The entropy equation

According to e.g. Lumley and Panofsky (1964) the following relation holds for the entropy (S)

$$dS = (\frac{\partial S}{\partial T})_p dT + (\frac{\partial S}{\partial P})_T dP = \frac{c_p}{T}dT - (\frac{\partial V}{\partial T})_p dP = \frac{c_p}{T}dT - R\frac{dP}{P} \ . \tag{A1.8}$$

122

Substituting this into (2.3) and using (A1.1) we arrive at

$$\underset{\sim}{\rho} \underset{\sim}{T} \frac{c_p}{T} \left(\frac{\partial \underset{\sim}{T}}{\partial t} + u_j \frac{\partial \underset{\sim}{T}}{\partial x_j} \right) - \frac{R}{\underset{\sim}{P}} \left(\frac{\partial \underset{\sim}{P}}{\partial t} + \underset{\sim}{u}_j \frac{\partial \underset{\sim}{P}}{\partial x_j} \right) = k \frac{\partial^2 \underset{\sim}{T}}{\partial x_k \partial x_k} \, .$$

Starting with the decomposition (2.5), putting $\partial \tilde{P}/\partial t = 0$
and $\tilde{u}_j \frac{\partial \tilde{P}}{\partial x_j} = 0$, using $|\tilde{T}/T_r| \ll 1$, $|\tilde{P}/P_r| \ll 1$ and finally

dividing by $\underset{\sim}{\rho} c_p$ we obtain

$$\frac{\partial \tilde{T}}{\partial t} + \tilde{u}_j \frac{\partial \tilde{T}}{\partial x_j} + \tilde{u}_j \frac{\partial T_r}{\partial x_j} - \frac{R T_r}{c_p P_r} \tilde{u}_j \frac{\partial P_r}{\partial x_j} = \kappa_H \frac{\partial^2 \tilde{T}}{\partial x_k \partial x_k} \, . \qquad (A1.9)$$

If for $\partial P_r/\partial x_j$ and $\partial T_r/\partial x_j$ the relations (2.7) and (2.9)
are substituted respectively and if also the equation of
state (2.10) is applied, the third and fourth term in (A1.9)
cancel each other. What remains is

$$\frac{\partial \tilde{T}}{\partial t} + \tilde{u}_j \frac{\partial \tilde{T}}{\partial x_j} = \kappa_H \frac{\partial^2 \tilde{T}}{\partial x_k \, x_k} \, ,$$

which to a good approximation may be written as

$$\frac{\partial \tilde{\Theta}}{\partial t} + \tilde{u}_j \frac{\partial \tilde{\Theta}}{\partial x_j} = \kappa_H \frac{\partial^2 \tilde{\Theta}}{\partial x_k \partial x_k} \, . \qquad (A1.10)$$

The next step, again, is the application of Reynolds' con-
vention (2.24) to equation (A1.10). Analogous to the deri-
vation in section A1.2 we obtain

$$\frac{\partial \Theta}{\partial t} + U_j \frac{\partial \Theta}{\partial x_j} = - \frac{\partial}{\partial x_j} (\overline{u_j \theta}) + \kappa_H \frac{\partial^2 \Theta}{\partial x_k \partial x_k} \, , \qquad (A1.11)$$

and

$$\frac{\partial \theta}{\partial t} + \frac{\partial}{\partial x_j} \left(U_j \theta + u_j \theta + u_j \theta - \overline{u_j \theta} \right) = \kappa_H \frac{\partial^2 \theta}{\partial x_k \partial x_k} \, , \qquad (A1.12)$$

for the mean and turbulent field respectively.

A1.4   The specific humidity equation

Without derivation the equations corresponding to (A1.11) and (A1.12) for the specific humidity are presented. These read for the mean and turbulent field respectively

$$\frac{\partial Q}{\partial t} + U_j \frac{\partial Q}{\partial x_j} = - \frac{\partial}{\partial x_j}(\overline{u_j q}) + \kappa_v \frac{\partial^2 Q}{\partial x_k \partial x_k} \; , \tag{A1.13}$$

$$\frac{\partial q}{\partial t} + \frac{\partial}{\partial x_j} U_j q + u_j q + u_j Q - \overline{u_j q} = \kappa_v \frac{\partial^2 q}{\partial x_k \partial x_k} \; . \tag{A1.14}$$

A1.5 Derivation of the second moment equations

A1.5.1   The Reynolds' stress equation

Multiplying (A1.7) for u_i with u_k, adding (A1.7) for u_k multiplied with u_i and averaging the result yields

$$\frac{\partial}{\partial t} \overline{u_i u_k} + (\overline{u_j u_k} \frac{\partial U_i}{\partial x_j} + \overline{u_j u_i} \frac{\partial U_k}{\partial x_j}) + U_j \frac{\partial}{\partial x_j} \overline{u_i u_k} =$$

$$- (\overline{u_j u_k \frac{\partial u_i}{\partial x_j} + u_j u_i \frac{\partial u_k}{\partial x_j}}) - \frac{1}{\rho_r}(\overline{u_k \frac{\partial p}{\partial x_i}} + \overline{u_i \frac{\partial p}{\partial x_k}}) +$$

$$+ \frac{1}{T_r}(g_i \overline{u_k \theta_v} + g_k \overline{u_i \theta_v}) + (\overline{\nu u_k \frac{\partial^2 u_i}{\partial x_j \partial x_j}} + \overline{\nu u_i \frac{\partial^2 u_k}{\partial x_j \partial x_j}}) +$$

$$- 2\Omega_j(\varepsilon_{ijl} \overline{u_l u_k} + \varepsilon_{kjl} \overline{u_l u_i}), \tag{A1.15}$$

where terms like $\overline{u_k \frac{\partial}{\partial x_j} \overline{u_i u_j}}$ and $\overline{u_i \frac{\partial}{\partial x_j} \overline{u_k u_j}}$ are equal to zero and can be omitted. Moreover, (A1.2) and (A1.3) were used several times.

The viscous terms in (A1.15) can be transformed as follows

$$\overline{\nu u_k \frac{\partial^2 u_i}{\partial x_j \partial x_j}} + \overline{\nu u_i \frac{\partial^2 u_k}{\partial x_j \partial x_j}} = \nu \frac{\partial}{\partial x_j}(\overline{u_k \frac{\partial u_i}{\partial x_j}}) - \nu(\overline{\frac{\partial u_k}{\partial x_j} \frac{\partial u_i}{\partial x_j}}) +$$

124

$$\nu \frac{\partial}{\partial x_j}(u_i \overline{\frac{\partial u_k}{\partial x_j}}) - \nu \overline{(\frac{\partial u_i}{\partial x_j} \frac{\partial u_k}{\partial x_j})} = \nu \frac{\partial}{\partial x_j}(\overline{\frac{\partial u_i u_k}{\partial x_j}}) - \nu \frac{\partial}{\partial x_j}(u_i \overline{\frac{\partial u_k}{\partial x_j}}) +$$

$$\nu \frac{\partial}{\partial x_j}(u_i \overline{\frac{\partial u_k}{\partial x_j}}) - 2\nu \overline{\frac{\partial u_i}{\partial x_j} \frac{\partial u_k}{\partial x_j}} .$$

This yields

$$\nu u_k \overline{\frac{\partial^2 u_i}{\partial x_j \partial x_j}} + \nu u_i \overline{\frac{\partial^2 u_k}{\partial x_j \partial x_j}} = \nu \frac{\partial^2 \overline{u_i u_k}}{\partial x_j \partial x_j} - 2\nu \overline{\frac{\partial u_i}{\partial x_j} \frac{\partial u_k}{\partial x_j}} . \tag{A1.16}$$

The first term on the right hand side of (A1.16) represents
molecular diffusion of $\overline{u_i u_k}$ and can be neglected in high Re-
number flows (Wyngaard, 1982; Hinze, 1959). The second term
on the right hand side of (A1.16) represents molecular des-
truction and cannot be ignored. If isotropy of the small
scale structure of turbulence is assumed then

$$2\nu \overline{\frac{\partial u_i}{\partial x_j} \frac{\partial u_k}{\partial x_j}} = -\frac{2}{3}\nu \overline{(\frac{\partial u_i}{\partial x_j})^2} \delta_{ik} = -\frac{2}{3}\bar{\epsilon}\, \delta_{ik}. \tag{A1.17}$$

This implies that molecular destruction only affects the
normal components of the Reynolds' stress tensor i.e. the
variances $\overline{u_i u_i}$.

With this transformation of the viscous terms, (A1.15) reads

$$\frac{\partial}{\partial t} \overline{u_i u_k} + (\overline{u_j u_k} \frac{\partial U_i}{\partial x_j} + \overline{u_j u_i} \frac{\partial U_k}{\partial x_j}) + U_j \frac{\partial}{\partial x_j} \overline{u_i u_k} =$$

$$- \frac{\partial}{\partial x_j}(\overline{u_i u_j u_k}) - \frac{1}{\rho_r}(\overline{u_k \frac{\partial p}{\partial x_i}} + \overline{u_i \frac{\partial p}{\partial x_k}}) + \frac{1}{T_r}(g_i \overline{u_k \theta_v}$$

$$+ g_k \overline{u_i \theta_v}) - \frac{2}{3}\bar{\epsilon}\, \delta_{ik} - 2\Omega_j(\epsilon_{ijl} \overline{u_l u_k} + \epsilon_{kjl} \overline{u_l u_i}) , \tag{A1.18}$$

where (A1.3) has been used once again to obtain the third

125

order term $\frac{\partial}{\partial x_j}(\overline{u_j u_i u_k})$

A1.5.2 The turbulent flux equations

The result of multiplying (A1.7) with θ, (A1.12) with u_i, adding and averaging is

$$\frac{\partial}{\partial t}\,\overline{u_i\theta} + U_j\,\frac{\partial}{\partial x_j}\,\overline{u_i\theta} + (\overline{u_i u_j}\,\frac{\partial\Theta}{\partial x_j} + \overline{u_j\theta}\,\frac{\partial U_i}{\partial x_j}) = -\frac{\partial}{\partial x_j}(\overline{u_i u_j \theta}) -$$

$$\frac{1}{\rho_r}\,\overline{\theta\frac{\partial p}{\partial x_i}} + g_i\,\overline{\frac{\theta\theta}{T_r}}v + \nu\,\overline{\theta\frac{\partial^2 u_i}{\partial x_j \partial x_j}} + \kappa_H\,\overline{u_i\frac{\partial^2\theta}{\partial x_j \partial x_j}} -$$

$$\qquad\qquad\qquad\qquad\qquad\qquad\qquad\qquad\qquad\qquad\qquad\text{(A1.19)}$$

$$2\Omega_j\varepsilon_{ijk}\,\overline{\theta u_k}\ .$$

The molecular terms can be written as

$$\nu\,\overline{\theta\frac{\partial^2 u_i}{\partial x_j \partial x_j}} = \nu\,\frac{\partial^2\overline{\theta u_i}}{\partial x_j \partial x_j} - \nu\,\frac{\partial}{\partial x_j}(\overline{u_i\frac{\partial\theta}{\partial x_j}}) - \nu\,\overline{\frac{\partial\theta}{\partial x_j}\frac{\partial u_i}{\partial x_j}}\ , \qquad \text{(A1.20)}$$

and

$$\kappa_H\,\overline{u_i\frac{\partial^2\theta}{\partial x_j \partial x_j}} = \kappa_H\,\frac{\partial^2\,\overline{u_i\theta}}{\partial x_j \partial x_j} - \kappa_H\,\frac{\partial}{\partial x_j}(\overline{\theta\frac{\partial u_i}{\partial x_j}}) - \kappa_H\,\overline{\frac{\partial\theta}{\partial x_j}\frac{\partial u_i}{\partial x_j}}\ . \qquad \text{(A.21)}$$

The first term on the right hand side of (A1.20) and (A1.21) represents molecular diffusion of $\overline{u_i\theta}$ and can be neglected in flows with a high Re and Pe number. According to Wyngaard (1982) the second term in both equations is negligible also. Hence only the third term remains. However, if isotropy of the smallest scales is assumed, these terms, because of their odd number of indices, must also equal zero. This means that the molecular terms in (A1.19) disappear altogether. Thus

$$\frac{\partial}{\partial t}\,\overline{u_i\theta} + U_j\,\frac{\partial\overline{u_i\theta}}{\partial x_j} + (\overline{u_i u_j}\,\frac{\partial\Theta}{\partial x_j} + \overline{u_j\theta}\,\frac{\partial U_i}{\partial x_j}) =$$

$$- \frac{\partial}{\partial x_j}(\overline{u_i u_j \theta}) - \frac{1}{\rho_r} \overline{\theta \frac{\partial p}{\partial x_i}} + g_i \frac{\overline{\theta \theta_v}}{T_r} - 2\Omega_j \epsilon_{ijk} \overline{u_k \theta} \ , \tag{A1.22}$$

The derivation of the humidity flux transport equation is analogous to the derivation given above.

A1.5.3   The other (co)variance equations

The derivation of the $\overline{\theta^2}$, $\overline{q^2}$ and $\overline{q\theta}$ equations is straight-forward. For the $\overline{\theta^2}$ equation we multiply (A1.12) with θ and average, this yields

$$\frac{1}{2} \frac{\partial}{\partial t} \overline{\theta^2} + \frac{1}{2} U_j \frac{\partial \overline{\theta^2}}{\partial x_j} + \frac{1}{2} \frac{\partial}{\partial x_j}(\overline{u_j \theta^2}) + \overline{u_j \theta} \frac{\partial \Theta}{\partial x_j} = \kappa_H \overline{\theta \frac{\partial^2 \theta}{\partial x_k \partial x_k}} \ , \tag{A1.23}$$

where the molecular term must be transformed. To this end we write

$$\kappa_H \overline{\theta \frac{\partial^2 \theta}{\partial x_k \partial x_k}} = \kappa_H \overline{\frac{\partial}{\partial x_k}(\theta \frac{\partial \theta}{\partial x_k})} - \kappa_H \overline{(\frac{\partial \theta}{\partial x_k})^2} =$$

$$= \frac{1}{2} \kappa_H \frac{\partial^2 \overline{\theta^2}}{\partial x_k \partial x_k} - \kappa_H \overline{(\frac{\partial \theta}{\partial x_k})^2} \ .$$

The first term on the right hand side represents molecular diffusion again and can be neglected. The second term cannot be neglected, even when isotropy of the smallest scales is assumed. Thus

$$\kappa_H \overline{\theta \frac{\partial^2 \theta}{\partial x_k \partial x_k}} = - \kappa_H \overline{(\frac{\partial \theta}{\partial x_k})^2} = - \overline{\epsilon}_\theta \ . \tag{A1.24}$$

Equation (A1.23) then reads

$$\frac{\partial}{\partial t} \overline{\theta^2} + U_j \frac{\partial \overline{\theta^2}}{\partial x_j} + 2 \overline{u_j \theta} \frac{\partial \Theta}{\partial x_j} = - \frac{\partial}{\partial x_j}(\overline{u_j \theta^2}) - 2 \overline{\epsilon}_\theta \ . \tag{A1.25}$$

For the $\overline{q^2}$ and $\overline{q\theta}$ equation we find accordingly

$$\frac{\partial}{\partial t}\,\overline{q^2} + U_j\,\frac{\partial \overline{q^2}}{\partial x_j} + 2\,\overline{u_j q}\,\frac{\partial Q}{\partial x_j} = -\,\frac{\partial}{\partial x_j}(\overline{u_j q^2}) - 2\,\overline{\varepsilon}_q \quad, \tag{A1.26}$$

and

$$\frac{\partial}{\partial t}\,\overline{q\theta} + U_j\,\frac{\partial \overline{q\theta}}{\partial x_j} + \overline{u_j q}\,\frac{\partial \Theta}{\partial x_j} + \overline{u_j \theta}\,\frac{\partial Q}{\partial x_j} = -\,\frac{\partial}{\partial x_j}(\overline{u_j q\theta}) - \overline{\varepsilon}_{q\theta} \quad, \tag{A1.27}$$
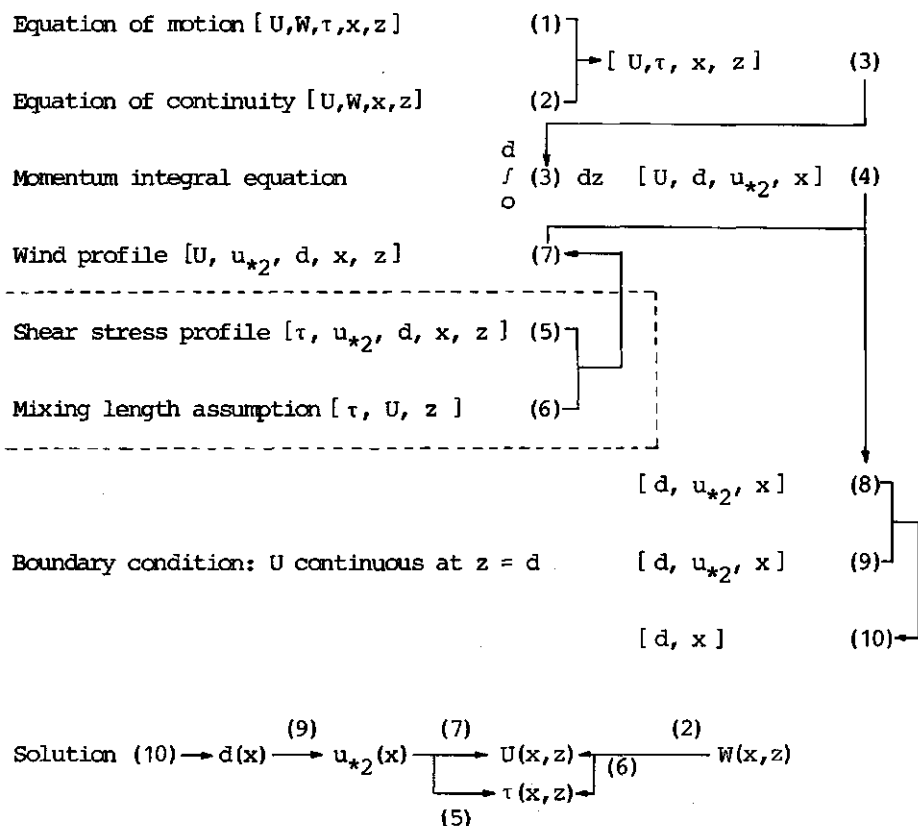
where

$$\overline{\varepsilon}_q = -\,\kappa_v \overline{\left(\frac{\partial q}{\partial x_k}\right)^2} \quad, \quad \text{and} \quad \overline{\varepsilon}_{q\theta} = -\,(\kappa_v + \kappa_H)\overline{\frac{\partial q}{\partial x_k}\,\frac{\partial \theta}{\partial x_k}} \quad. \tag{A1.28 a,b}$$

Appendix 2

SOLUTION PROCEDURE FOR INTEGRAL METHODS

If square brackets are used to denote a relation between the
dependent and independent variables placed within these brackets,
the solution procedure used in integral models can be summarized
as follows:

Equation of motion $[U, W, \tau, x, z]$ (1)

$[U, \tau, x, z]$ (3)

Equation of continuity $[U, W, x, z]$ (2)

$\int\limits_{o}^{d} (3)\ dz$ $[U, d, u_{*2}, x]$ (4)

Momentum integral equation

Wind profile $[U, u_{*2}, d, x, z]$ (7)

Shear stress profile $[\tau, u_{*2}, d, x, z]$ (5)

Mixing length assumption $[\tau, U, z]$ (6)

$[d, u_{*2}, x]$ (8)

Boundary condition: U continuous at $z = d$ $[d, u_{*2}, x]$ (9)

$[d, x]$ (10)

Solution $(10) \rightarrow d(x) \xrightarrow{(9)} u_{*2}(x) \xrightarrow{(7)} U(x,z) \xrightarrow[\ (6)\ ]{(2)} W(x,z)$
$ \xrightarrow[(5)]{} \tau(x,z)$

Using the equation of continuity (2), it is possible to
eliminate the vertical velocity W from the equation of motion
(1), resulting in eq. (3). If this equation is integrated over
the depth d of the IBL, the shear stress at $z = 0$ (u_{*2}) and the

IBL height enter the analysis in (4). When a prescribed form of
the horizontal velocity U is used (7) we are able to eliminate
U as a dependent variable from (4) resulting in (8). Finally,
if the boundary condition of a continuous velocity at $z = d$ (9)
is used, two equations (9) and (8) with two unknowns (d and u_{*2})
are obtained. Combining these equations will generate a differ-
ential equation in d (10) which can be solved either analytical-
ly or numerically, giving d as a function of x.

Substituting backwards will result in the other dependent
variables as shown in the bottom line diagram.
We did not include the parameters z_{01}, z_{02} and u_{*1} in these
diagrams. The part of the diagram behind the dashed line indi-
cates that the prescription of a shear stress profile within
the IBL is, as Peterson (1969) notices, a fourth equation, which
creates a system with more equations than unknowns. But as
Taylor (1969) notices, the mixing length hypothesis is necessary
to obtain the vertical distribution of the shear stress.

Appendix 3

SUMMARY OF CLOSURE APPROXIMATIONS AND BOUNDARY CONDITIONS

A3.1 Closure approximation and modeled equations

Although a full description of the closure approximations in the
present model is given by Rao et al. (1974b) they are summarized
in this Appendix for completeness and easy reference. Some clo-
sure approximations were modified in the course of this study
and these modified expressions are also presented here. As
k = 0.41 was used instead of k = 0.35 (Rao et al., 1974b), the
value of various constants in the closure approximations is
changed accordingly.

Turbulent transport terms
The turbulent transport terms are approximated by a gradient
transport model (see Chapter 4):

$$\overline{Mu_i} = - a_t \frac{\partial M}{\partial x_j} \overline{u_i u_j} \, \tau \tag{A3.1}$$

where M can be $\overline{\theta u_j}$, $\overline{q u_j}$, $\overline{\theta^2}$, $\overline{q^2}$, $\overline{q\theta}$ or $\overline{\epsilon}$ and $\tau = \overline{u_i u_i}/\epsilon$ is a
turbulent time scale. The third moment $\overline{u_i u_j u_k}$ in the $\overline{u_i u_k}$
equation is expressed as

$$\overline{(u_i u_j + \frac{2}{3}p\delta_{ij})u_k} = a_t \frac{\partial(-\overline{u_i u_j})}{\partial x_m} \overline{u_m u_k} \, \tau \tag{A3.2}$$

where a_t in both equations is a transport constant. In the
original model $a_t = 0.15$ was used, except in the $\overline{\epsilon}$ -equation,
where the surface layer constraints require $a_t = (4-4a)/16.6$
(see Wyngaard et al., 1974a).

Pressure covariance terms
Rao et al. (1974b) modeled the pressure covariance terms
in Eqs. (4.1)-(4.3) respectively by

131

$$-\overline{(u_k \frac{\partial p}{\partial x_i} + u_i \frac{\partial p}{\partial x_k})} + 2 \frac{\partial}{\partial x_j}(\overline{u_j p}) \frac{\delta_{ik}}{3} =$$

$$- (\overline{u_i u_k} - \overline{u_i u_i} \frac{\delta_{ik}}{3}) \frac{c_{ik}}{\tau} \tag{A3.3}$$

$$- \overline{\theta \frac{\partial p}{\partial x_i}} = - d_i \frac{\overline{\theta u_i}}{\tau} \tag{A3.4}$$

$$- \overline{q \frac{\partial p}{\partial x_i}} = - d_i \frac{\overline{q u_i}}{\tau} \tag{A3.5}$$

where the constants $c_{ii} = 6.7$, c_{ik} ($i \neq k$) $= 13.1$, $d_1 = 5.0$ and $d_3 = 13.1$. In these modeling approximations no mean strain and buoyancy effects have been incorporated. The extension to account for these effects is given by Wyngaard (1975) and was added in a later version of the model in this study, hence

$$- \overline{(u_k \frac{\partial p}{\partial x_i} + u_i \frac{\partial p}{\partial x_k})} + \frac{2}{3} \frac{\partial}{\partial x_j}(\overline{u_j p}) \delta_{ik} = A_{ik} \tag{A3.6}$$

where

$$A_{ik} = - \frac{C}{\tau}(\overline{u_i u_k} - \overline{u_i u_i} \frac{\delta_{ik}}{3}) + \frac{1}{2} C_1 \overline{u_i u_i}(\frac{\partial U_i}{\partial x_k} + \frac{\partial U_k}{\partial x_i}) +$$

$$+ C_2 (\overline{u_i u_j} \frac{\partial U_k}{\partial x_j} + \overline{u_k u_j} \frac{\partial U_i}{\partial x_j} - \frac{2}{3} \delta_{ik} \overline{u_m u_j} \frac{\partial U_j}{\partial x_m}) +$$

$$+ C_3 (\frac{g_i}{T_r} \overline{\theta u_k} + \frac{g_k}{T_r} \overline{\theta u_i} - \frac{2}{3} \frac{g_j}{T_r} \overline{\theta u_j} \delta_{ik}) \tag{A3.7}$$

The C-term is identical to the right hand side of eq. (A3.3). The C_1 and C_2 terms represent mean strain effects, while the C_3 term parameterizes the buoyancy effects. Applying the lower boundary neutral surface layer limit, these constants are related by:

$C = 6.67 \ (1-C_2)$

$C_1 = 0.23 \ (1-C_2)$ $\hspace{4cm}$ (A3.8)

Unfortunately, Wyngaard (1975) only presents values of the various C's for the stable surface layer. For the turbulent heat and humidity flux, the approximation read respectively:

$$\overline{\theta \frac{\partial p}{\partial x_i}} = d_i \frac{\overline{\theta u_i}}{\tau} + a_1 \frac{g_i}{T_r} \overline{\theta \theta_v} + a_2 \frac{\partial U_i}{\partial x_j} \overline{\theta u_j} \hspace{2cm} (A3.9)$$

and

$$\overline{q \frac{\partial p}{\partial x_i}} = d_i \frac{\overline{q u_i}}{\tau} + a_1 \frac{g_i}{T_r} \overline{q \theta_v} + a_2 \frac{\partial U_i}{\partial x_j} \overline{q u_j} \hspace{2cm} (A3.10)$$

where (A3.9) has been slightly modified with respect to the expression given by Wyngaard (1975) to account for humidity. The a_1 and a_2 terms parameterize buoyancy and mean strain effects respectively. The value of d_i is the same as in Eqs. (A3.4) and (A3.5), while $a_2 = -0.5$ was used as suggested by Launder (1975). The value of a_1 is determined by the gradient Richardson number:

$a_1 = 0.5$ $\hspace{2cm}$ if $R_i < 0$

$a_1 = 0.5 + 1.5 \ R_i^2 - R_i^3$ if $0 < R_i < 1$ $\hspace{1.5cm}$ (A3.11)

$a_1 = 1.0$ $\hspace{2cm}$ if $R_i > 1$

where $Ri = (g/T) \ (\partial \theta / \partial z)/(\partial U/\partial z)^2$

Modeled equations

The modeling expressions originally given by Rao et al. (1974a) presented in this Appendix are now applied to Eqs. (4.1)-(4.6) and (4.14). If homogeneity is assumed i.e. $\partial/\partial x = 0$ and, by virtue of the equation of continuity, als $W = 0$, the following equations apply to the various turbulence quantities:

$$2 \, \overline{uw} \, \frac{\partial U}{\partial z} = -a_t \frac{\partial}{\partial z}(\overline{w^2}\tau \, \frac{\partial \overline{u^2}}{\partial z}) - \left[\overline{u^2} - \frac{1}{3}(\overline{u^2} + \overline{v^2} + \overline{w^2})\right]\frac{C_{11}}{\tau} - \frac{2}{3}\,\overline{\varepsilon} \tag{A3.12}$$

$$0 = -a_t \frac{\partial}{\partial z}(\overline{w^2}\tau \, \frac{\partial \overline{v^2}}{\partial z}) - \left[\overline{v^2} - \frac{1}{3}(\overline{u^2} + \overline{v^2} + \overline{w^2})\right]\frac{C_{22}}{\tau} - \frac{2}{3}\,\overline{\varepsilon} \tag{A3.13}$$

$$- 2 \frac{g}{T_r} \, \overline{w\theta}_v = -a_t \frac{\partial}{\partial z}(\overline{w^2}\tau \, \frac{\partial \overline{w^2}}{\partial z}) - \left[\overline{w^2} - \frac{1}{3}(\overline{u^2} + \overline{v^2} + \overline{w^2})\right]\frac{C_{33}}{\tau} - \frac{2}{3}\,\overline{\varepsilon} \tag{A3.14}$$

$$\overline{w^2} \, \frac{\partial U}{\partial z} - \frac{g}{T_r} \, \overline{u\theta}_v = - a_t \frac{\partial}{\partial z}(\overline{w^2}\tau \, \frac{\partial \overline{uw}}{\partial z}) - \overline{uw} \, \frac{c}{\tau} \tag{A3.15}$$

$$\overline{w\theta} \, \frac{\partial U}{\partial z} + \overline{uw} \, \frac{\partial \Theta}{\partial z} = - a_t \frac{\partial}{\partial z}(\overline{w^2}\tau \, \frac{\partial \overline{u\theta}}{\partial z}) - \overline{u\theta} \, \frac{d_1}{\tau} \tag{A3.16}$$

$$\overline{w^2} \, \frac{\partial \Theta}{\partial z} - \frac{g}{T_r} \, \overline{\theta\theta}_v = - a_t \frac{\partial}{\partial z}(\overline{w^2}\tau \, \frac{\partial \overline{w\theta}}{\partial z}) - \overline{w\theta} \, \frac{d_3}{\tau} \tag{A3.17}$$

$$\overline{wq} \, \frac{\partial U}{\partial z} + \overline{uw} \, \frac{\partial Q}{\partial z} = - a_t \frac{\partial}{\partial z}(\overline{w^2}\tau \, \frac{\partial \overline{uq}}{\partial z}) - \overline{uq} \, \frac{d_1}{\tau} \tag{A3.18}$$

$$\overline{w^2} \, \frac{\partial Q}{\partial z} - \frac{g}{T_r} \, \overline{q\theta}_v = - a_t \frac{\partial}{\partial z}(\overline{w^2}\tau \, \frac{\partial \overline{wq}}{\partial z}) - \overline{wq} \, \frac{d_3}{\tau} \tag{A3.19}$$

$$\overline{wq} \, \frac{\partial \Theta}{\partial z} + \overline{w\theta} \, \frac{\partial Q}{\partial z} = - a_t \frac{\partial}{\partial z}(\overline{w^2}\tau \, \frac{\partial \overline{q\theta}}{\partial z}) - \overline{q\theta} \, \frac{2b}{\tau} \tag{A3.20}$$

$$2 \, \overline{w\theta} \, \frac{\partial \Theta}{\partial z} = - a_t \frac{\partial}{\partial z}(\overline{w^2}\tau \, \frac{\partial \overline{\theta^2}}{\partial z}) - \overline{\theta^2} \, \frac{2b}{\tau} \tag{A3.21}$$

$$2 \, \overline{wq} \, \frac{\partial Q}{\partial z} = - a_t \frac{\partial}{\partial z}(\overline{w^2}\tau \, \frac{\partial \overline{q^2}}{\partial z}) - \overline{q^2} \, \frac{2b}{\tau} \tag{A3.22}$$

$$\frac{- 4 \, \overline{\varepsilon}}{\overline{u^2} + \overline{v^2} + \overline{w^2}}(\overline{\varepsilon} - aP) = - a_t \frac{\partial}{\partial z}(\overline{w^2}\tau \, \frac{\partial \overline{\varepsilon}}{\partial z}) \tag{A3.23}$$

134

A3.2 Summary of boundary conditions

The lower boundary conditions used in the model of Rao et al.
(1974b) were based on the equilibrium flux-profile relations
defined by the Kansas experiment results (Businger et al.,
1971). In the present study modified expressions are used
in accordance with k = 0.41 instead of k = 0.35. Thus:

at $z = z_{oi}$ (x < 0, upstream conditions: i = 1)

$$U = W = 0, \quad \Theta = \Theta_o , \quad Q = Q_o ,$$

$$\frac{kz_{oi}}{u_{*i}} \frac{\partial U}{\partial z} = \frac{kz_{oi}}{T_{*i}} \frac{\partial \Theta}{\partial z} = \frac{kz_{oi}}{q_{*i}} \frac{\partial Q}{\partial z} = 1 ,$$

$$\overline{uw}/u_{*i}^2 = -1.0 , \quad \overline{u^2}/u_{*i}^2 = 4.0 , \quad \overline{v^2}/u_{*i}^2 = \overline{w^2}/u_{*i}^2 = 1.75$$

$$\overline{w\theta}/u_{*i}T_{*i} = \overline{wq}/u_{*i}q_{*i} = -1.0, \quad \overline{u\theta}/u_{*i}T_{*i} = \overline{uq}/u_{*i}q_{*i} = 4.0 ,$$

$$\overline{\theta^2}/T_{*i}^2 = \overline{q^2}/q_{*i}^2 = \overline{q\theta}/q_{*i}T_{*i} = 4.0 , \quad \frac{kz_o}{u_{*i}^3}\overline{\varepsilon} = 1.0 \qquad \text{(A3.24)}$$

In part II of the model (x > 0, downstream conditions:
i = 2) the value of $u_{*2}(x)$, $T_{*2}(x)$ and $q_{*2}(x)$ is deter-
mined by U(x,z), $\Theta(x,z)$ and $Q(x,z_2)$ at the lowest two
levels (z_1 and z_2) where the lowest level z_1 coincides
with the surface roughness height z_{02}. The value of
$U(x,z_2)$, $\Theta(x,z_2)$ and $Q(x,z_2)$ is calculated by the model
using the finite difference computation scheme. But at
$z = z_1 = z_{02}$ only U is known, as by definition $U(x,z_1)$
= 0. This allows the computation of $u_{*2}(x)$ by means of
(5.4). The boundary value of the temperature and speci-
fic humidity must somehow be obtained by inferring
equations relating these quantities to others already
known. Rao et al (1974b) used the energy balance equation

135

$$H_{02}(x) + \lambda E_{02}(x) = R_n - G \tag{A3.25}$$

with a predetermined constant value of $R_n - G$. That the
available energy is constant throughout the flow,
(either for $x < 0$ and $x > 0$), seems questionable but appears
to be a reasonable assumption. Experimental data (Lang,
et al., 1983) indicate that this is, at least within some
10% a good approximation. Using the equilibrium flux-
profile relations, (A3.25) can be expressed in terms of
mean quantities

$$(\frac{\partial \theta}{\partial z})_{z_{02}} + \frac{\lambda}{c_p}(\frac{\partial Q}{\partial z})_{z_{02}} = \frac{u_{*1}(T_{*1} + \frac{\lambda}{c_p} q_{*1})}{k z_{02} u_{*2}(x)} \tag{A3.26}$$

where $u_{*2}(x) = k z_{02}(\frac{\partial U}{\partial z})_{z_{02}}$ and the gradients of Q and θ

are approximated by finite differences:

$$(\frac{\partial Q}{\partial z})_{z_{02}} = \frac{Q(x,z_2) - Q(x,z_1)}{z_2 - z_1} ,$$

and

$$(\frac{\partial \theta}{\partial z})_{z_{02}} = \frac{\theta(x,z_2) - \theta(x,z_1)}{z_2 - z_1} .$$

A second equation is necessary to solve (A3.26) for
$\theta(x,z_1)$ and $Q(x,z_1)$. Rao et al. postulated that

$$Q(x,z_1) = R_{02} \cdot Q_s(\theta(x,z_1)) \tag{A3.27}$$

where R_{02} is the surface relative humidity, which is
assumed to be constant for $x > 0$. $Q_s(\theta(x,z_1))$ is the
saturation specific humidity for the temperature at
$z = z_1 = z_{02}$. Solving (A3.26) and (A3.27) for $\theta(x,z_1)$
and $Q(x,z_1)$ enables the calculation of $T_{*2}(x)$ and
$q_{*2}(x)$ which, together with $u_{*2}(x)$ determine the lower

boundary condition for every variable by means of (A3.24).
Instead of using (A3.27), an alternative method to close
(A3.26) was suggested by McNaughton (1984) and is discussed
in Appendix 4.

The upper boundary conditions in Part I ($x < 0$, upstream
situation) are also determined by the existing flux-profile
relations and the predetermined height of the atmospheric
boundary layer height (z_I).
At $z = z_{max}$ ($x < 0$, upstream conditions: $i = 1$)

$$\frac{k\ z_{max}}{u_{*i}} \frac{\partial U}{\partial z} = \phi_m(\frac{z_{max}}{L}) , \qquad \frac{k\ z_{max}}{T_{*i}} \cdot \frac{\partial \theta}{\partial z} = \phi_h(\frac{z_{max}}{L}) ,$$

$$\frac{k\ z_{max}}{q_{*i}} \frac{\partial Q}{\partial z} = \phi_w(\frac{z_{max}}{L})$$

$$\overline{u^2}/u_{*i}^2 = 0.2(w_*^2/u_{*i}^2) + 4 ,$$

$$\overline{v^2}/u_{*i}^2 = 0.2(w_*^2/u_{*i}^2) + 1.75 ,$$

$$\overline{w^2}/u_{*i}^2 = 2(- \frac{z_{max}}{L})^{2/3} + 1.75$$

$$\overline{w\theta}/u_{*i}T_{*i} = \overline{wq}/u_{*i}q_{*i} = \overline{uw}/u_{*i}^2 = \frac{z_{max}}{z_I} - 1$$

$$\overline{u\theta}/u_{*i}T_{*i} = \overline{uq}/u_{*i}q_{*i} = 4\ \phi_m\ \phi_h$$

$$\overline{\theta^2}/T_{*i}^2 = \overline{q^2}/q_{*i}^2 = \overline{q\theta}/q_{*i}T_{*i} = 4(1 - 8.3\ \frac{z_{max}}{L})^{-2/3}$$

$$\overline{\varepsilon} = - \overline{uw}\ \frac{\partial U}{\partial z} + \frac{g}{T_r}\ \overline{w\theta}_v \qquad\qquad (A3.28)$$

137

In part II (x > 0, downstream conditions) the upper boundary
value of every variable, except W, remains fixed, i.e. sta-
tionary conditions aloft are assumed. Gradients are supposed
to be very small hence the vertical windspeed W does not sub-
stantially affect the upper boundary values. This implies that
calculations cannot be extended beyond the value of x where the
IBL coincides with the highest calculation level.

Appendix 4

RECONSIDERATION OF THE LOWER BOUNDARY CONDITION

In order to avoid the, rather unrealistic, assumption that R_{02} has a constant value for $x > 0$, and thus discarding Eq. (A3.27) McNaughton (1984) suggested the following procedure.

Use the Penman-Monteith equation to calculate the latent heat flux density

$$\lambda E = \frac{(\frac{s}{s+\gamma})(R_n - G) + \frac{\rho c_p}{s+\gamma} \cdot \frac{1}{r_a}[Q_s(\theta(x,z_2)) - Q(x,z_2)]}{1 + (\frac{\gamma}{s+\gamma}) r_s/r_a} \qquad (A4.1)$$

where r_a is the aerodynamic resistance,
  r_s is the surface resistance,
  s is the slope of the saturation specific humidity
    curve
and $\gamma = c_p/\lambda$.

Multiplying this equation by $(\frac{s+\gamma}{\gamma}) r_a$ yields

$$\lambda E = \frac{(\frac{s}{\gamma})(R_n - G) r_a + \rho\lambda[Q_s(\theta(x,z_2)) - Q(x,z_2)]}{(1 + s/\gamma) r_a + r_s} \qquad (A4.2)$$

The aerodynamic resistance r_a is obtained from the wind profile by

$$r_a = U(x,z_2)/u_*^2(x) \qquad (A4.3)$$

This leaves r_s undetermined, and hence a new independent parameter is introduced.

The latent heat flux density at each step downstream is
calculated by solving Eqs. (A4.2) and (A4.3), using an
empirical function for $Q_s(\theta)$. The energy balance (A3.25)
provides the accompanying sensible heat flux density.
The value of $Q(x,z_1)$ and $\theta(x,z_1)$ is obtained by using

$$H = \rho c_p (\theta(x,z_1) - \theta(x,z_2))/r_a \qquad\qquad\qquad (A4.4)$$

and

$$\lambda E = \rho \lambda (Q(x,z_1) - Q(x,z_2))/r_a \qquad\qquad\qquad (A4.5)$$

In daytime situations when R_n - G is positive, all variables
in (A4.2) are positive and hence a negative value of the la-
tent heat flux density λE is precluded.

The boundary conditions (A4.2)-(A4.5) were inserted into the
present model and the same upstream situation as discussed
in Chapter 4 was used (Figs. 4.10 and 4.11). The value of
the surface resistance r_s for the upstream terrain was cal-
culated from the equilibrium profiles and amounted to 37 s/m.
As the air moves over a warmer, dryer and rougher surface
downstream, the latent heat flux and the aerodynamic resis-
tance (r_a) must decrease. According to (A4.2) the value of
r_s must be greater than 37 s/m. For this experiment r_s was
set to 5000 s/m.

The results, as far as the temperature and the absolute
humidity are concerned, are presented in Figs. (A4.1) and
(A4.2). Fig. (A4.1) clearly shows that the gradient of the
absolute humidity is negative everywhere, hence the latent
heat flux is directed upwards throughout the flow. The
negative (i.e. downwards) latent heat flux in Fig. (4.10)
releases latent heat at the surface which is physically
unrealistic. Because of this additional input of energy at
the surface, the surface temperature must increase substan-
tially. This is visible in Fig. (4.11). In the present situ-

ation no latent heat is released at the surface and hence the increase of the surface temperature after x = 0 will be much smaller.

Though the problem of the negative latent heat flux has been effectively eliminated by the procedure outlined in this appendix, one problem still remains. Instead of using the assumption of a constant relative humidity at the surface it is now assumed that the surface resistance r_s remains un-changed. Although, on observing Eq. (A4.2), the solution is not very sensitive for this assumption, it remains in doubt. Furthermore, the application of equation (A4.2) implies that the surface is at saturation point. In this example the Penman-Monteith equation is used above a very dry surface, this seems contradictory.

Finally, for a change from a dry, warm surface to a cool and humid one, the problem of a downwards latent heat flux will not arise. In that case the sensible heat flux will be direc-ted downwards, this is not an uncommon feature.
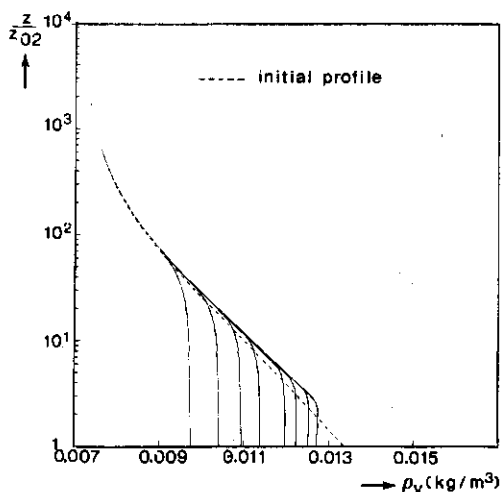

Figure A4.1   Absolute humidity profiles after a change in surface conditions for various distances downstream.
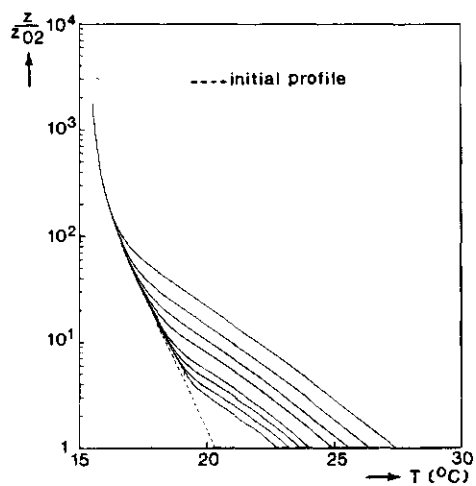
Figure A4.2 Temperature profiles after a change in surface conditions for various distances downstream.

Appendix 5

TRANSFORMATION OF THE SECOND ORDER FLUX-PROFILE RELATIONS

We want to transform the flux profile relations, derived from
the modeled transport equations of the second moments, into
relations resembling the "standard" flux-profile relations
(5.22)-(5.24). The additional equations for $\overline{u\theta}$, $\overline{\theta^2}$ and $\overline{q\theta}$
(A3.16), (A3.21) and (A3.20) are then needed.

The following two assumptions are made:

(i) the buoyancy terms $\dfrac{g}{T_r}\dfrac{\overline{m\theta}}{\overline{w^2}}v$ in (5.28)-(5-30) can be approxi-
mated by $\dfrac{g}{T}\dfrac{\overline{m\theta}}{\overline{w^2}}$ (m = u, θ or q). Thus the influence of water
vapour on the buoyancy term will be neglected.

(ii) the turbulent transport term in the equation for $\overline{u\theta}$, $\overline{\theta^2}$ and
$\overline{q\theta}$ is negligibly small. This can be inferred from Figs. 4.3 and
4.4 for $\overline{\theta^2}$ and $\overline{u\theta}$, respectively. Calculations show that this also
applies for the $\overline{q\theta}$ equation.

Hence we start with the following equations:

$$\overline{uw} = -\frac{\overline{w^2}\tau}{c_{13}}\left(\frac{\partial U}{\partial z} - \frac{g}{T_r}\frac{\overline{u\theta}}{\overline{w^2}}\right) , \qquad (A5.1)$$

$$\overline{w\theta} = -\frac{\overline{w^2}\tau}{d_3}\left(\frac{\partial\Theta}{\partial z} - \frac{g}{T_r}\frac{\overline{\theta^2}}{\overline{w^2}}\right) , \qquad (A5.2)$$

$$\overline{wq} = -\frac{\overline{w^2}\tau}{d_3}\left(\frac{\partial Q}{\partial z} - \frac{g}{T_r}\frac{\overline{q\theta}}{\overline{w^2}}\right) , \qquad (A5.3)$$

$$\overline{u\theta} = -\frac{\tau}{d_1}\left(\overline{w\theta}\frac{\partial U}{\partial z} + \overline{uw}\frac{\partial\Theta}{\partial z}\right) , \qquad (A5.4)$$

$$\overline{\theta^2} = -\frac{\tau}{b}\left(\overline{w\theta}\frac{\partial\Theta}{\partial z}\right) , \qquad (A5.5)$$

143

$$\overline{q\theta} = - \frac{\tau}{2b}(\overline{wq}\,\frac{\partial\theta}{\partial z} + \overline{w\theta}\,\frac{\partial Q}{\partial z}) , \qquad\qquad (A5.6)$$

where $c_{13} = d_3 = c$.

Substitute $\overline{\theta^2}$ (A5.5) into (A5.2), this results in:

$$\overline{w\theta} = - \frac{\overline{w^2}\tau}{c}\,\frac{\partial\theta}{\partial z}/(1 + \frac{\tau^2}{bc}\,\frac{g}{T_r}\,\frac{\partial\theta}{\partial z}) . \qquad\qquad (A5.7)$$

Substitute $\overline{u\theta}$ (A5.4) and subsequently $\overline{w\theta}$ (A5.7) into (A5.1).
This yields after rearranging:

$$\overline{uw} = - \frac{\overline{w^2}\tau}{c}\,\frac{\partial U}{\partial z}\,\frac{1 - P_1/(1 + P_2)}{1 + P_1} , \qquad\qquad (A5.8)$$

where $P_1 = \frac{\tau^2}{d_1 c}\,\frac{g}{T_r}\,\frac{\partial\theta}{\partial z}$,

and $P_2 = \frac{\tau^2}{bc}\,\frac{g}{T_r}\,\frac{\partial\theta}{\partial z}$.

Analogously we will find for $\overline{wq}$ after substituting $\overline{q\theta}$ (A5.6)
and $\overline{w\theta}$ (A5.7):

$$\overline{wq} = - \frac{\overline{w^2}\tau}{c}\,\frac{\partial Q}{\partial z}\,\frac{1 - P_3/(1 + P_2)}{1 + P_3} , \qquad\qquad (A5.9)$$

where $P_3 = \frac{\tau^2}{2bc}\,\frac{g}{T_r}\,\frac{\partial\theta}{\partial z}$

Equations (A5.8) and (A5.9) can be reduced to simpler forms
if $P_i \ll 1$ (i = 1,2,3) is assumed. We then obtain:

$$\overline{uw} = - \frac{\overline{w^2}\tau}{c}\,\frac{\partial U}{\partial z}/(1 + \frac{2\tau^2}{d_1 c}\,\frac{g}{T_r}\,\frac{\partial\theta}{\partial z}) , \qquad\qquad (A5.10)$$

and

144

$$\overline{wq} = - \frac{\overline{w^2}\tau}{c} \frac{\partial Q}{\partial z} / (1 + \frac{\tau^2}{bc} \frac{g}{T_r} \frac{\partial \theta}{\partial z}) \tag{A5.11}$$

Note the similarity of the expressions for the fluxes of sensible- and latent heat (A5.7) and (A5.11). This is in accordance with eqs. (5.23) and (5.24) and the assumption (5.13). In the next step only the buoyancy correction factors in (5.22) and (A5.10) are considered. Hence it is assumed that the influence of buoyancy on $\overline{w^2}\tau/c$ is small. Then we are left to show that:

$$\phi_m = 1 + \frac{2\tau^2}{cd_1} \frac{g}{T_r} \frac{\partial \theta}{\partial z} \tag{A5.12}$$

Using eqs. (5.11) and (5.7), the left hand side of the above equation reads

$$\phi_m = (1 - 16 \frac{z}{L})^{-\frac{1}{4}} \cong 1 + 4 \frac{z}{L} = 1 + 4 z \frac{g}{T_r} k \frac{T_*}{u_*^2}$$

which after applying eq. (5.5) yields

$$\phi_m = 1 + 4 k^2 z^2 \frac{g}{T_r} \frac{1}{u_*^2} \frac{\partial \theta}{\partial z} \tag{A5.13}$$

Finally, it is assumed that $\tau \cong \kappa z / u_*$. If eqs. (A5.13) and (A5.12) are substituted we obtain

$$1 + 4 \frac{k^2 z^2}{u_*^2} \frac{g}{T_r} \frac{\partial \theta}{\partial z} = 1 + \frac{2}{cd_1} \frac{\kappa^2 z^2}{u_*^2} \frac{g}{T_r} \frac{\partial \theta}{\partial z} \tag{A5.14}$$

The assumption of the distribution of τ is of course not rigorous, as part of the buoyancy effect is still contained within the $\overline{w^2}\tau/c$ term. Attempts to solve also for $\overline{e^2}$ and $\overline{\epsilon}$ are frustrated by the fact that the turbulent transport terms of $\overline{u^2}$, $\overline{v^2}$ and $\overline{w^2}$ are not negligible, compared to the production and dissipation terms. This renders the whole set of equations analytically untractable.

Samenvatting

De bepaling van de verticale fluxdichtheden van impuls, voel-
bare- en latente warmte aan het aardoppervlak is van groot
belang in diverse wetenschappen zoals bijvoorbeeld meteorologie,
landbouwkunde en hydrologie. De fluxdichtheid van een grootheid
wordt gedefinieerd als het transport van die grootheid per een-
heid van oppervlak en per tijdseenheid.

Een directe meting van een fluxdichtheid aan het aardoppervlak
is vaak lastig uit te voeren, daarom neemt men gewoonlijk z'n
toevlucht tot metingen in de atmosfeer en in de bodem. Een veel
toegepaste techniek is die welke gebruik maakt van zogenaamde
"flux-profiel relaties". Deze relaties koppelen de verticale
fluxdichtheid van bijvoorbeeld de voelbare warmte aan een verti-
caal temperatuurprofiel. Bij zo'n methode kan dan volstaan wor-
den met een relatief eenvoudige meting van de temperatuur op 2
of meerdere hoogten. Echter, bij het gebruik van flux-profiel
relaties gaat men er vanuit dat aan een aantal voorwaarden is
voldaan. De belangrijkste voorwaarde is wel dat de fluxdichtheid
onafhankelijk is van de hoogte, hetgeen alleen opgaat boven een
uitgestrekt, homogeen terrein. Daar aan deze eis in de praktijk
meestal niet (voldoende) voldaan is, rijst de vraag in hoeverre
dit de meetresultaten beïnvloedt. Het doel van dit onderzoek is
dan ook na te gaan hoe groot de fouten zijn die men maakt bij
het gebruik van de standaard flux-profiel relaties boven een
niet-homogeen terrein, en tevens na te gaan hoe die fouten
samenhangen met de structuur van de atmosfeer boven een inhomo-
geen terrein.

In hoofdstuk 1 wordt als inleiding de bovenstaande vraagstelling
gepresenteerd. Er wordt in aangegeven dat het onderzoek uitge-
voerd zal worden door gebruik te maken van een numeriek 2e orde
model. De numerieke aanpak in het algemeen wordt vergeleken met
de traditionele keuze: theoretisch of experimenteel.

146

Een nadere uitwerking van de probleemstelling wordt gegeven in hoofdstuk 2. Hierin wordt aangegeven dat de studie betrekking heeft op het onderste deel van de atmosfeer: de atmosferische oppervlakte laag (ASL) en op welke manier de ASL zich ruwweg aanpast aan een terreinovergang. Het doel van dit onderzoek wordt daarna in dit kader geplaatst. In het tweede deel van hoofdstuk 2 worden de voor het probleem relevante vergelijkingen behandeld.

In hoofdstuk 3 wordt een indeling in diverse klassen gemaakt van de bestaande modellen die een beschrijving geven van het gedrag van de atmosferische oppervlaktelaag na een terreinovergang. De voor- en nadelen van de diverse modelklassen worden besproken. Het blijkt dat voor het huidige onderzoek de numerieke modellen met een tweede orde sluiting, kortweg 2e orde modellen, de meeste mogelijkheden bieden en dat van dit soort modellen tevens de beste resultaten verwacht mogen worden.

Het 2e orde model van Rao, Wyngaard en Coté (1974b) dat gebruikt zal worden, wordt in hoofdstuk 4 nader bekeken. Dit model bestaat uit een gedeelte (deel 1) dat de beginprofielen berekent van de diverse grootheden zoals windsnelheid, temperatuur, luchtvochtigheid enz. (initialisatie). Het andere gedeelte (deel 2) van dit model berekent daarna het gedrag (= de verdeling) van de diverse grootheden na een terreinovergang.

De beginprofielen en de balansen van diverse vergelijkingen, berekend met deel 1 worden vergeleken met experimenteel gevonden waarden en enige universele functies. Hieruit blijkt dat de randvoorwaarden aan de bovengrens van het model problemen opleveren in een niet-neutrale atmosfeer. Tevens wordt duidelijk dat de modellering (= benadering) van met name de druktermen in de diverse vergelijkingen te wensen overlaat. Een en ander resulteert in beginprofielen, bijvoorbeeld van de verticale gradiënt van de windsnelheid ($\partial U/\partial z$), die niet exact overeenkomen met de verwachte universele functies. In deel 2 van het model wordt als randvoorwaarde aan de ondergrens van het model o.a.

147

verondersteld dat de relatieve vochtigheid (R_{02}) constant is.
Deze aanname levert een niet-realistische oplossing bij een
overgang van een nat en koel terrein, naar een droog en warm
terrein. Een methode om dit te verbeteren wordt aangegeven. Het
uitvoerig bespreken van deze zwakke punten wil natuurlijk niet
zeggen dat het model daarom onbruikbaar is. Een positief punt is
dat de oplossing stabiel blijkt te zijn bij een tijdelijke ver-
storing van de evenwichtssituatie: alle variabelen keren weer
terug naar hun oorspronkelijke toestand.

In hoofdstuk 5 wordt een samenvatting gegeven van de bestaande
flux-profiel methoden. De aannamen die aan elk van die methoden
ten grondslag liggen worden kort besproken. In de homogene
(evenwichts)situatie worden deze methoden vergeleken met elkaar
en met de zogenaamde "2e orde flux-profiel relaties". Dit laats-
te zijn flux-profiel relaties, welke afgeleid worden uit de
transportvergelijkingen van het model. Het blijkt dat in een
neutrale atmosfeer de fluxen, bepaald met beide soorten relaties,
vrijwel identiek zijn. In een niet-neutrale atmosfeer is de
interpretatie van de 2e orde relaties minder eenvoudig. Het
blijkt dat stabiliteitseffecten op 2 manieren de 2e orde flux-
profiel relaties beïnvloeden: via een extra term in de relatie
en via de verandering van de zogenaamde "2e orde eddy diffusie
constanten". Op 2 manieren wordt vervolgens nagegaan in hoeverre
de 2e orde relaties consistent zijn met de standaard flux-profiel
relaties. Het blijkt dat fluxen, bepaald met de Bowen verhouding
methode zeer goed (binnen 5%) overeenkomen met de fluxen bepaald
met de 2e orde relaties. Daarentegen blijkt dat de fluxen
bepaald met de aerodynamische methode een veel slechtere over-
eenkomst vertonen. Dit laatste is een gevolg van de tekortkoming
van het model, besproken in hoofdstuk 4.

De Bowen verhouding methode en de aerodynamische methode worden
in hoofdstuk 6 toegepast op de profielen van windsnelheid, tem-
peratuur en luchtvochtigheid welke berekend zijn met deel 2 van
het model. In deze inhomogene situatie blijkt dat de Bowen
verhouding methode warmtefluxen geeft die in absolute waarde

148

groter zijn dan de fluxen berekend met het model. Tenminste, dit is het geval in de zogenaamde aangepaste grenslaag (IAL), waarin de modelfluxen vrijwel onafhankelijk van de hoogte zijn. Het blijkt dat het verschil voornamelijk veroorzaakt wordt door de bijdragen van de advectietermen en de turbulente transporttermen in de modelvergelijkingen. Met deze effecten wordt in de Bowen verhouding methode per definitie geen rekening gehouden. De verschillen zijn echter gering (< 10%) indien het gebied vlak achter de terreinovergang (binnen 2 m.) buiten beschouwing wordt gelaten. Een bijzonder gunstige bijkomstigheid is overigens dat de Bowen verhouding methode zelfs een betere schatting van de warmtefluxen aan het aardoppervlak geeft dan de volledige modelvergelijkingen. Ver boven de IAL zijn de fluxen, bepaald met de Bowen verhouding methode, juist kleiner (in absolute zin) dan de fluxen bepaald met het model. Een mogelijke verklaring hiervoor wordt kort besproken.

De analyse van de aerodynamische methode, tenslotte, is zoals in hoofdstuk 5 werd opgemerkt, minder goed mogelijk door de afwijkingen in de beginprofielen. Hierdoor is de beschouwing van de resultaten van de aerodynamische methode beperkt en slechts kwalitatief. Het blijkt wel dat deze methode aanzienlijk grotere fouten geeft dan de Bowen verhouding methode. Dit wordt toegeschreven aan de grotere gevoeligheid van de aerodynamische methode voor de juiste hoogteverdeling van de diverse dimensieloze gradiënten.

In hoofdstuk 7, tenslotte, worden de resultaten van dit onderzoek samengevat, en wordt kort aangegeven wat in het algemeen de toepassingsmogelijkheden van het gebruikte model zijn.

References

Antonia, R.A. and Luxton, R.E. 1971: The response of a turbulent
    boundary layer to a step change in surface roughness.
    Part 1: smooth to rough. J. Fluid Mech. 48, p. 721-761.

Antonia, R.A. and Luxton, R.E. 1972: The response of a turbulent
    boundary layer to a step change in surface roughness. Part 2:
    rough to smooth. J. Fluid Mech. 53, p. 737-757.

Antonia, R.A., Dahn, H.Q. and Prabhu, A. 1977: Response of a
    turbulent boundary layer to a step change in surface heat
    flux. J. Fluid Mech. 80, p. 153-177.

Blackadar, A.K., Panofsky, H.A., Glass, P.E. and Boogaard, J.F.
    1967: Determination of the effect of roughness change on the
    wind profile. Boundary Layers and turbulence. Phys. of
    Fluids Suppl. 10 S, p. 209-211.

Blom, J. and Wartena, L. 1969: The influence of changes in sur-
    face roughness on the development of the turbulent boundary
    layer in the lower layers of the atmosphere. J. Atm. Sc. 26,
    p. 225-265.

Bowen, A.J. and Lindley, D. 1977: A wind-tunnel investigation of
    the wind speed and turbulence characteristics close to the
    ground over various escarpment shapes. B.L.M. 12, p. 259-271.

Bradley, E.F. 1968: A micrometeorological study of velocity
    profiles and surface drag in the region modified by a change
    in surface roughness. Q.J.R.M.S. 94, p. 361-379.

Bradley, E.F., Antonia, R.A. and Chambers, A.J. 1981:
    Temperature structure in the atmospheric surface layer.
    Part I. Budget of temperature variance. B.L.M. 20,
    p. 275-292.

Bradley, E.F., Antonia, R.A. and Chambers, A.J. 1982: Streamwise
    heat flux budget in the atmospheric surface layer. B.L.M. 23,
    p. 3-15.

Bradshaw, P. 1972: The understanding and prediction of turbulent
    flow. Aero. J. 76, p. 403-418.

Bradshaw, P., Ferriss, D.H. and Atwell, N.P. 1967: Calculation
    of boundary-layer development using the turbulent energy

equation. J. Fluid Mech. 28, p. 593-616.

Brutsaert, W.H. 1982: Evaporation into the atmosphere. Environ-
    mental Fluid Mechanics. D. Reidel Publ. Co., Dordrecht,
    Holland.

Businger, J.A., Wyngaard, J.C., Izumi, Y. and Bradley, E.F.
    1971: Flux-profile relationships in the atmospheric surface
    layer. J. Atm. Sc. 28, p. 181-189.

Champagne, F.H., Friehe, C.A., LaRue, J.C. and Wyngaard, J.C.
    1977: Flux measurements, flux estimation techniques, and
    fine-scale turbulence measurements in the unstable surface
    layer over land. J. Atm. Sc. 34, p. 515-530.

Corrsin, S. 1974: Limitations of gradient transport models in
    random walks and in turbulence. Adv. Geoph. 18A, p. 25-60.

Dawkins, R.A. and Davies, D.R. 1981: The effect of surface
    topography on momentum and mass transfer in a turbulent
    boundary layer. J. Fluid Mech. 108, p. 423-442.

Deardorff, J.W. 1966: The counter-gradient heat flux in the
    lower atmosphere and in the laboratory. J. Atm. Sc. 23,
    p. 503-506.

Deardorff, J.W. 1972: Numerical investigation of neutral and
    unstable planetary boundary layers. J. Atm. Sc. 29, p.
    p. 91-115.

De Bray, B.G. 1973: Atmospheric shear flows over ramps and
    escarpments. Industrial Aerodynamics Abstracts 5,
    sept.-oct. 1973.

De Bruin, H.A.R. 1982: The energy balance of the earth's surface:
    a practical approach. Ph. D. Thesis. KNMI Scientific Report
    W.R. 82-1.

Douwes, J.T.G. 1980: The calculation of a turbulent boundary
    layer following a step change in surface conditions.
    Rep. no. R-438-A, University Eindhoven.

DuFort, E.C. and Frankel, S.P. 1953: Stability conditions in the
    numerical treatment of parabolic differential equations.
    Math. Tables Aid Comput. 7, p. 135-152.

Dutton, J.A. and Fichtl, G.H. 1969: Approximate equations of
    motion for gases and liquids. J. Atm. Sc. 26, p. 241-254.

Dyer, A.J. 1963: The adjustment of profiles and eddy fluxes.

Q.J.R.M.S. 89, p. 276-280.

Dyer, A.J. 1974: A review of flux-profile relationships. B.L.M. 7, p. 363-372.

Dyer, A.J. and Crawford, T.V. 1965: Observations of the modification of the microclimate at a leading edge. Q.J.R.M.S. 91, p. 345-348.

Elliott, W.P. 1958: The growth of the atmospheric internal boundary layer. Trans. Am. Geoph. Union 36 no. 6, p. 1048-1054.

Fuchs, M. and Tanner, C.B. 1970: Error analysis of Bowen ratios measured by differential psychrometry. Agric. Meteorol. 7, p. 329-334.

Gandin, L.S. 1952: On the transformation of the wind profile. Trudy GGO 33, p. 71-84.

Harsha, P.T. 1977: Kinetic energy models. Chapter 8 of "Handbook of Turbulence", vol.1 Fundamentals and Applications. W. Frost and T.H. Moulden (editors) Plenum Press.

Hinze, J.O. 1959: Turbulence. McGraw-Hill Book Co., New York.

Højstrup, J. 1981: A simple model for the adjustment of velocity spectra in unstable conditions downstream of an abrupt change in roughness and heat flux. B.L.M. 21, p. 341-356.

Huang, C.H. and Nickerson, E.C. 1972: Numerical simulation of wind, temperature, shear stress and turbulent energy over nonhomogeneous terrain. Project Themis Report No. 12, Fluid Mechanics Program, Colorado State University.

Huang, C.H. and Nickerson, E.C. 1974a: Stratified flow over non-uniform surface conditions: mixing-length model. B.L.M. 5, p. 395-417.

Huang, C.H. and Nickerson, E.C. 1974b: Stratified flow over non-uniform surfaces: turbulent energy model. B.L.M. 7, p. 107-123.

Izumi, Y. 1971: Kansas 1968 field program data report. AFCRL-72-0041., Air Force Cambridge Research Laboratories (LYB), L.G. Hanscom Field, Bedford, MA.

Izumi, Y. and Caughey, S.J. 1976: Minnesota 1973 atmospheric boundary layer experiment data report. AFGL Environmental Research Paper no. 547.

Johnson, D.S. 1955: Turbulent heat transfer in a boundary layer
    with discontinuous wall temperature. Dissertation, Johns
    Hopkins Univ., Baltimore.

Lang, A.R.G., McNaughton, K.G., Chen Fazu, Bradley, E.F. and
    Eiji Ohtaki, 1983a: Inequality of eddy transfer coefficients
    for vertical transport of sensible and latent heats during
    advective inversions. B.L.M. 25, p. 25-41.

Lang, A.R.G., McNaughton, K.G., Chen Fazu, Bradley, E.F. and
    Eiji Ohtaki, 1983b: An experimental appraisal of the terms
    in the heat and moisture flux equations for local advection.
    B.L.M. 25, p. 89-102.

Launder, B.E. 1975: On the effects of a gravitational field on
    the turbulent transport of heat and momentum. J. Fluid Mech.
    67, p. 569-581.

Launder, B.E. and Spalding, D.B. 1972: Lectures in: Mathematical
    models of turbulence. Academic Press (3rd. printing 1979).

Logan, E. and Fichtl, G.H. 1975: Rough to smooth transition of
    an equilibrium neutral constant stress layer. B.L.M. 8,
    p. 525-528.

Lumley, J.L. 1979: Computational modeling of turbulent flows.
    Adv. Appl. Mech. 18, p. 123-176.

Lumley, J.L. and Panofsky, H. 1964: The structure of the atmos-
    pheric turbulence. Interscience Publishers, New York.

Lumley, J.L. and Khajeh-Nouri, B. 1974: Computational modeling
    of turbulent transport. Adv. in Geoph. 18A, p. 169-193.
    Academic Press, New York.

McNaughton, K.G. 1976a: Evaporation and advection I: evaporation
    from extensive homogeneous surfaces. Q.J.R.M.S. 102,
    p. 181-191.

McNaughton, K.G. 1967b: Evaporation and advection II: evapora-
    tion downwind of a boundary separating regions having
    different surface resistances and available energies.
    Q.J.R.M.S. 102, p. 193-202.

McNaughton, K.G. 1984: private communication.

Mellor, G.L. and Herring, H.J. 1973: A survey of the mean
    turbulent field closure models. AIAA Journal 11, (no. 5),
    p. 590-599.

Monin, A.S. and Yaglom, A.M. 1971: Statistical Fluid Mechanics: Mechanics of Turbulence, Vol. 1. The MIT Press, Cambridge, Mass.

Mulhearn, P.J. 1977: Relations between surface fluxes and mean profiles of velocity, temperature and concentration, downwind of a change in surface roughness. Q.J.R.M.S. 103, p. 785-802.

Nickerson, E.C. 1968: Boundary layer adjustment as an initial value problem. J. Atm. Sc. 25, p. 207-213.

Obukhov, A.M. 1946: Turbulence in an atmosphere with non-uniform temperature. Trudy Instit. Teoret. Geofiz: AN-S.S.S.R., No. 1 (English translation: 1971: B.L.M. 2, p. 7-29).

Onishi, G. and Estoque, M.A. 1968: Numerical study on atmospheric boundary layer flow over inhomogeneous terrain. J. Met. Soc. of Japan 46, p. 280-285.

Panofsky, H.A. and Townsend, A.A. 1964: Change of terrain roughness and the wind profile. Q.J.R.M.S. 90, p. 147-155.

Peterson, E.W. 1969a: A numerical model of the mean wind and turbulent energy downstream of a change in surface roughness. Rep. no. 102-69, Center for Air Environment Studies, Penn. State Univ.

Peterson, E.W. 1969b: Modification of mean flow and turbulent energy by a change in surface roughness under conditions of neutral stability. Q.J.R.M.S. 95, p. 561-575.

Peterson, E.W. 1972: Relative importance of terms in the turbulent-energy and momentum equations as applied to the problem of a surface roughness change. J. Atm. Sc. 29, p. 1470-1476.

Peterson, E.W., Jensen, N.O. and Højstrup, J. 1979: Observations of downwind development of wind speed and variance profiles at Bognaes and comparison with theory. Q.J.R.M.S. 105, p. 521-529.

Philip, J.R. 1959: The theory of local advection: I. J. Meteor. 16, p. 535-547.

Plate, E.J. 1971: Aerodynamic characteristics of atmospheric boundary layers. AEC Critical Review Series, U.S. Atomic Energy Commission, Div. Techn. Info.

Plate, E.J. and Hidy, G.M. 1967: Laboratory study of air flowing
    over a smooth surface onto small water waves. J. Geoph. Res.
    72 (no. 18), p. 4627-4641.
Rao, K.S. 1975: Effect of thermal stratification on the growth
    of the internal boundary layer. B.L.M. 8, p. 227-234.
Rao, K.S., Wyngaard, J.C. and Coté, O.R. 1974a: The structure of
    the two-dimensional internal boundary layer over a sudden
    change of surface roughness. J. Atm. Sc. 31, p. 738-746.
Rao, K.S., Wyngaard, J.C. and Coté, O.R. 1974b: Local advection
    of momentum, heat and moisture in micrometeorology. B.L.M. 7,
    p. 331-348.
Revfeim, K.J.A. and Jordan, R.B. 1976: Precision of evaporation
    measurements using the Bowen ratio. B.L.M. 10, p. 97-111.
Rider, N.E., Philip. J.R. and Bradley, E.F. 1963: The horizontal
    transport of heat and moisture - a micrometeorological study.
    Q.J.R.M.S. 89, p.507-531.
Rider, N.E., Philip, J.R. and Bradley, E.F. 1965: Discussion on:
    Horizontal transport of heat and moisture - a micrometeoro-
    logical study. Q.J.R.M.S. 91, p. 236-240.
Rodi W. 1979: Prediction methods for turbulent flows. Lecture
    series VKI 1979-2 Von Karman Institute, Belgium.
Rotta, J.C. 1951: Statistische Theorie nichthomogener Turbulenz.
    Z. Phys. 129, p. 547-572; 131, p. 51-77.
Schols, J.L.J. 1979: The response of a turbulent boundary layer
    to a step change in surface roughness. Report R-386-A,
    Dept. of Physics, Heat transfer section, University of
    Eindhoven, The Netherlands.
Schols, J.L.J. 1984: The determination of turbulent structures
    in the atmospheric surface layer. Ph. D.-thesis Agricultural
    Univ. Wageningen.
Shir, C.C. 1972: A numerical computation of air flow over a sud-
    den change of surface roughness. J. Atm. Sc. 29, p. 304-310.
Sinclair, T.R., Allen, L.H. and Lemon, E.R. 1975: An analysis
    of errors in the calculation of energy flux densities above
    vegetation by a Bowen-ratio method. B.L.M. 8, p. 129-139.
Tani, I 1968: Review of some experimental results on the response
    of a turbulent boundary layer to sudden perturbations.

Proc. of AFOSR-IFP-Stanford Conference on computation of turbulent boundary layers. Vol. I, p. 483-494.

Taylor, P.A. 1969a: On wind and shear stress profiles above a change in surface roughness. Q.J.R.M.S. 95, p. 77-91.

Taylor, P.A. 1969b: The planetary boundary layer above a change in surface roughness. J. Atm. Sc. 26, p. 432-440.

Taylor, P.A. 1970: A model of airflow above changes in surface heat flux, temperature and roughness for neutral and unstable conditions. B.L.M. 1, p. 18-39.

Taylor, P.A. 1971: Airflow above changes in surface heat flux, temperature and roughness; an extension to include the stable case. B.L.M. 1, p. 474-497.

Taylor, P.A. 1973: Some comparisons between mixing-length and turbulent energy equation models of flow above a change in surface roughness. Proc. 3rd. Int. Conf. on Numerical Models in Fluid Dynamics. Univ. of Paris VI, July 3-7, 1972. Springer-Verlag, Vol. II, p. 246-253.

Tennekes, H. 1973: The logarithmic wind profile. J. Atm. Sc. 30, p. 234-238.

Tennekes, H. and Lumley, J.L. 1972: A first course in turbulence. The MIT Press, Cambridge, Mass.

Tieleman, H.W. and Derrington, D.B. 1977: An experimental study of the atmospheric boundary layer modified by a change in surface roughness and surface temperature. Report VPI-E-77-17, Dept. of Engineering Science and Mech. Virginia Polytechnic Institute and State University.

Townsend, A.A. 1965a: Self-preserving flow inside a turbulent boundary layer. J. Fluid Mech. 22, p. 773-797.

Townsend, A.A. 1965b: The response of a turbulent boundary layer to abrupt changes in surface conditions. J. Fluid Mech. 22, p. 799-822.

Townsend, A.A. 1966: The flow in a turbulent boundary layer after a change in surface roughness. J. Fluid Mech. 26, p. 255-266.

Viswanadham, Y. 1982: Examination of the empirical flux-profile models in the atmospheric surface boundary layer. B.L.M. 22, p. 61-77.

Vugts, H.F. and Businger, J.A. 1977: Air modification due to a
    step change in surface temperature. B.L.M. 11, p. 295-305.
Wagner, N.K. 1966: A two-dimensional, time dependent numerical
    model of atmospheric boundary layer flow over inhomogeneous
    terrain. Final Report for U.S. Army Electronic Res. and Dev.
    Activity, Arizona, part I. Hawaii Institute of Geophysics.
Weisman, R.N. 1975: A developing boundary layer over an evapo-
    rating surface. B.L.M. 8, p. 437-445.
Wood, D.H. 1978: Calculation of the neutral wind profile
    following a large step change in surface roughness.
    Q.J.R.M.S. 104, p. 383-392.
Wyngaard, J.C. 1975: Modeling the planetary boundary layer -
    extension to the stable case. B.L.M. 9, p. 441-460.
Wyngaard, J.C. 1978: Progress in research on turbulent flow.
    Paper presented at: WMO symposium on boundary layer physics
    applied to specific problems of air pollution. Norrköping,
    19-23 June 1978.
Wyngaard, J.C. 1982: Boundary-layer modeling. Chapter 3 in:
    Atmospheric Turbulence and Air Pollution Modelling.
    Atmospheric Sciences Library. D. Reidel Publishing Company
    Dordrecht, Holland.
Wyngaard, J.C., Arya, S.P.S. and Coté, O.R. 1974: Some aspects
    of the structure of convective planetary boundary layers.
    J. Atm. Sc. 31, p. 747-754.
Wyngaard, J.C. and Coté, O.R. 1971: The budgets of turbulent
    kinetic energy and temperature variance in the atmospheric
    surface layer. J. Atm. Sc. 28, p. 190-202.
Wyngaard, J.C., Coté, O.R. and Izumi, Y. 1971: Local free
    convection, similarity, and the budgets of shear stress
    and heat flux. J. Atm. Sc. 28, p. 1171-1183.
Wyngaard, J.C. and Coté, O.R. 1974a: The evolution of a convec-
    tive planetary boundary layer - A higher-order-closure model
    study. B.L.M. 7, p. 289-308.
Wyngaard, J.C. Coté, O.R. and Rao, K.S. 1974b: Modeling the
    atmospheric boundary layer, Adv. in Geoph. 18A, p. 193-212.
    Academic Press, New York.
Wyngaard, J.C., Pennell, W.T., Lenschow, D.H. and LeMone, M.A.

1978: The temperature humidity covariance budget in the convective boundary layer. J. Atm. Sc. 35, p. 47-58.

Yaglom, A.M. 1977: Comments on wind and temperature flux-profile relationships. B.L.M. 11, p. 89-102.

Yeh, G.T. amd Brutsaert, W. 1970: A numerical solution of the two dimensional steady-state turbulent transfer equation. Monthly Weath. Rev. 99, p. 494-500.

Yeh, G.T. and Nickerson, E.C. 1970: Airflow over roughness discontinuity. Techn. Report. No. 8. Project Themis. Fluid Dynamics and Diffusion Laboratory, College of Engineering, Colorado State Univ., Ft. Collins, Colo.

Zeman, O. 1981: Progress in the modeling of planetary boundary layers. Ann. Rev. Fluid Mech. 13, p. 253-272.

Curriculum vitae

Leonardus Johannes Maria Kroon werd op 5 januari 1952 geboren
te Rotterdam. In deze stad doorliep hij de lagere- en middelbare
school. In 1970 behaalde hij het diploma HBS-B aan het
St. Franciscuscollege, en schreef hij zich in aan de
Rijksuniversiteit te Utrecht. Het kandidaatsexamen natuurkunde,
studierichting N3, legde hij af in 1973. Het doctoraaldiploma
Geofysica, hoofdrichting Meteorologie, werd behaald in 1976 met
als afstudeeronderwerp "Ladingsscheiding in onweerswolken"
(prof. dr. F.H. Schmidt en dr. J.C.H. van der Hage). Tevens werd
de eerstegraads onderwijsbevoegdheid in de wis- en natuurkunde
behaald. Hierna volgde een periode tot 1980 waarin hij naast een
aanstelling als wetenschappelijk medewerker werkzaam was als
leraar natuurkunde in het middelbaar onderwijs. De wetenschappe-
lijke werkzaamheden werden verricht op het Instituut voor
Meteorologie en Fysische Oceanografie (IMOU) van de RUU en had-
den betrekking op het verdampingsonderzoek en de ontwikkeling
van geventileerde psychrometers. De leraarsfunctie werd achter-
eenvolgens vervuld bij SG. Spieringshoek te Schiedam (0.5 jaar),
Het Nieuwe Lyceum te Bilthoven (1 jaar) en Het Nieuwe Lyceum te
Hilversum (6 jaar). Door een zwak, maar overigens perfect
getimed, moment van de toenmalige minister van defensie
Vredeling, werd de mogelijkheid geschapen, en gebruikt, om
legaal aan de "vaderlandsplicht" te ontsnappen. In 1980 volgde
een aanstelling als promotieassistent bij de Vakgroep Natuur-
en Weerkunde van de Landbouwhogeschool te Wageningen. Naast deze
aanstelling bleef hij echter als leraar verbonden aan het
middelbaar onderwijs, totdat hij in 1984 volledig in dienst trad
bij de laatstgenoemde vakgroep als universitair docent.